

Z2615

AEGEHANDELD

Prepared for:

National Institute for Coastal and Marine
Management/RIKZ

Large-scale sandpits

Hydrodynamic and morphological modelling of large-scale sandpits

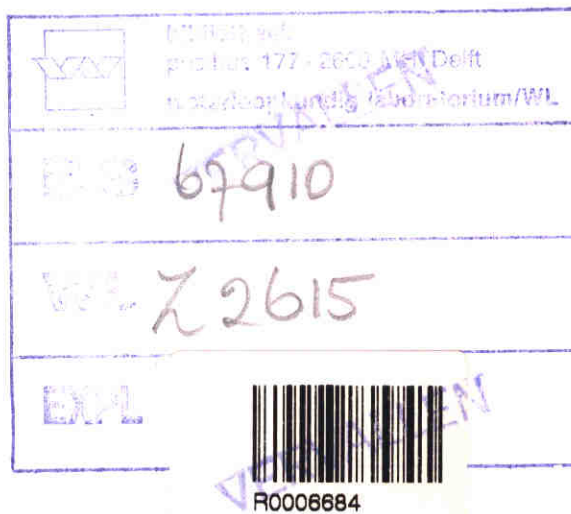
M.Sc. Thesis

June 1999

Z2615_2

z2615

wL | delft hydraulics

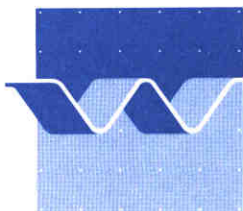


Large-scale sandpits

Hydrodynamic and morphological modelling of large-scale sandpits

M.D. Klein

M.Sc. Thesis



wl | delft hydraulics

List of Figures

Figure 3.1: The computational grid of Delft3D-FLOW*

Figure 4.1: Direction definitions*

Figure 4.2: The Delft3D-MOR process tree*

Figure 5.1: Stationary current pattern

Figure 5.2: Current velocities in center longitudinal section of a $40 \times 5 \text{ km}^2$ sandpit

Figure 5.3: Relation between water level difference and discharge into the sandpit

Figure 5.4: Three options for the maximum current velocity*

Figure 5.5: Definitions of the parameters in Equation (5.5)*

Figure 5.6: Area of influence around 30 m deep sandpits

Figure 5.7: Current velocity in an infinitely wide and a 5 km wide sandpit

Figure 5.8: Distribution of v-velocities in three cross-sections

Figure 5.9: Maximum current velocity vs. length of the sandpit

Figure 5.10: Maximum current velocity vs. length-width ratio of the sandpit

Figure 5.11: Maximum current velocity vs. length-depth ratio of the sandpit

Figure 5.12: Resultant discharges into and out of the sandpit*

Figure 6.1: Stationary boundary conditions including correction for Coriolis*

Figure 6.2: Current pattern around $+45^\circ$ rotated $40 \times 5 \text{ km}^2$ sandpit

Figure 6.3: Current pattern around $+22.5^\circ$ rotated $40 \times 5 \text{ km}^2$ sandpit

Figure 6.4: Current pattern around a parallel $40 \times 5 \text{ km}^2$ sandpit

Figure 6.5: Current pattern around -22.5° rotated $40 \times 5 \text{ km}^2$ sandpit

Figure 6.6: Current pattern around -45° rotated $40 \times 5 \text{ km}^2$ sandpit

Figure 6.7: Influence of the length and width on the stationary current pattern

Figure 7.1: Influence of the boundary conditions

Figure 7.2: Influence of the boundary conditions

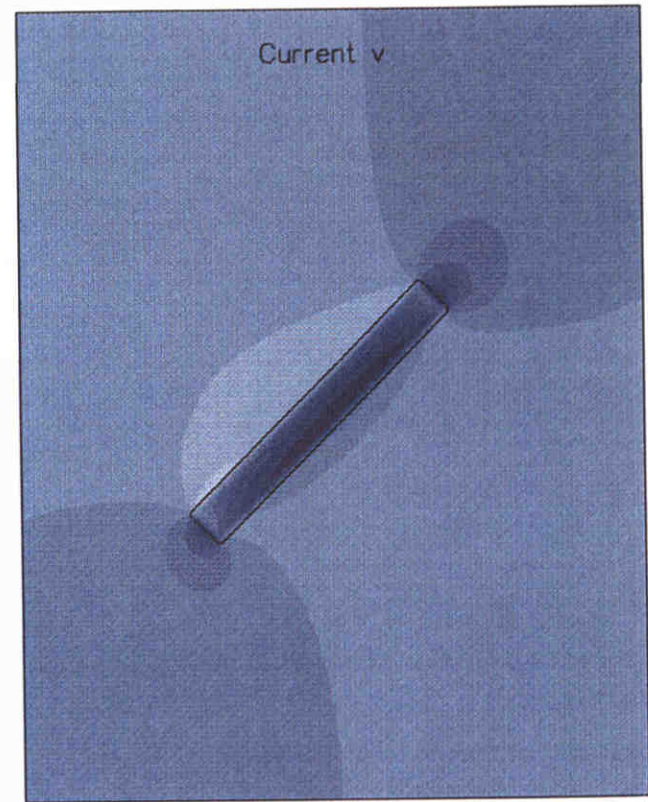
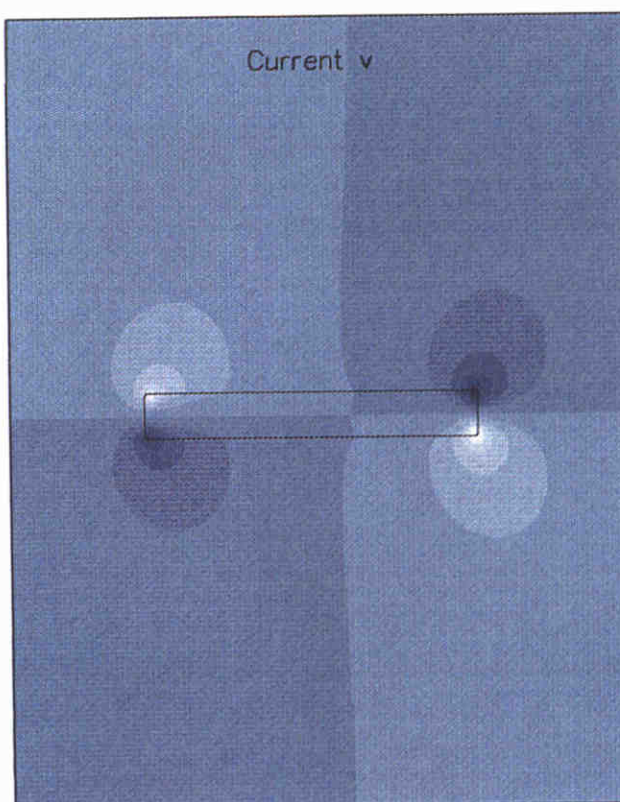
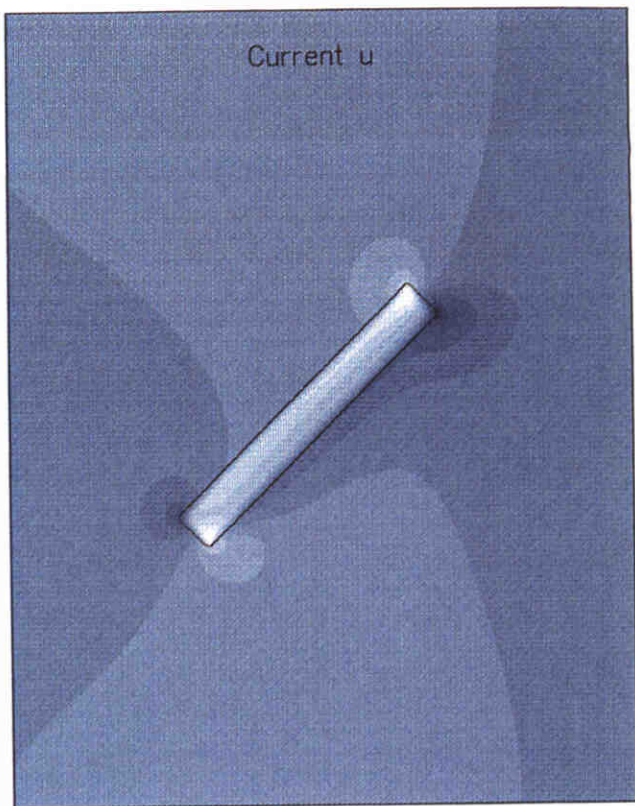
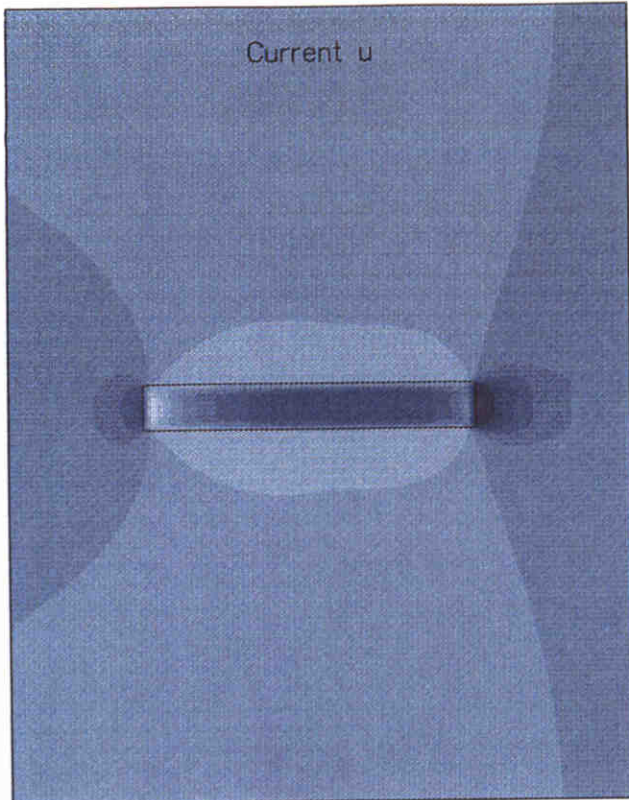
Figure 7.3: Tide-averaged current pattern around $+45^\circ$ rotated $40 \times 5 \text{ km}^2$ sandpit

Figure 7.4: Tide-averaged current pattern around a parallel $40 \times 5 \text{ km}^2$ sandpit

- Figure 7.5: Influence of the tidal amplitude and the width of the sandpit
- Figure 7.6: Influence of the length of the sandpit
- Figure 7.7: Tide-averaged current pattern around $+45^\circ$ rotated $40 \times 5 \text{ km}^2$ sandpit
- Figure 7.8: Tide-averaged current pattern around a parallel $40 \times 5 \text{ km}^2$ sandpit
- Figure 7.9: Tide-averaged current pattern around -45° rotated $40 \times 5 \text{ km}^2$ sandpit
- Figure 7.10: Tide-averaged current pattern around $10 \times 5 \text{ km}^2$ sandpits
- Figure 7.11: Tide-averaged current pattern around $10 \times 10 \text{ km}^2$ sandpits
- Figure 8.1: A sandpit considered as a tidal bank*
- Figure 8.2: Influence of the transport mode while α_{bd} is 1
- Figure 8.3: Influence of the transport mode while α_{bd} is 5
- Figure 8.4: Influence of the transport mode while α_{bd} is 10
- Figure 8.5: Influence of α_{bd} on the results of the total transport mode
- Figure 8.6: Influence of α_{bd} on the results of the bed and suspended transport mode
- Figure 8.7: Influence of α_{bd} on a $10 \times 10 \text{ km}^2$ sandpit with total transport
- Figure 8.8: Influence of the grid cell size on the morphological results
- Figure 8.9: Influence of slope of the sandpit on the morphological results
- Figure 8.10: Influence of the number of bottom computations per flow computation
- Figure 8.11: Data points for the tide analysis
- Figure 8.12: Results of the tide analysis
- Figure 8.13: SUTRENCH and Delft3D results of a reference trench
- Figure 8.14: SUTRENCH results of Walstra et al. (1998)
- Figure 8.15: Morphological computations of a $+45^\circ$ rotated $25 \times 5 \text{ km}^2$ sandpit
- Figure 8.16: Morphological computations of a parallel $25 \times 5 \text{ km}^2$ sandpit
- Figure 8.17: Morphological computations of a -45° rotated $25 \times 5 \text{ km}^2$ sandpit
- Figure 8.18: Comparison of tide-averaged current patterns
- Figure 8.19: Morphological computations of a parallel $10 \times 5 \text{ km}^2$ sandpit
- Figure 8.20: Morphological computations of a $+45^\circ$ rotated, 22m deep $25 \times 5 \text{ km}^2$ sandpit
- Figure 8.21: Morphological computations of a parallel, 22m deep $25 \times 5 \text{ km}^2$ sandpit
- Figure 8.22: Morphological computations of a -45° rotated, 22m deep $25 \times 5 \text{ km}^2$ sandpit
- Figure 8.23: Morphological computations of a parallel, 22m deep $10 \times 5 \text{ km}^2$ sandpit

- Figure 8.24: Morphological computations of a parallel $10 \times 5 \text{ km}^2$ sandpit with increased velocity of the M0 component
- Figure 8.25: Morphological development in time of a parallel $10 \times 5 \text{ km}^2$ sandpit with increased velocity of the M0 component
- Figure 8.26: Morphological computations of a parallel $10 \times 10 \text{ km}^2$ sandpit
- Figure 8.27: Morphological computations of a $+45^\circ$ rotated $10 \times 10 \text{ km}^2$ sandpit
- Figure 8.28: Morphological computations of a flat bottom
- Figure 8.29: Corrected bottom levels
- Figure 8.30: Corrected bottom changes

*) These figures are included in the text



Current velocity components u and v [m/s]

Influence of obliquity of a 40x5 km² sandpit

Stationary boundary conditions

Figure 5.2: Current velocities in the center longitudinal section of a $40 \times 5 \text{ km}^2$ sandpit

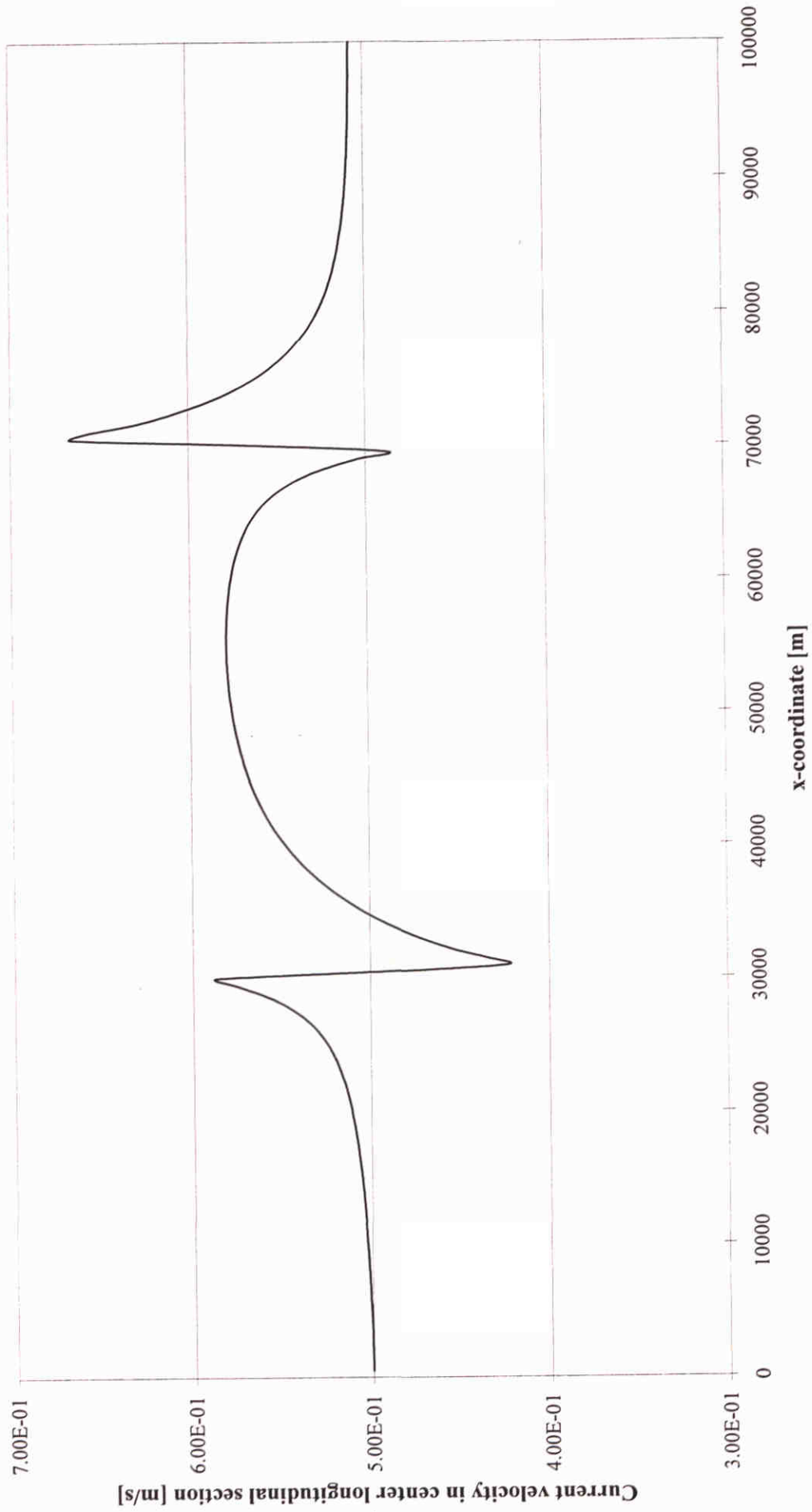
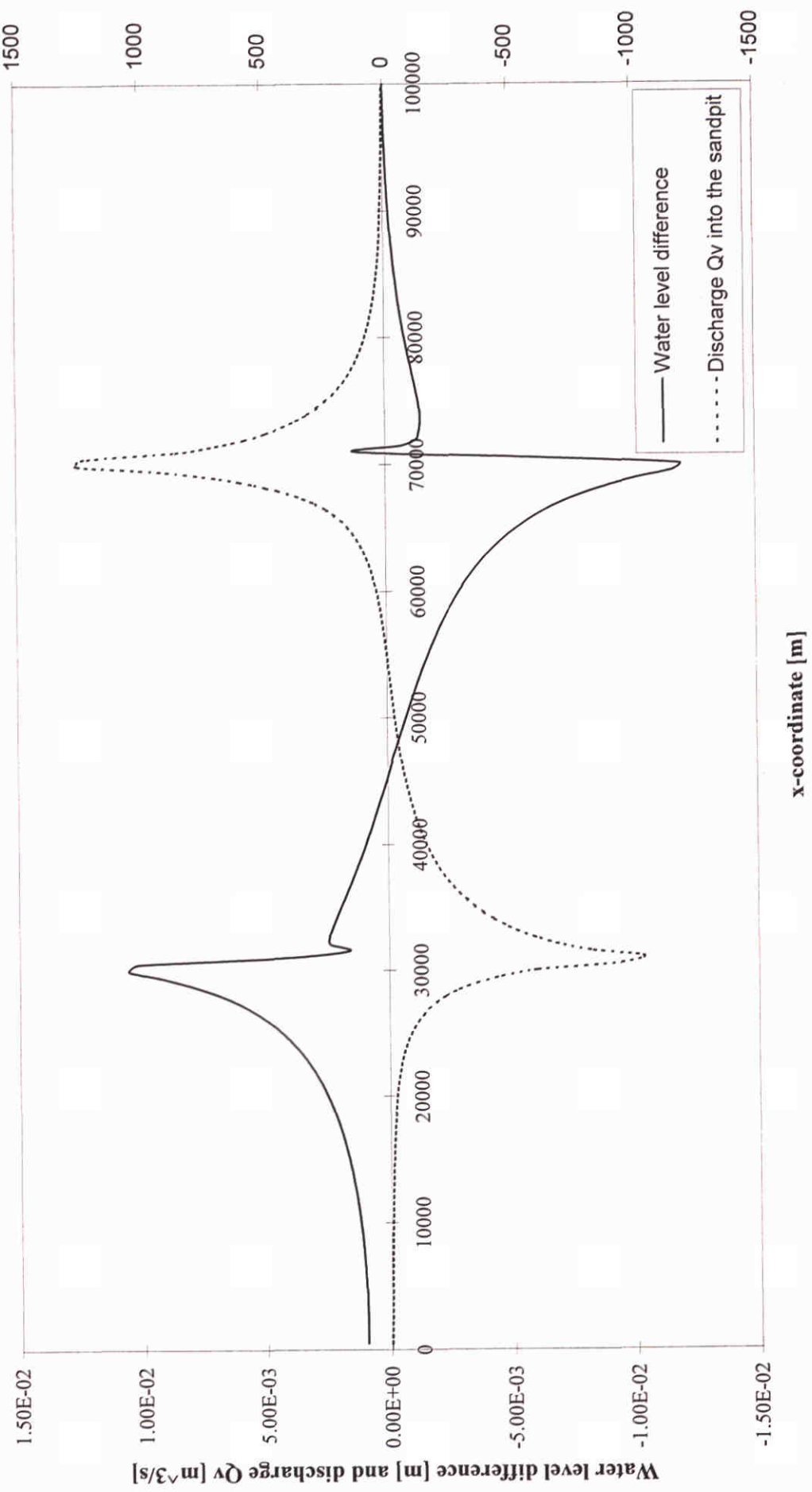
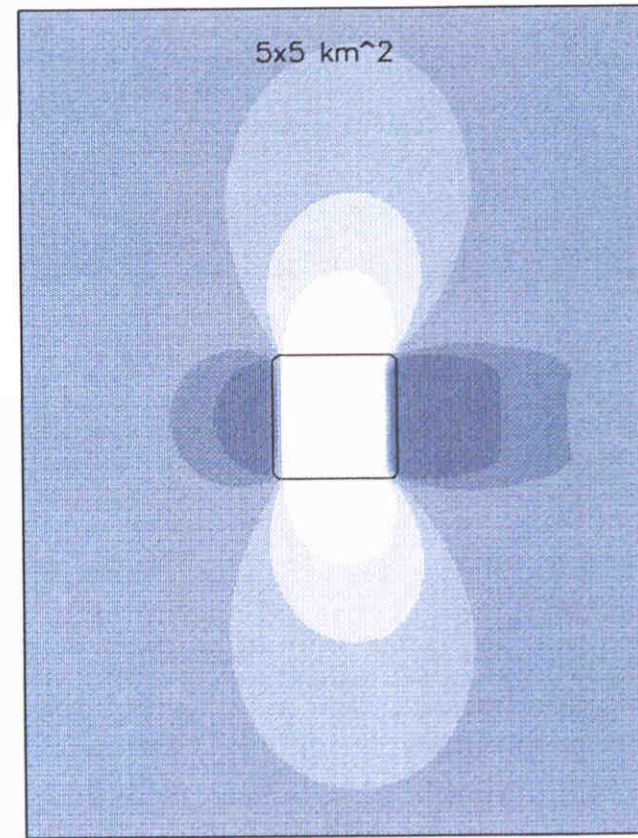
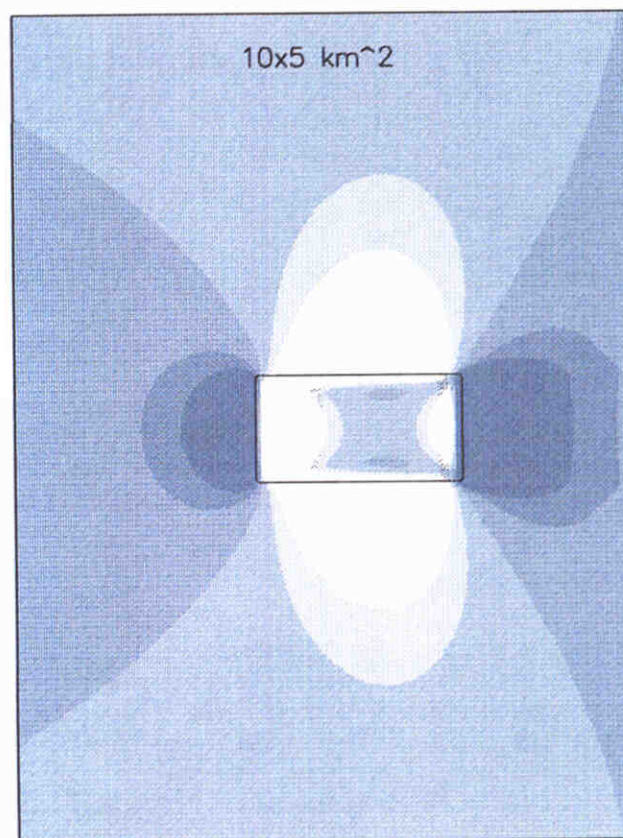
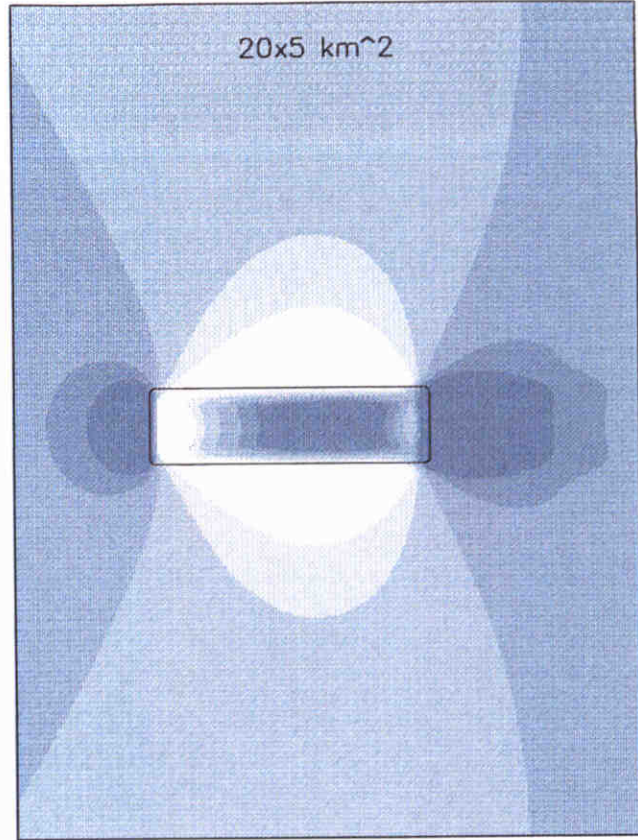
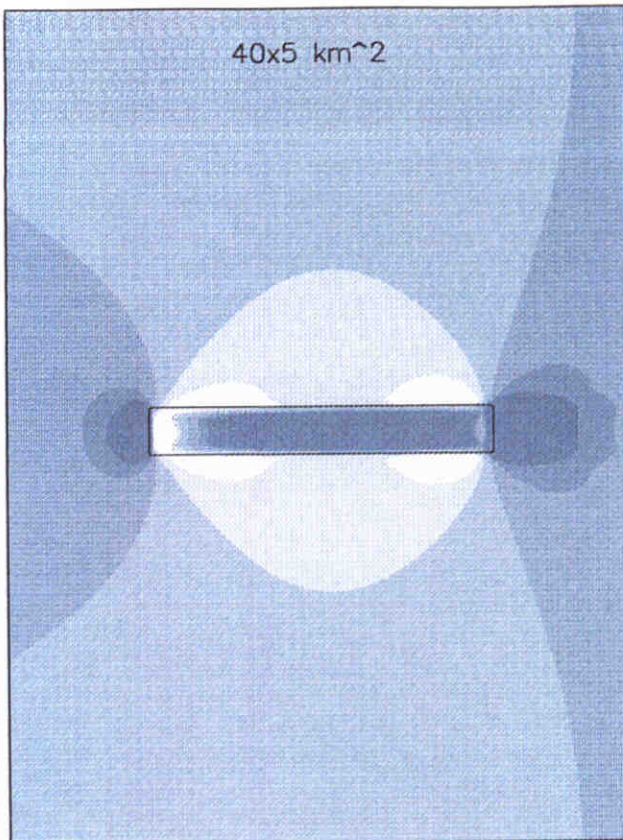


Figure 5.3: Relation between water level difference and discharge into the sandpit





<input type="checkbox"/> <0.47500	<input type="checkbox"/> <0.50000	<input type="checkbox"/> <0.52500
<input checked="" type="checkbox"/> <0.48500	<input type="checkbox"/> <0.51500	<input type="checkbox"/> >0.52500

Current magnitude [m/s]

Area of influence around 30 m deep sandpits, varying in length

Stationary boundary conditions

Figure 5.7: Current velocities in an infinitely wide and a 5 km wide sandpit

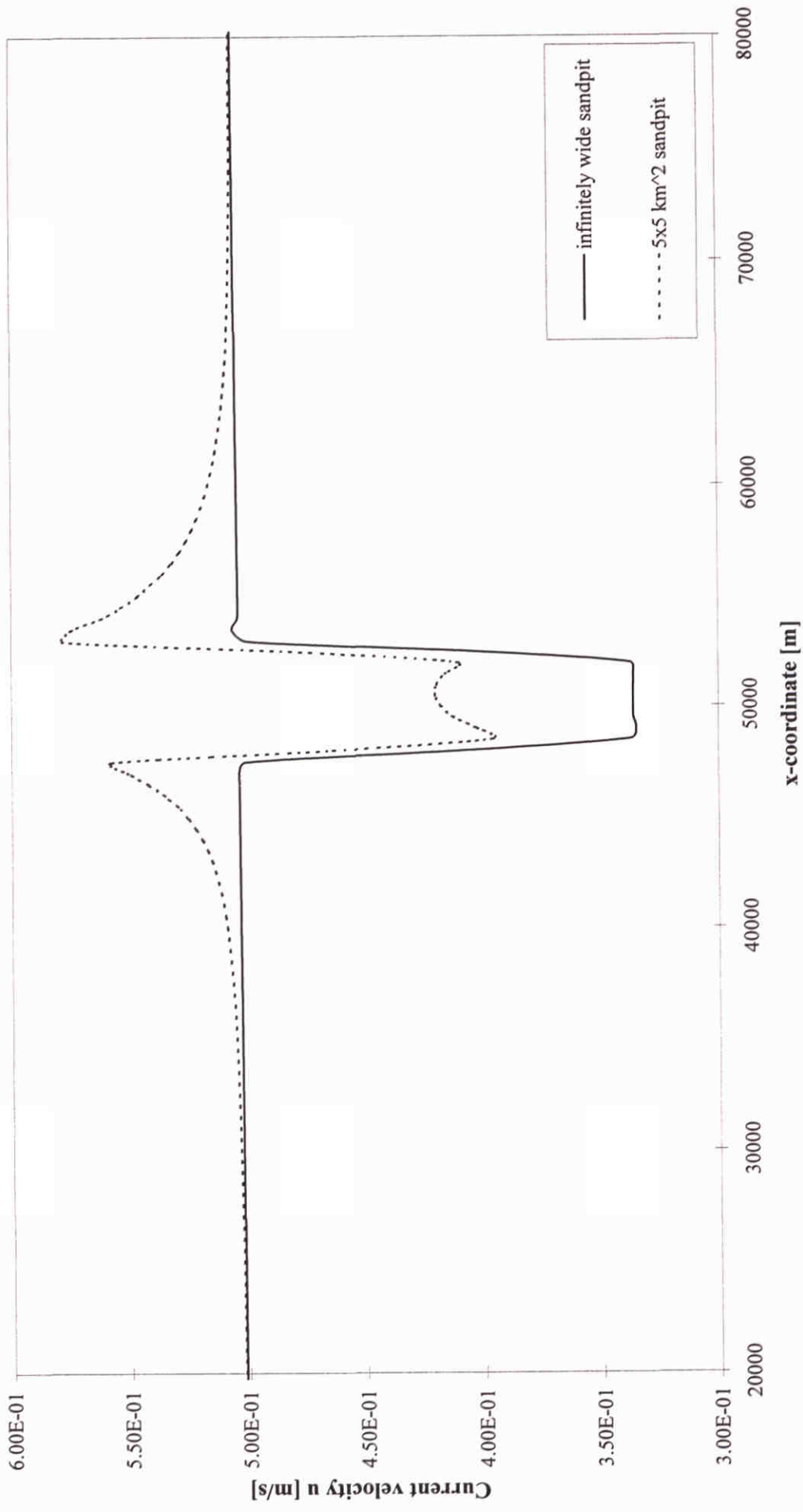
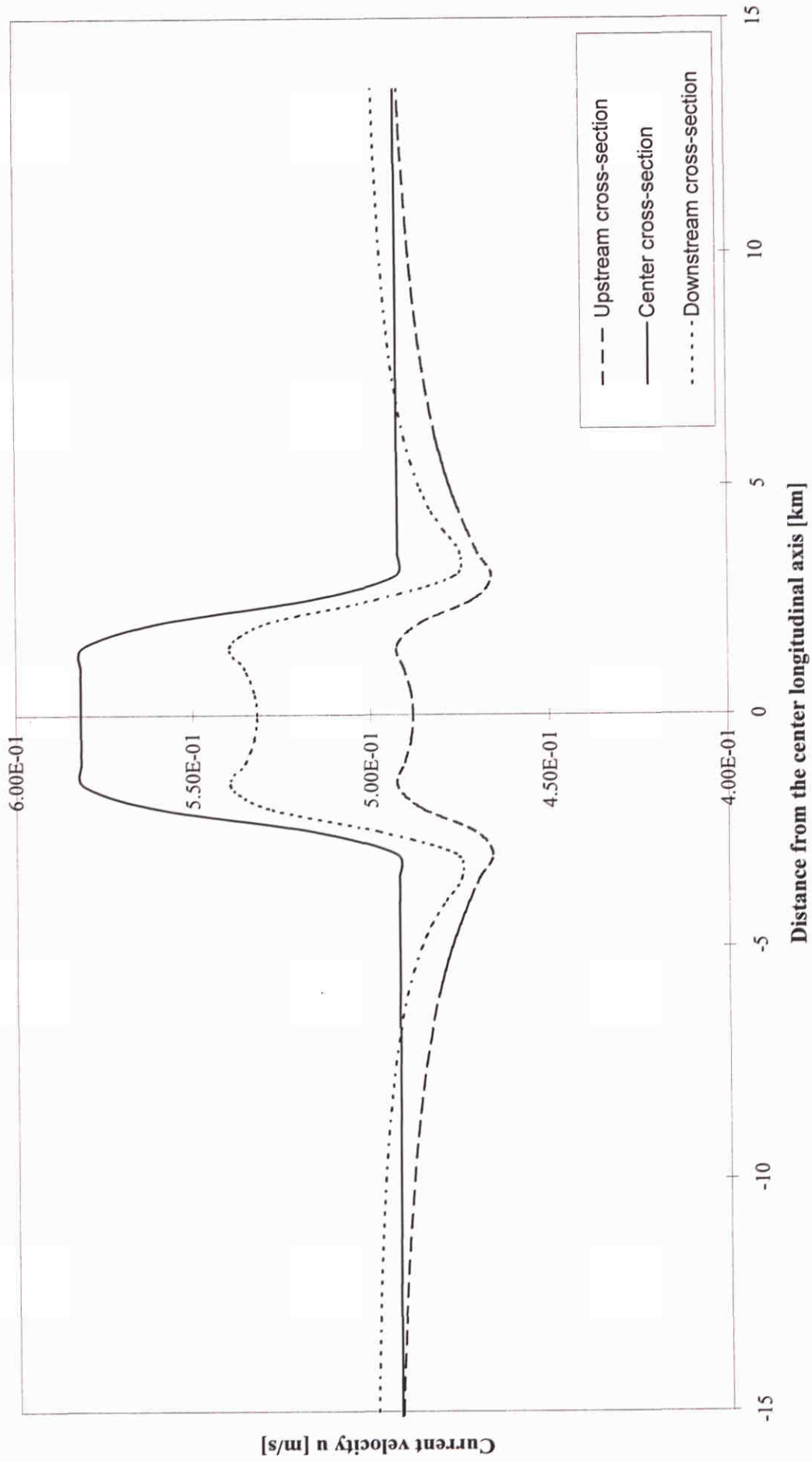
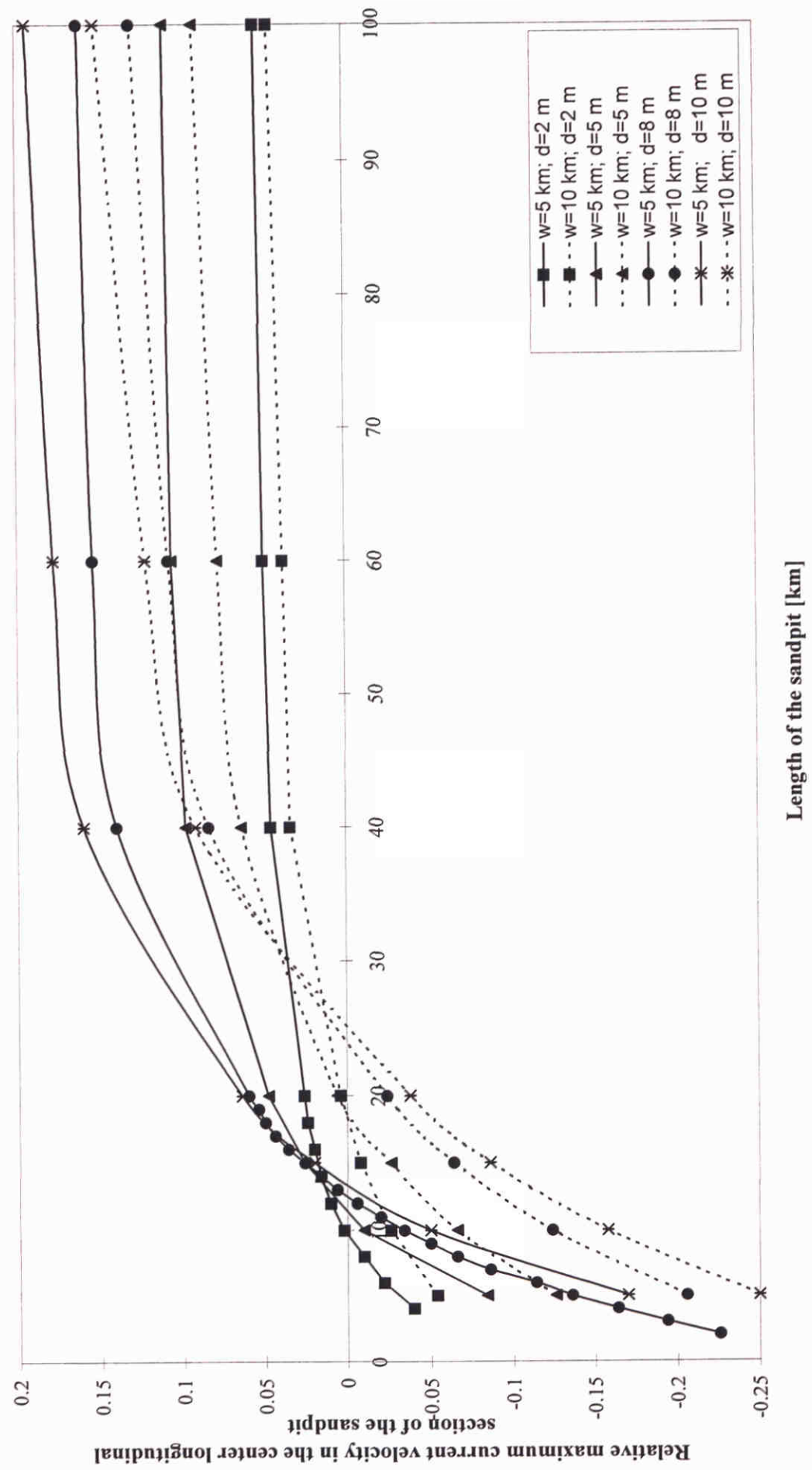


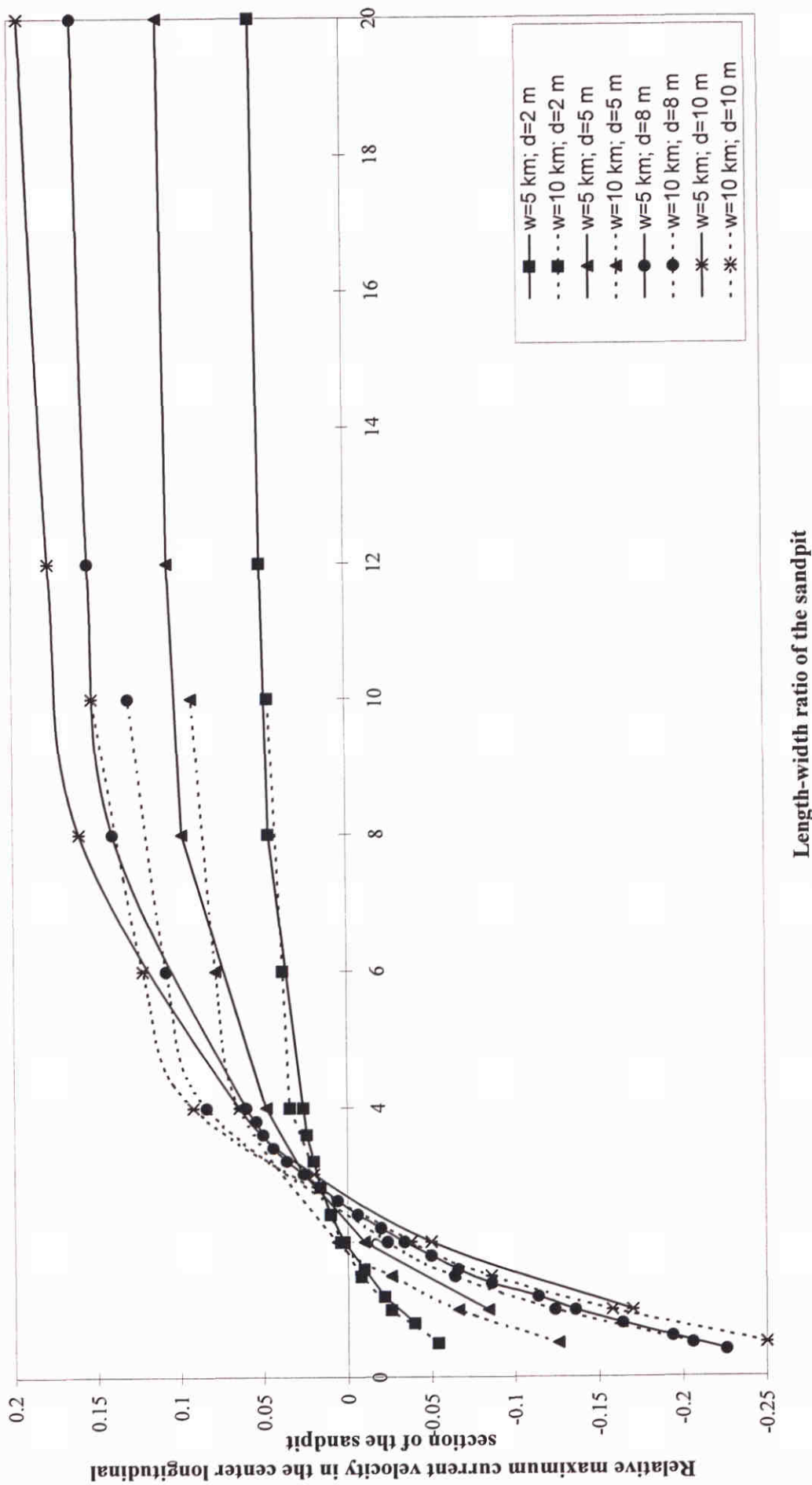
Figure 5.8: Distribution of u-velocity in three cross-sections



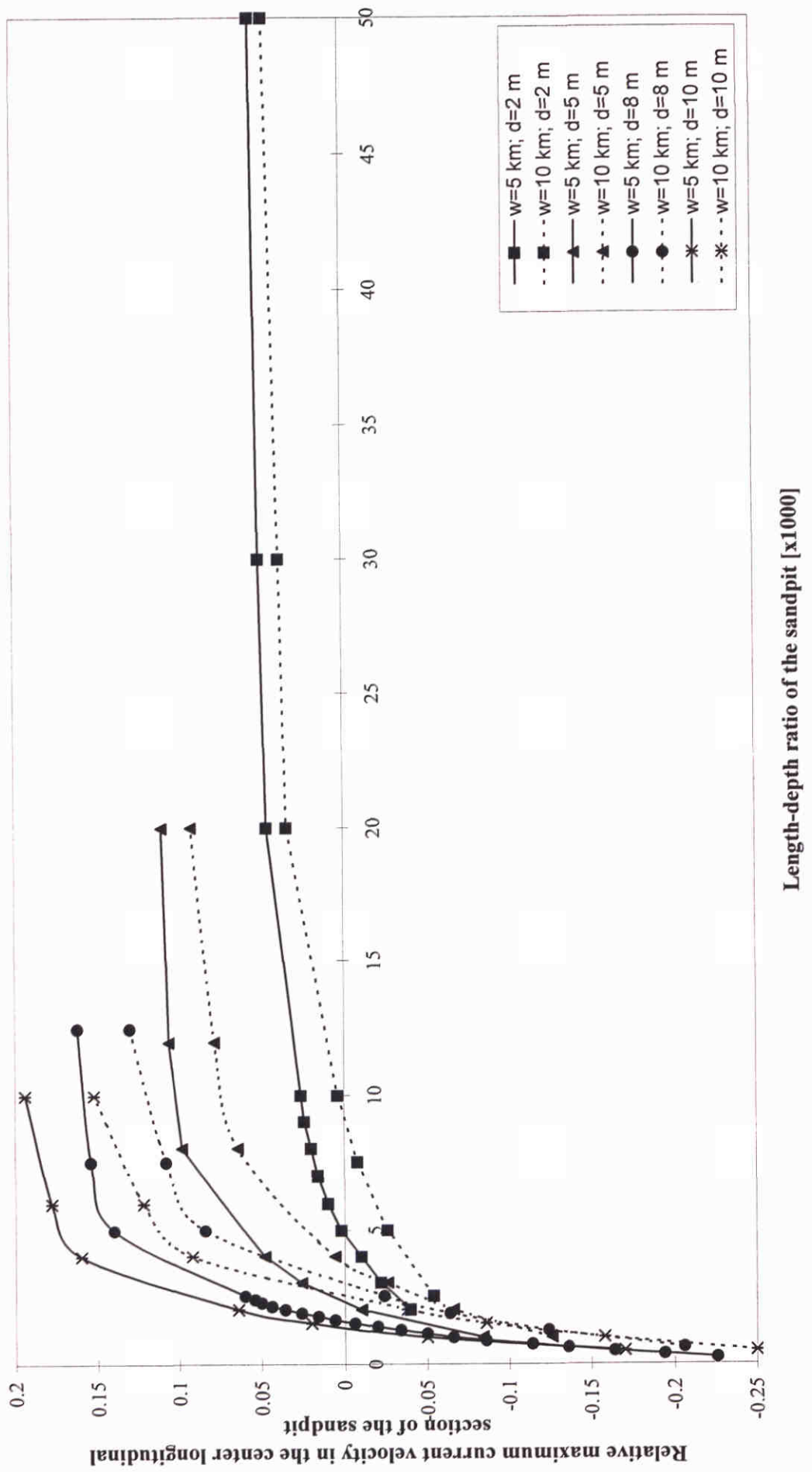
Figuur 5.9: Maximum current velocity vs. length of the sandpit

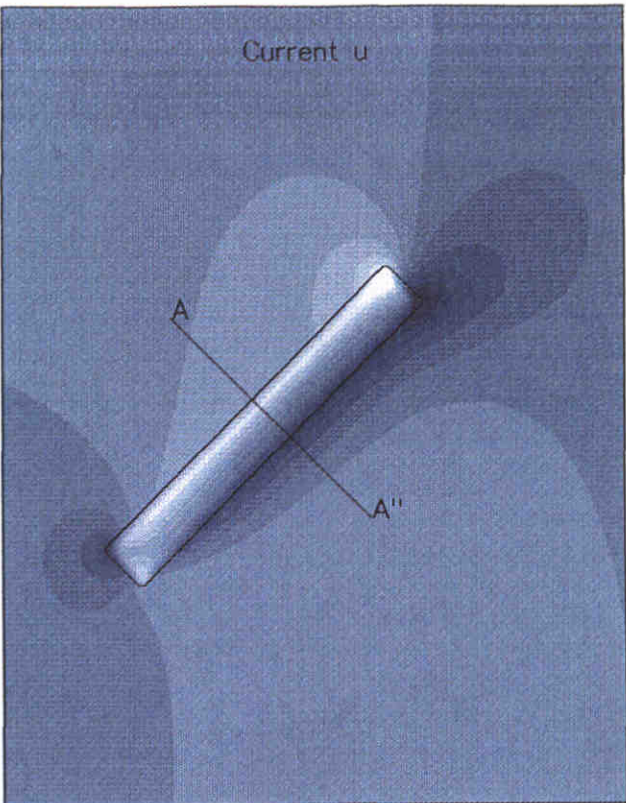


Figuur 5.10: Maximum current velocity vs. length-width ratio of the sandpit

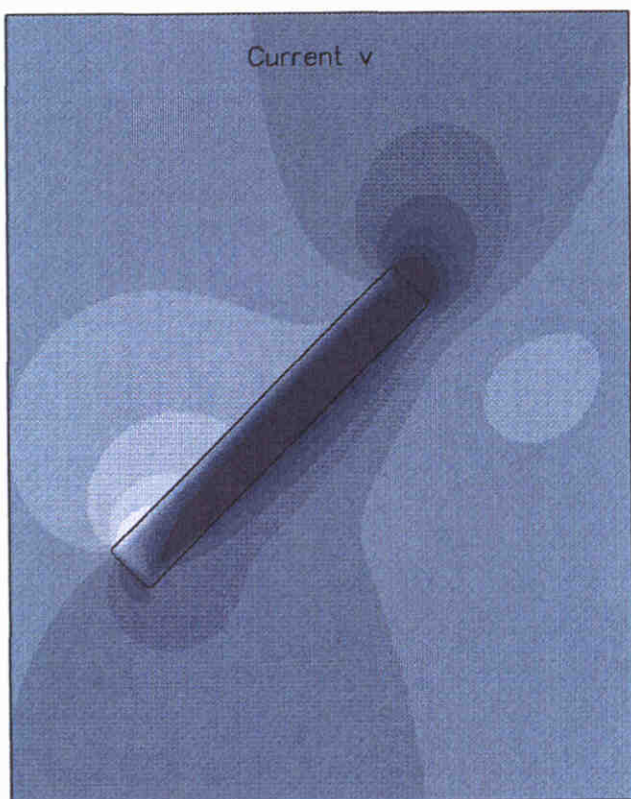
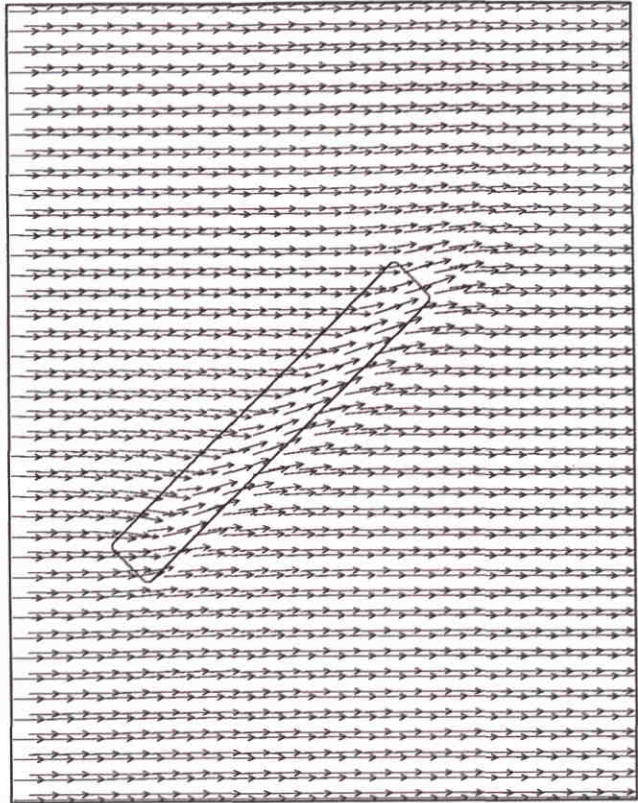


Figuur 5.11: Maximum current velocity vs. length-depth ratio of the sandpit

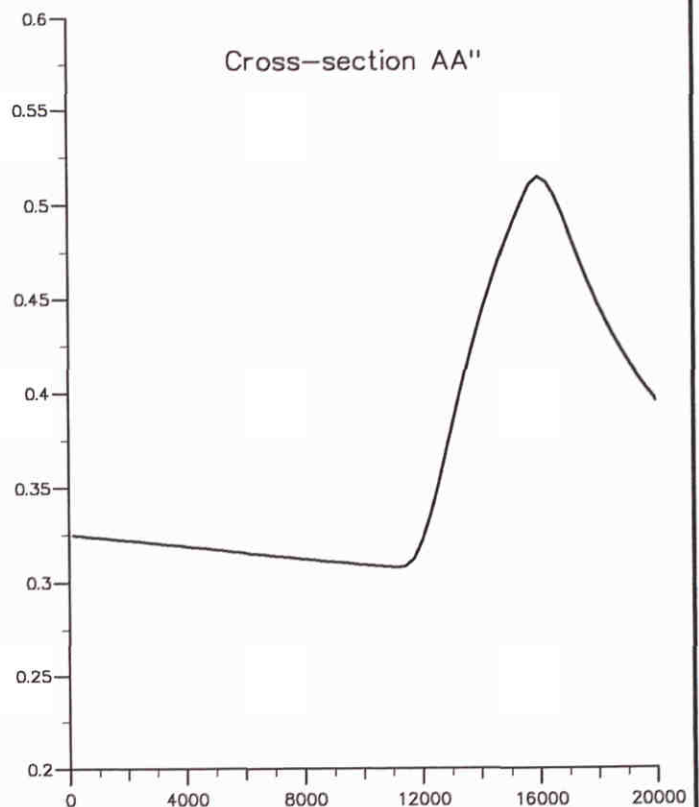




<0.40	<0.44	<0.48	<0.52	<0.56	<0.60
<0.42	<0.46	<0.50	<0.54	<0.58	>0.60



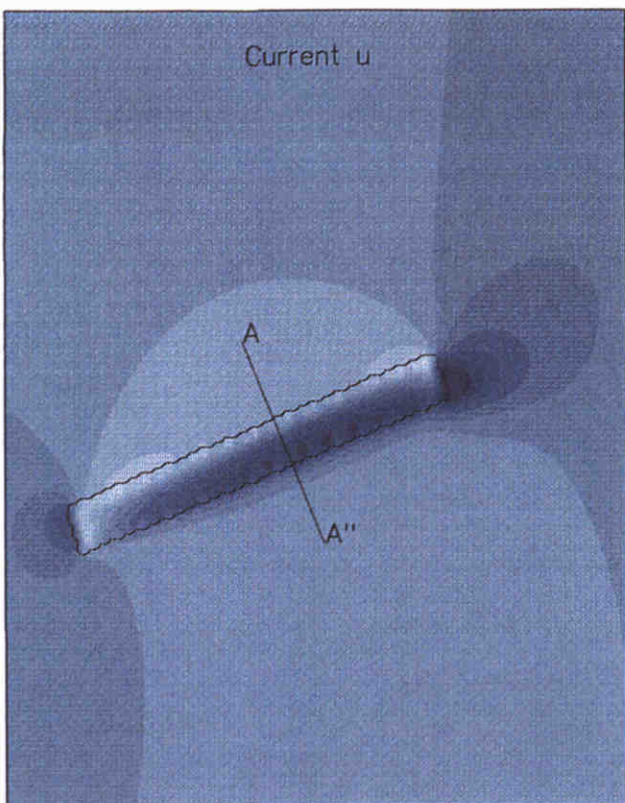
<-0.10	<-0.06	<-0.02	<0.02	<0.06	<0.10
<-0.08	<-0.04	<0.00	<0.04	<0.08	>0.10



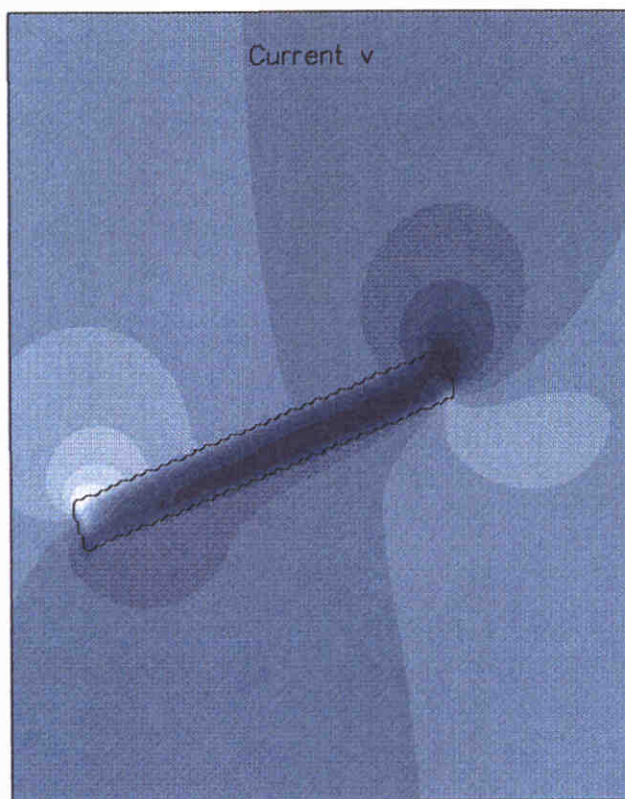
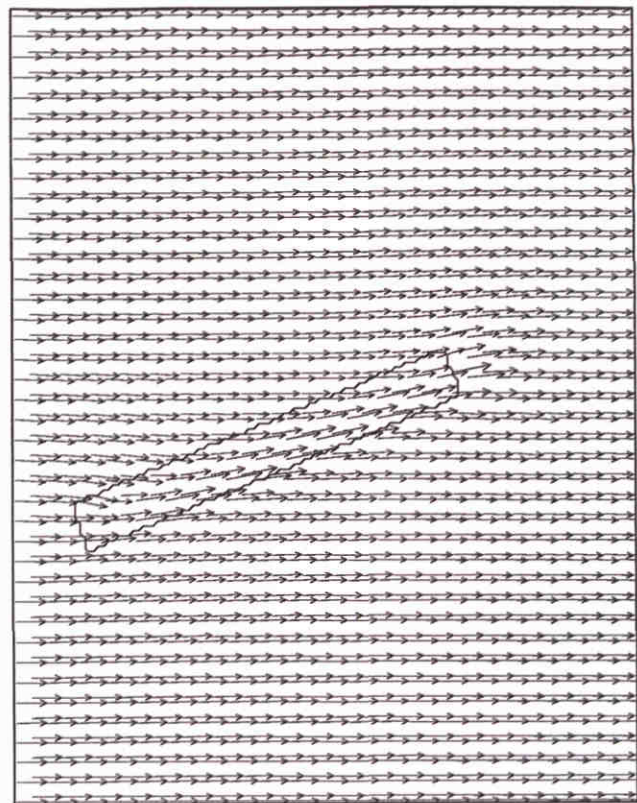
Current velocities u and v [m/s]

Stationary current pattern and current velocities in cross-section AA''

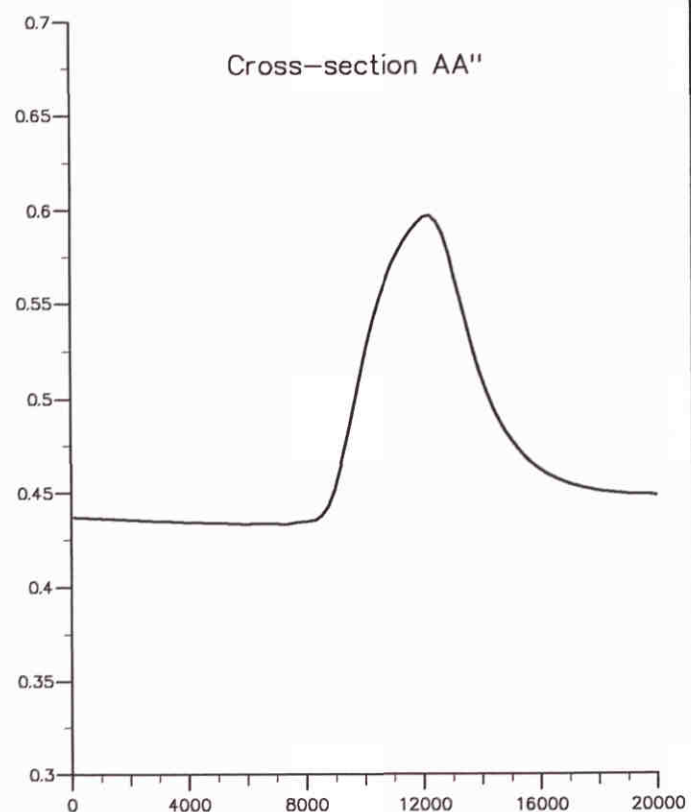
Stationary boundary conditions including Coriolis



<-0.40	<0.44	<0.48	<0.52	<0.56	<0.60
<0.42	<0.46	<0.50	<0.54	<0.58	>0.60



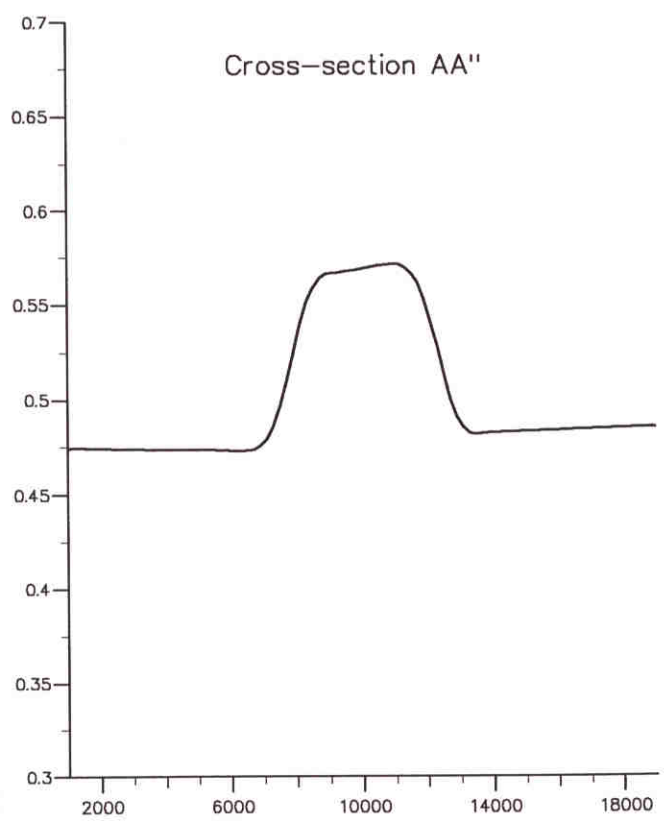
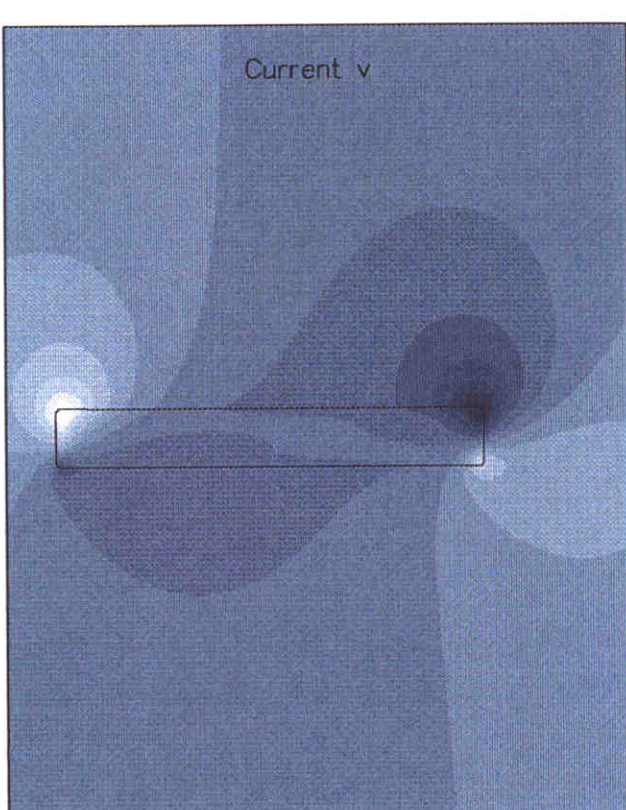
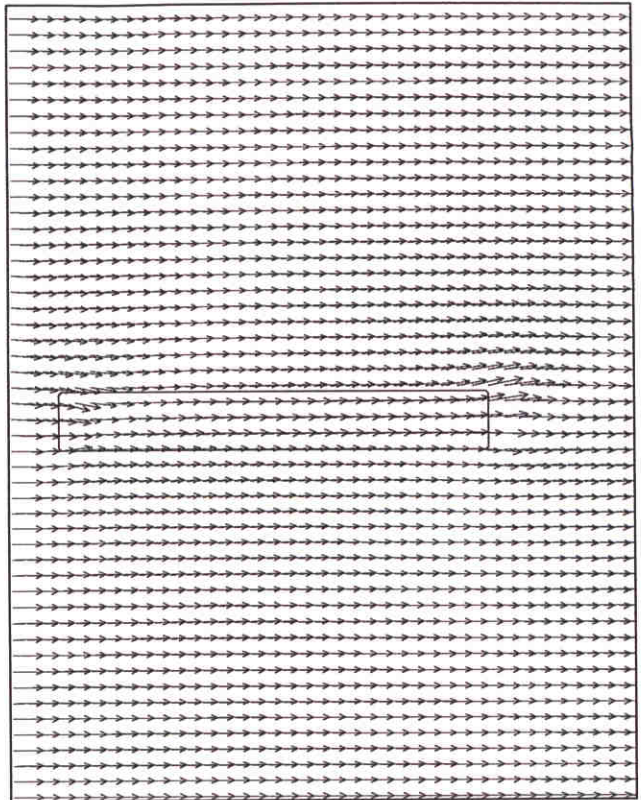
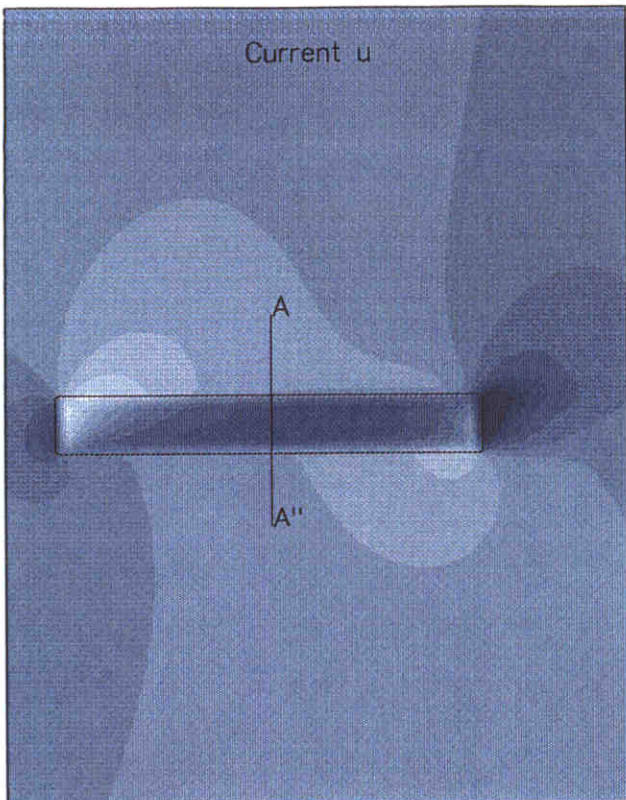
<-0.10	<-0.06	<-0.02	<0.02	<0.06	<0.10
<-0.08	<-0.04	<0.00	<0.04	<0.08	>0.10



Current velocities u and v [m/s]

Stationary current pattern and current velocities in cross-section AA''

Stationary boundary conditions including Coriolis

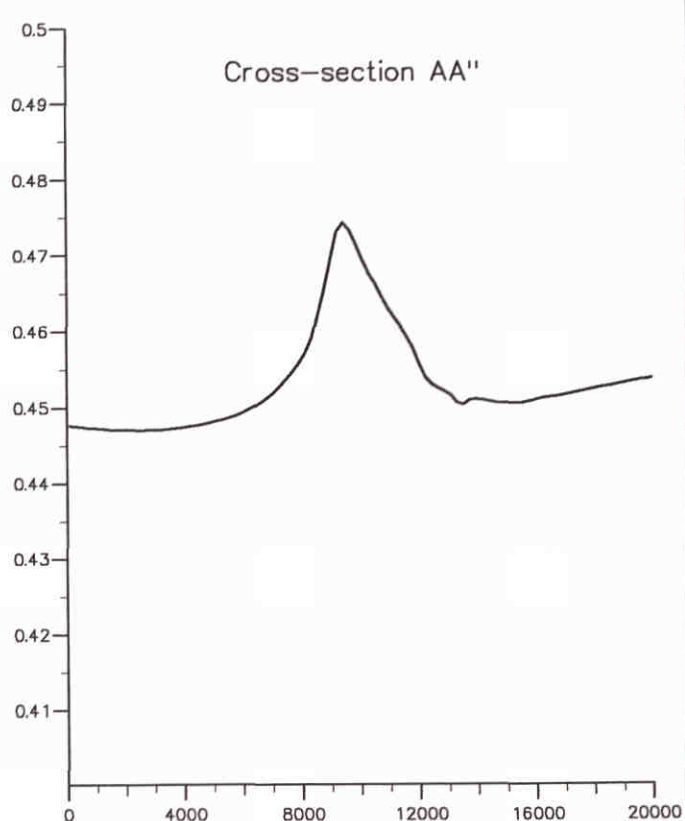
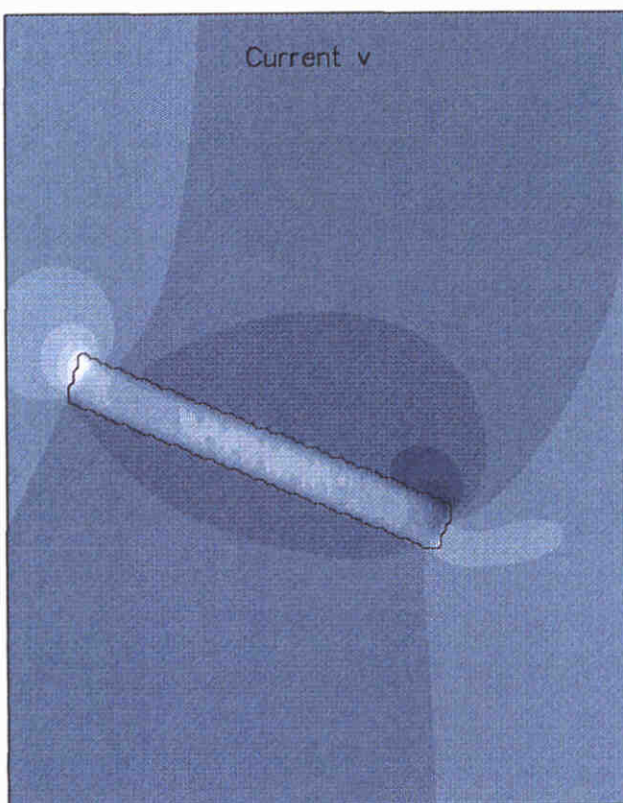
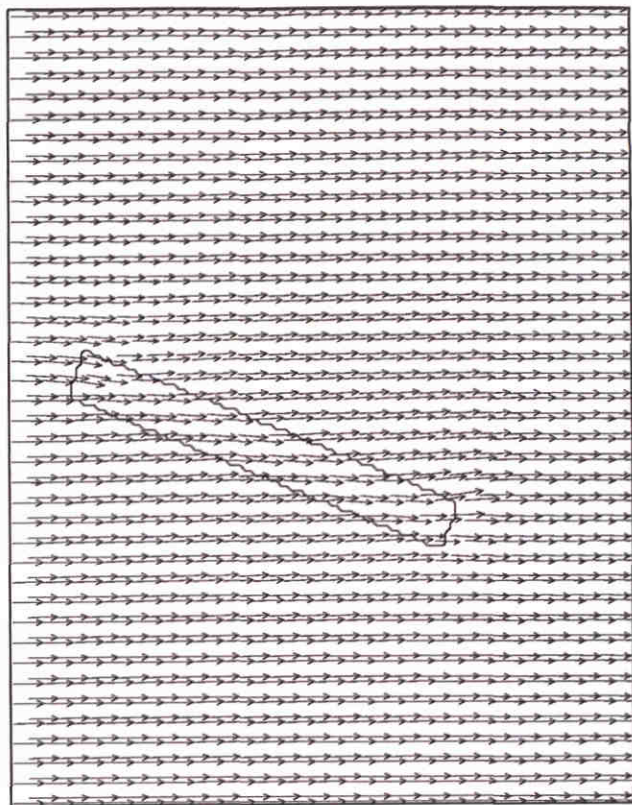
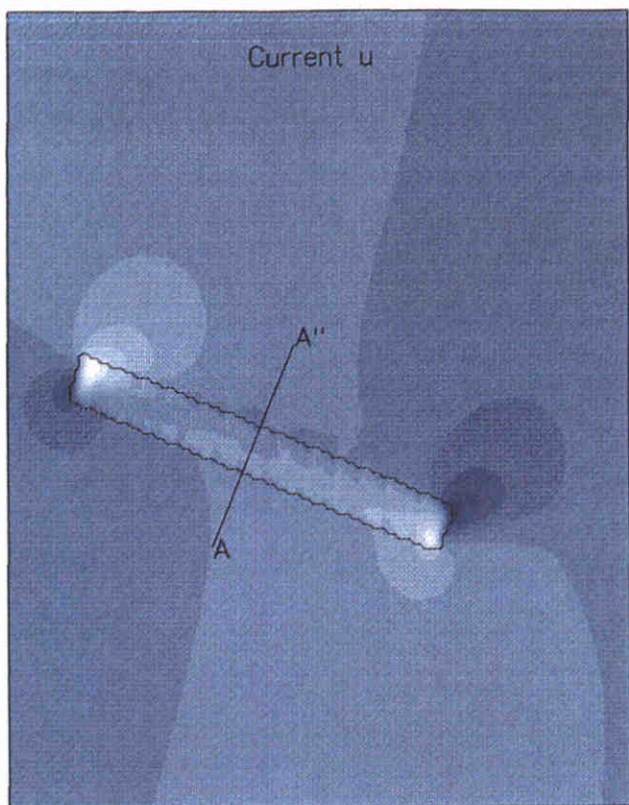


<-0.10	<-0.06	<-0.02	<0.02	<0.06	<0.10
<-0.08	<-0.04	<0.00	<0.04	<0.08	>0.10

Current velocities u and v [m/s]

Stationary current pattern and current velocities in cross-section AA''

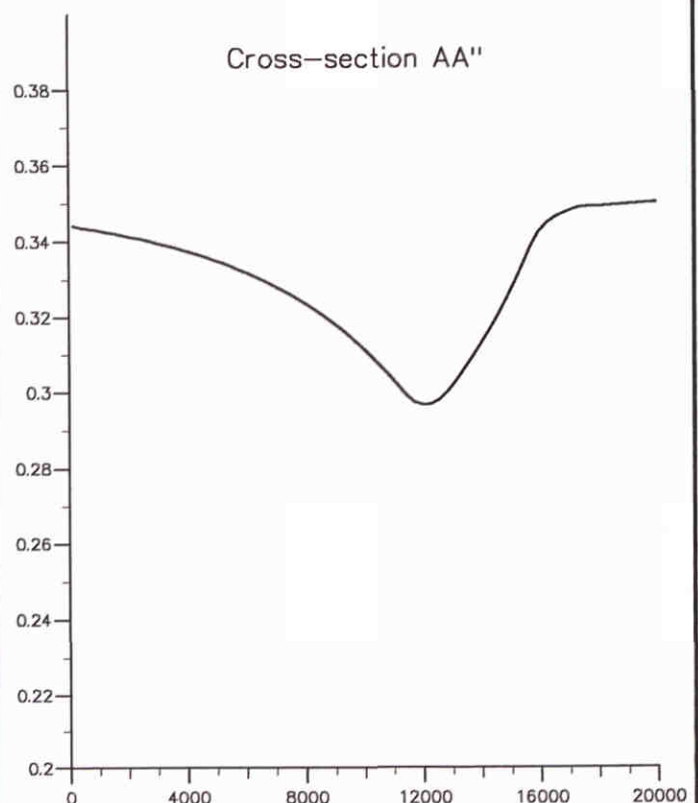
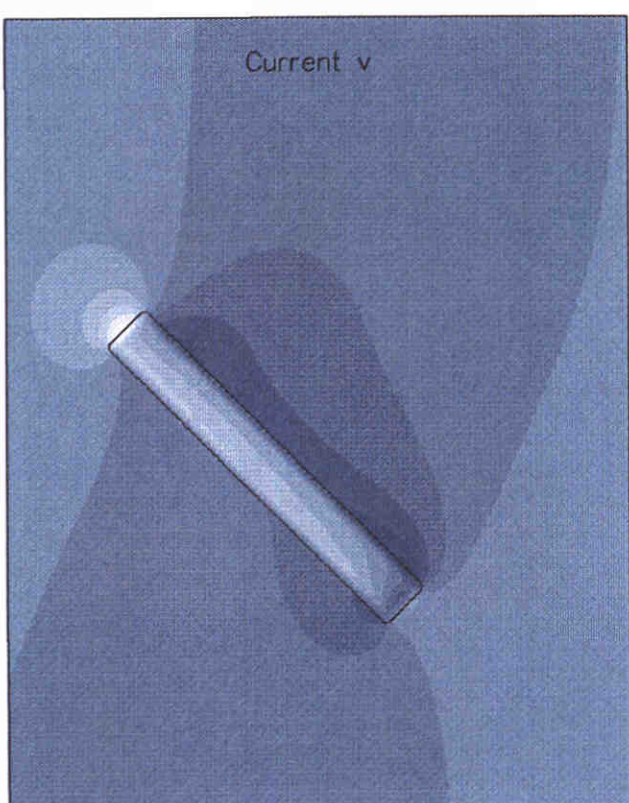
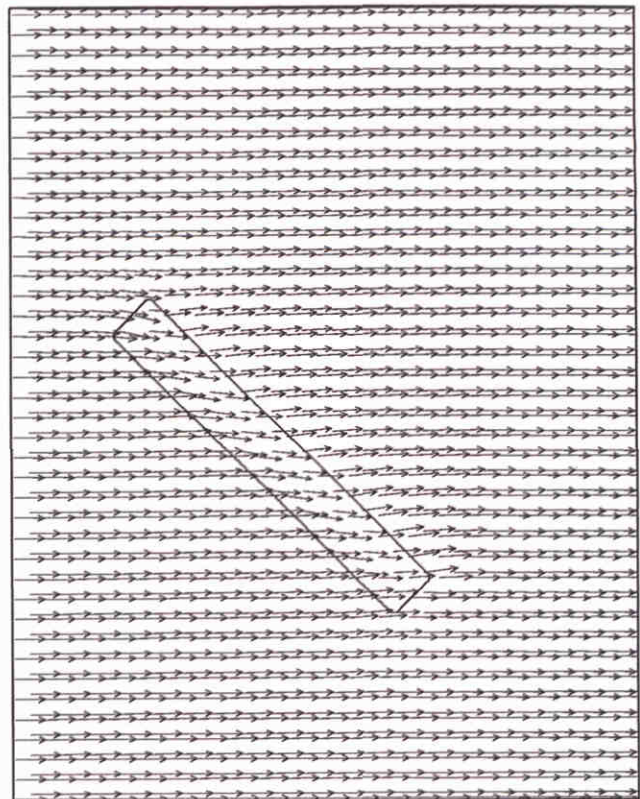
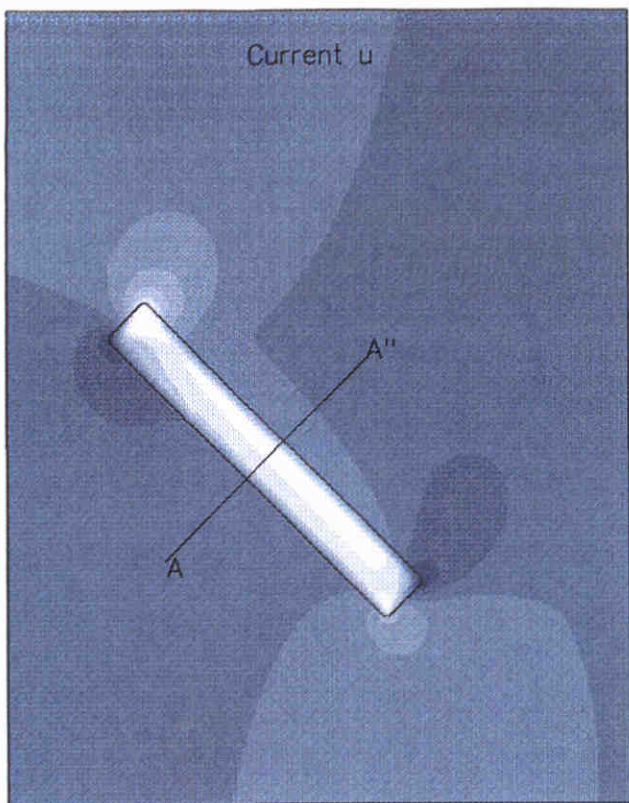
Stationary boundary conditions including Coriolis



Current velocities u and v [m/s]

Stationary current pattern and current velocities in cross-section AA''

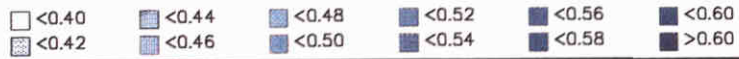
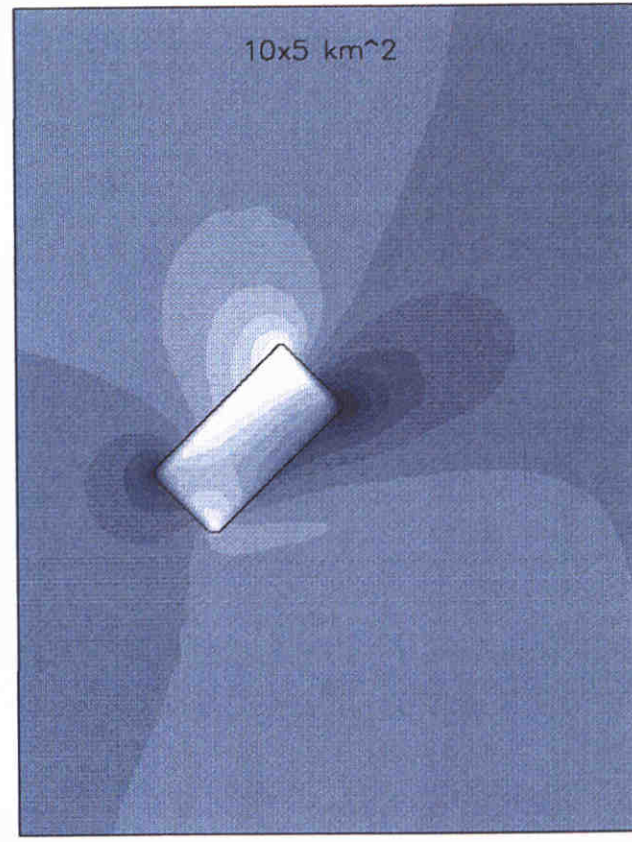
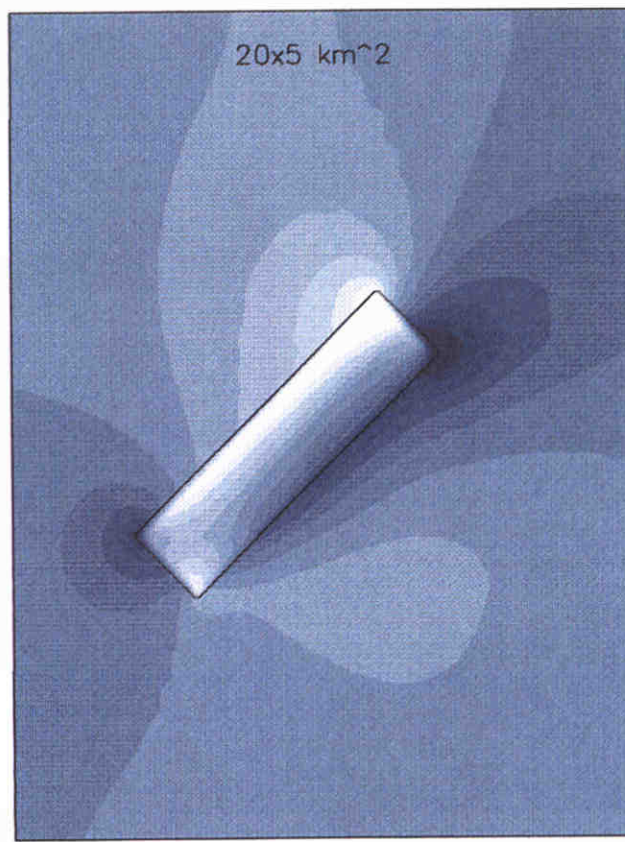
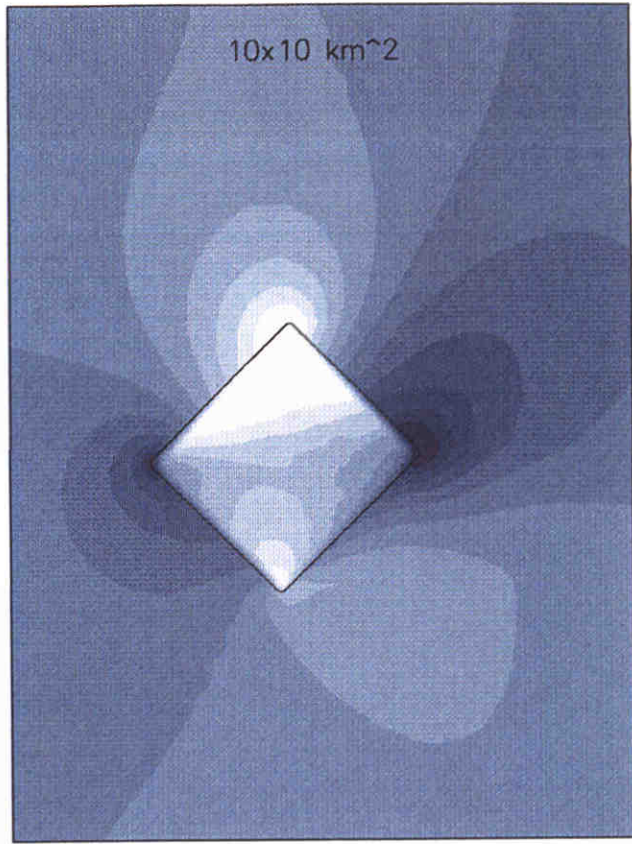
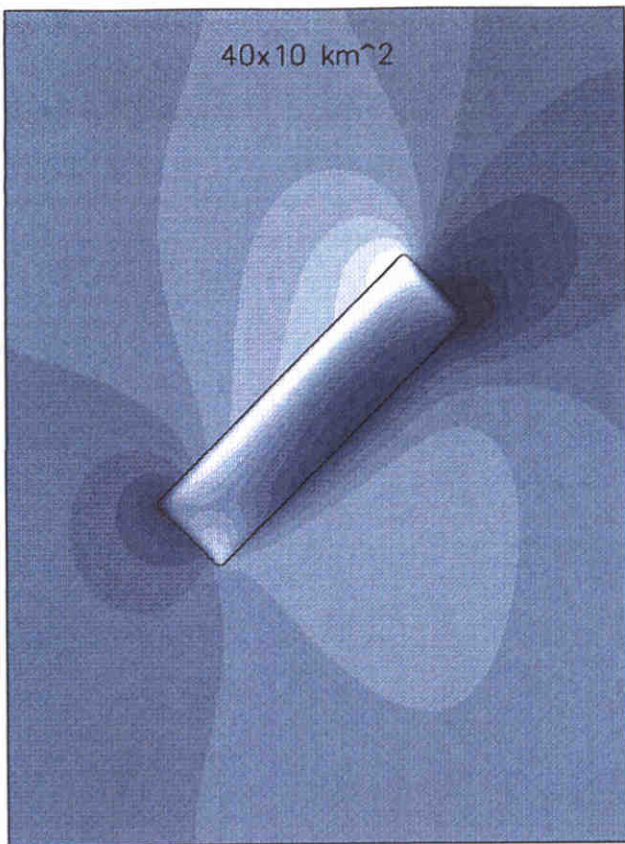
Stationary boundary conditions including Coriolis



Current velocities u and v [m/s]

Stationary current pattern and current velocities in cross-section AA''

Stationary boundary conditions including Coriolis



Current magnitude [m/s]

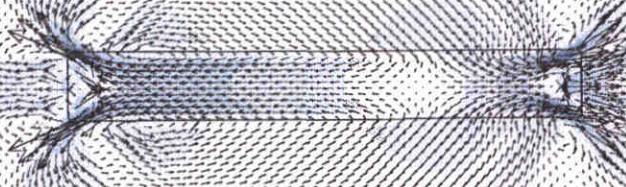
Influence of the length and the width on the current pattern

Stationary boundary conditions including Coriolis

u-h boundary conditions; no phase shift



u-h boundary conditions; 1 hour phase shift

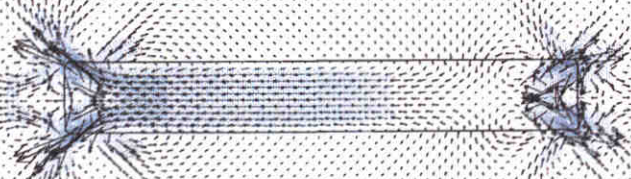


Tide-averaged current velocities [m/s]

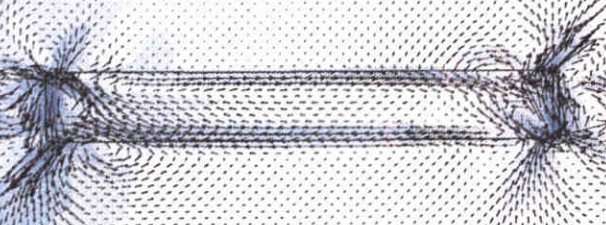
Influence of the boundary conditions on the tide-averaged current pattern

Tidal boundary conditions

$u-u$ boundary conditions; no Coriolis



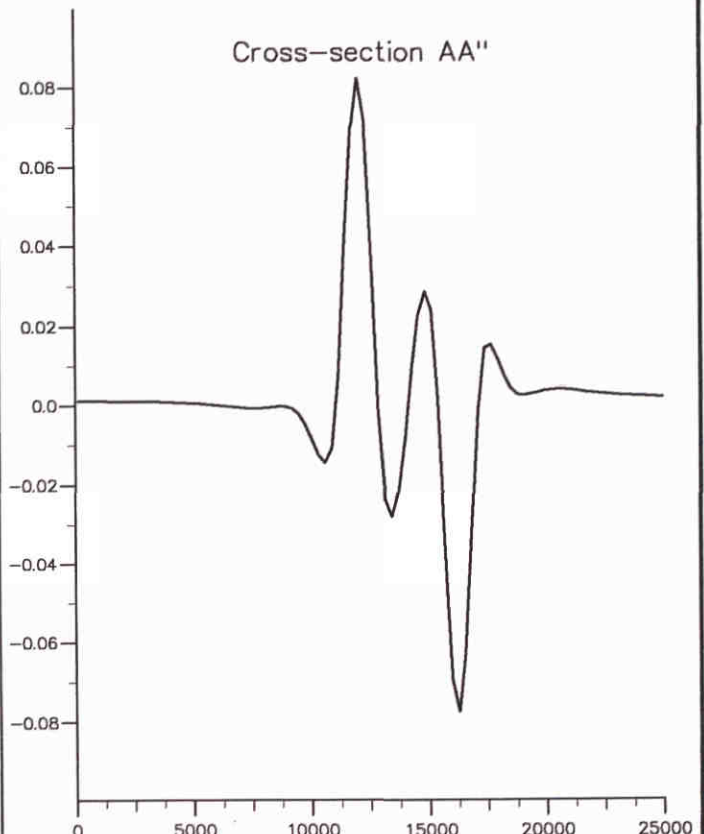
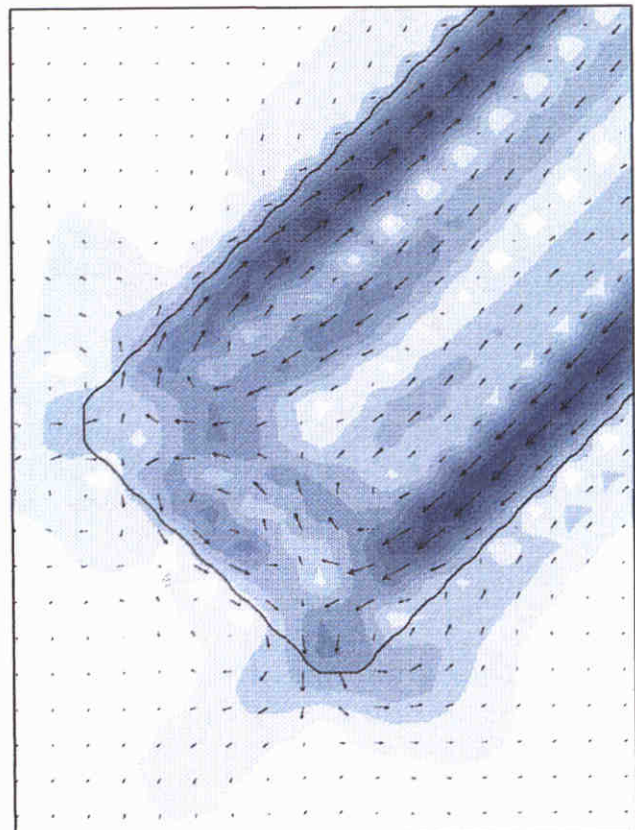
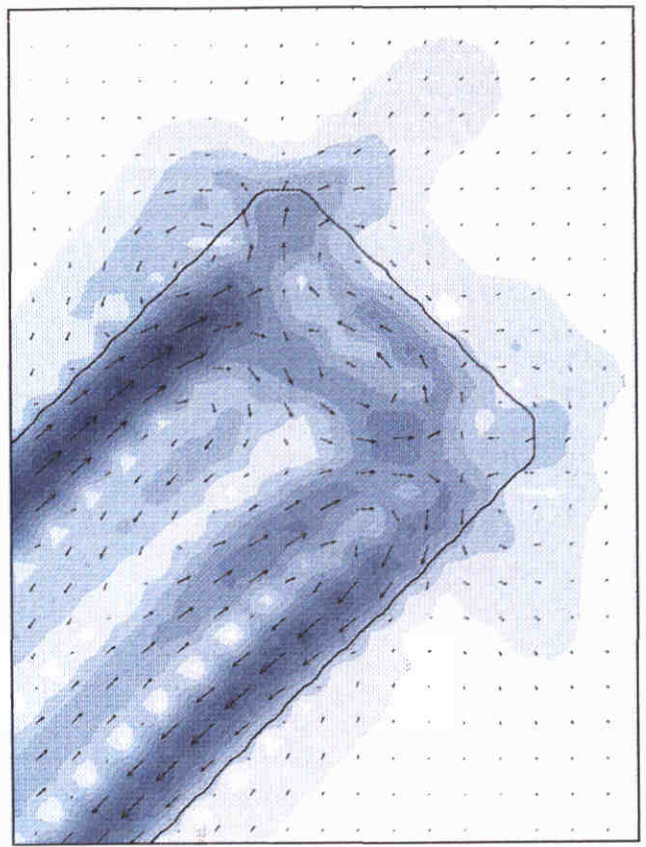
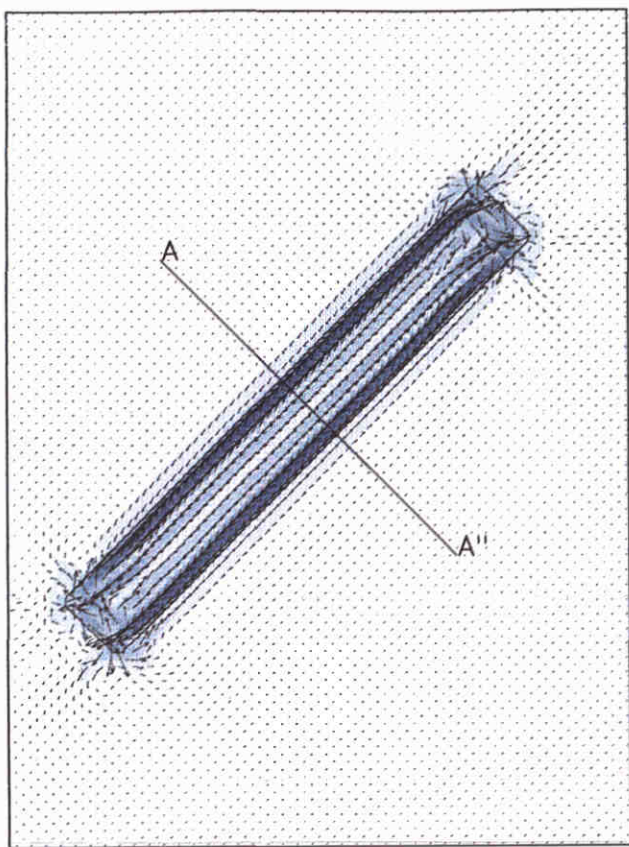
$u-u$ boundary conditions; including Coriolis



Tide-averaged current velocities [m/s]

Influence of Coriolis on the tide-averaged current pattern

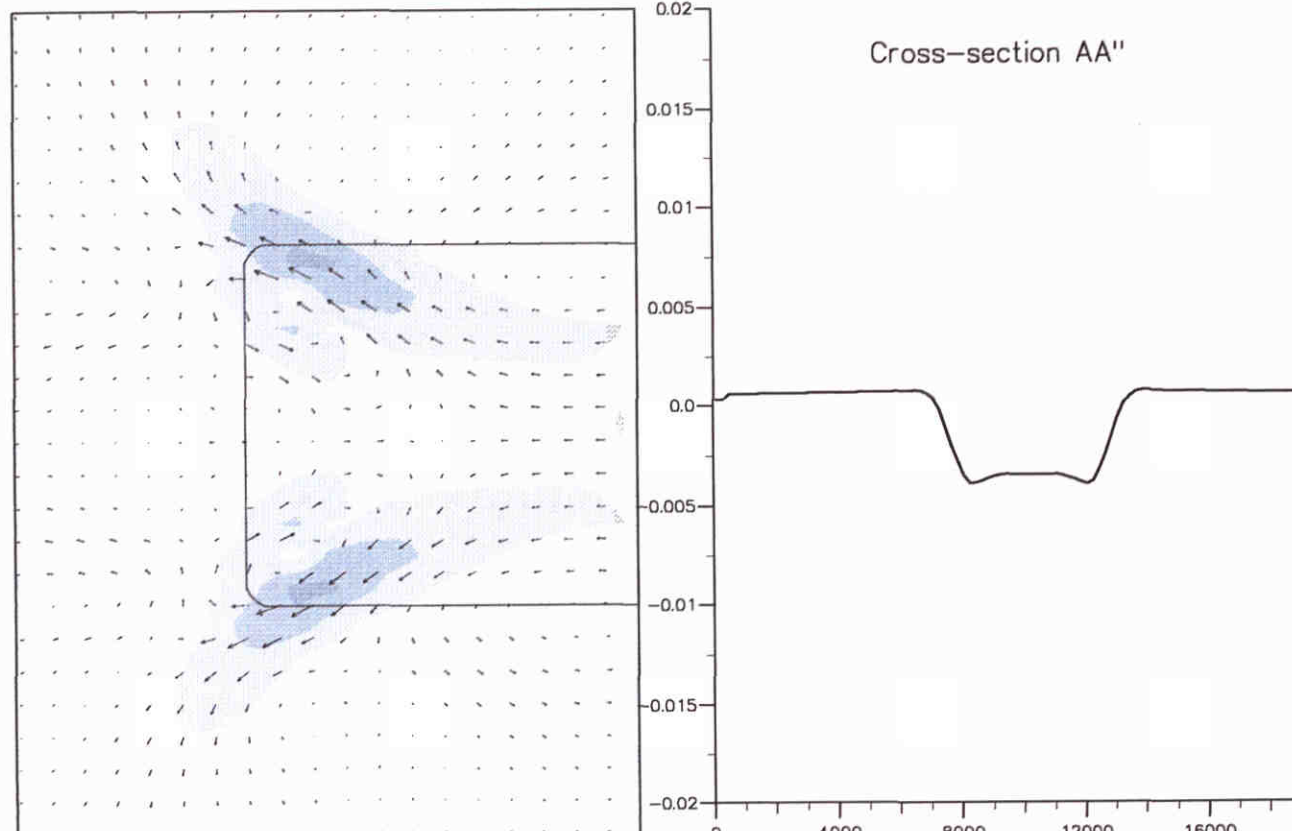
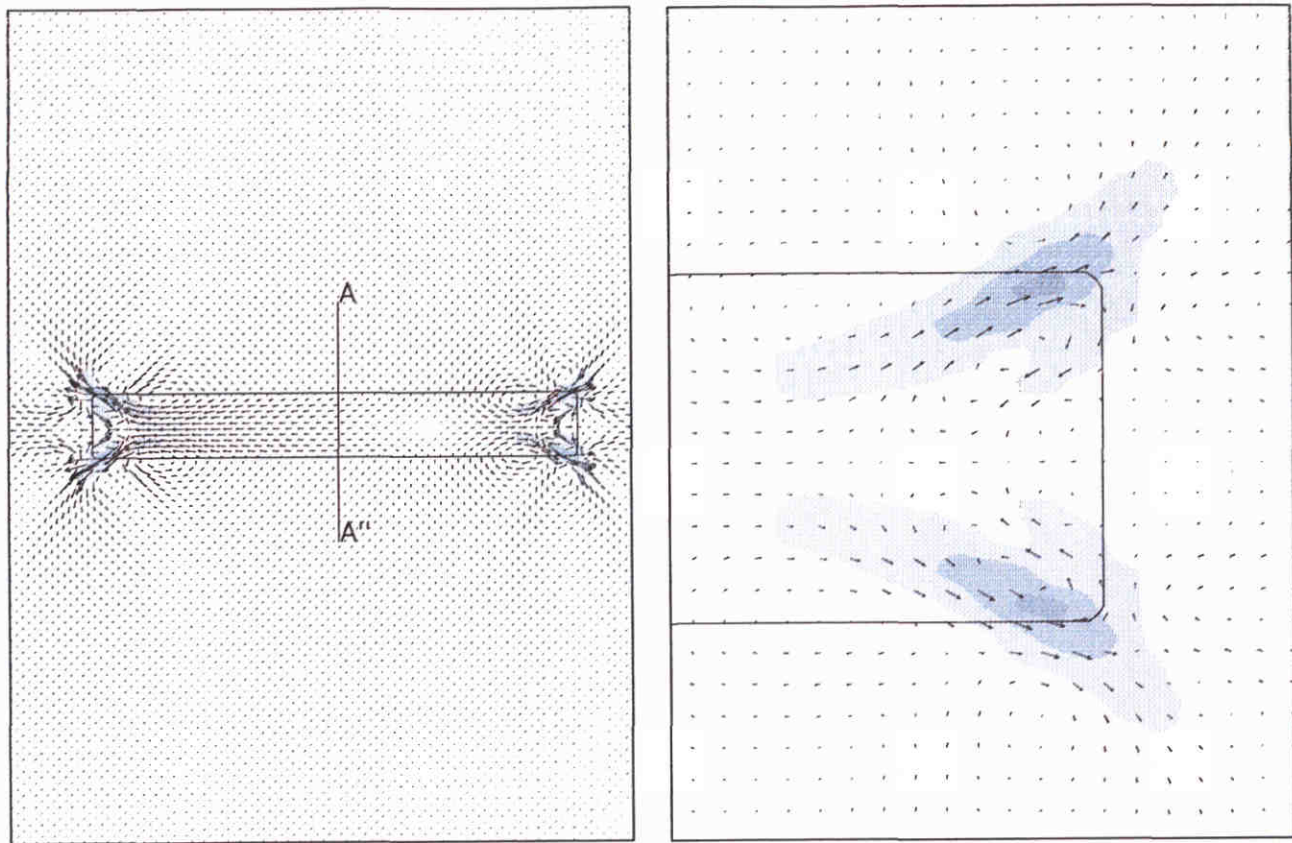
Tidal boundary conditions with and without Coriolis



Tide-averaged current velocities [m/s]

Tide-averaged current pattern and tide-averaged velocities in cross-section AA''

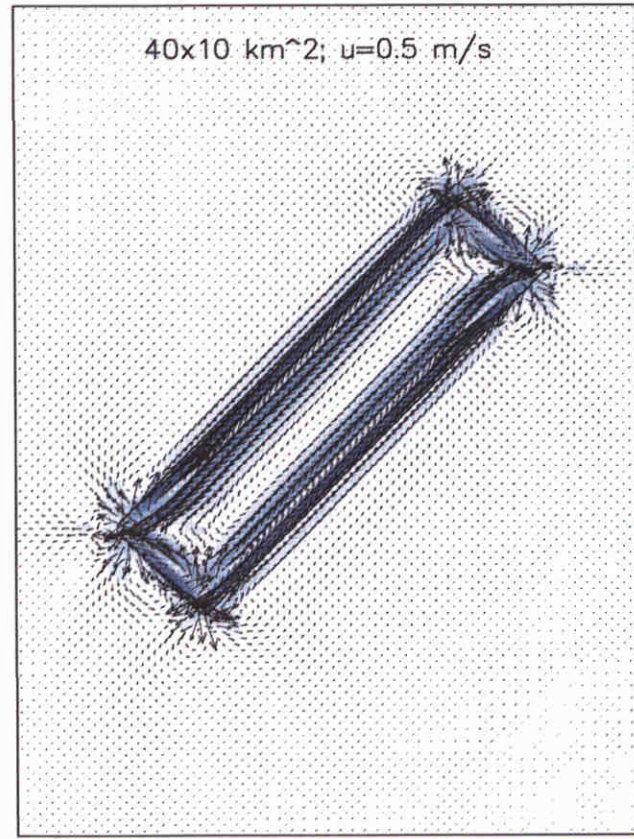
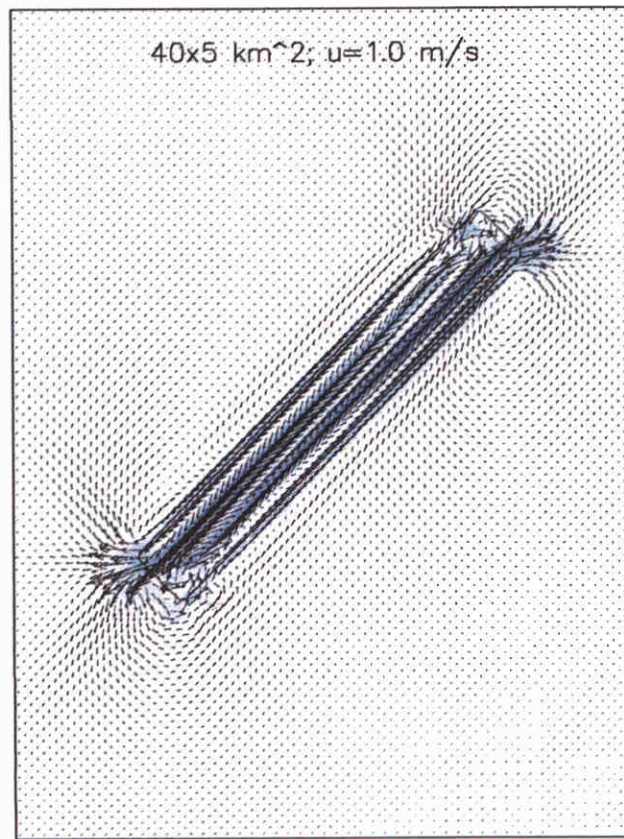
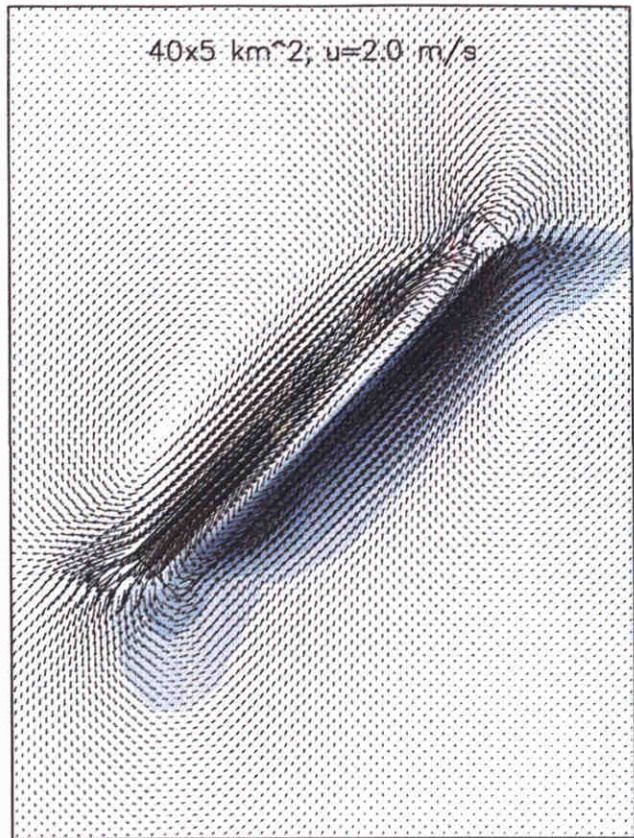
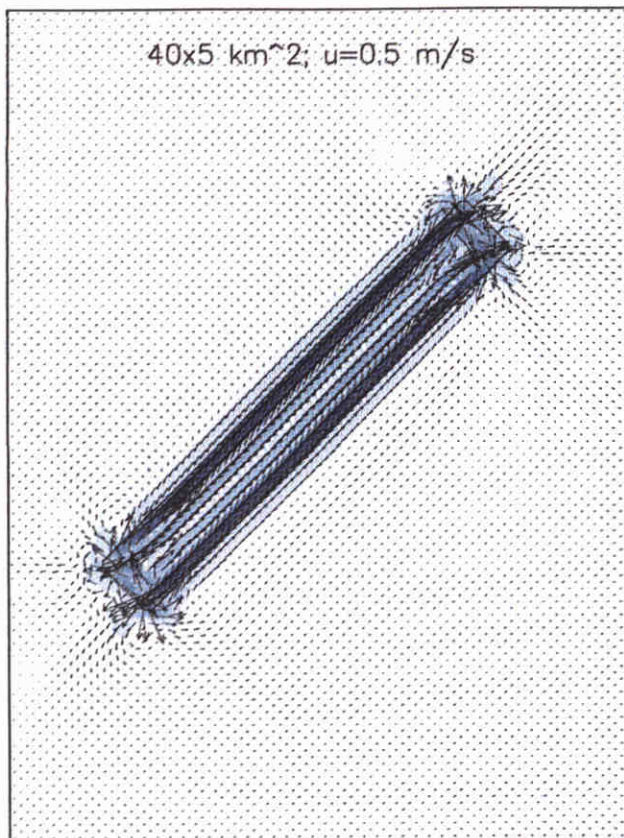
Tidal boundary conditions



Tide-averaged current velocities

Tide-averaged current pattern and tide-averaged velocities in cross-section AA''

Tidal boundary conditions

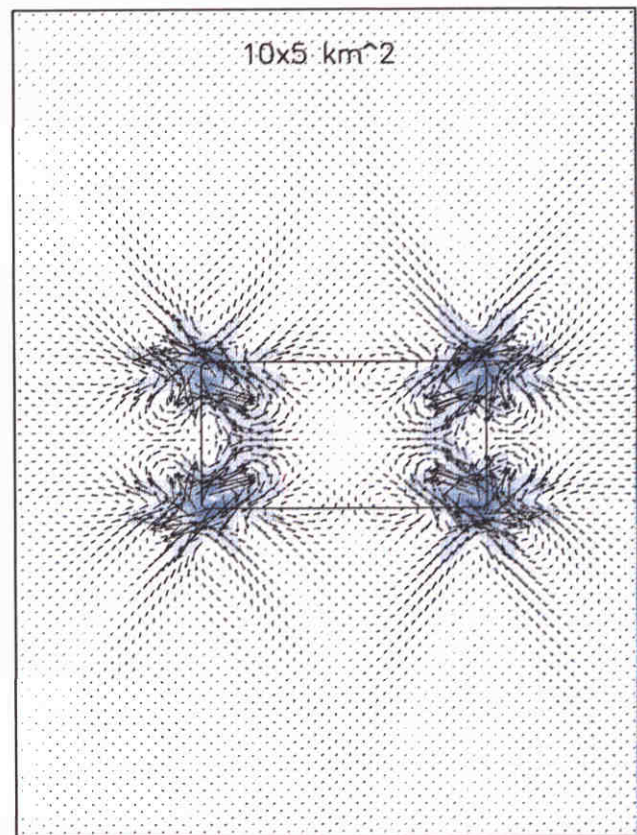
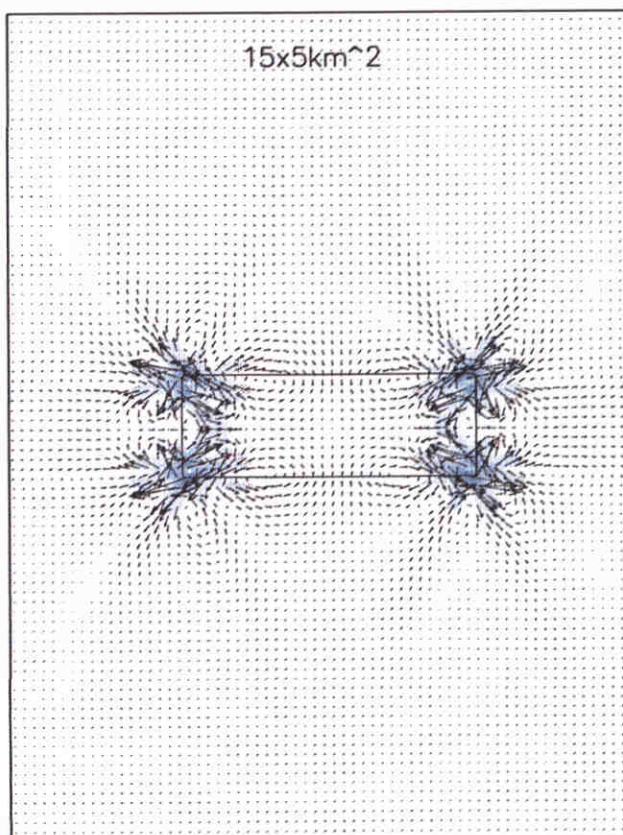
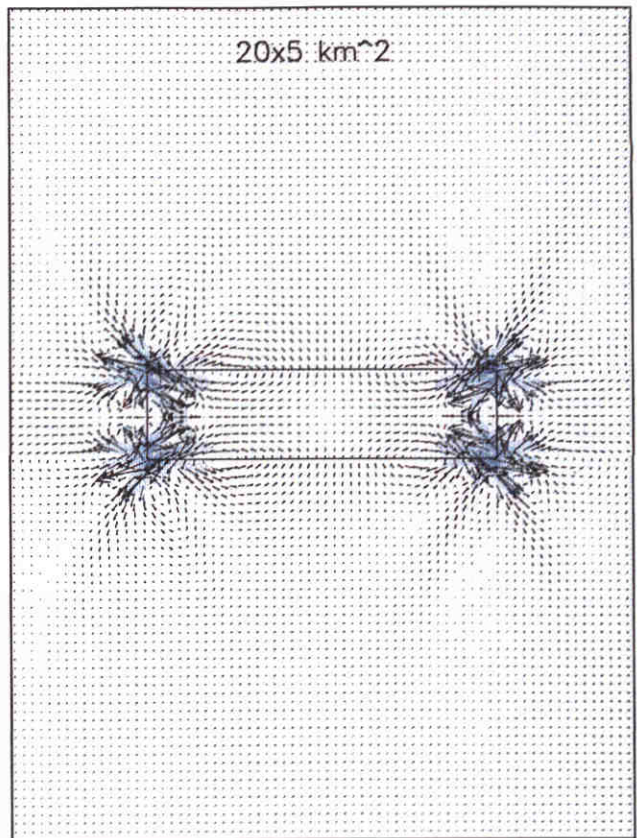
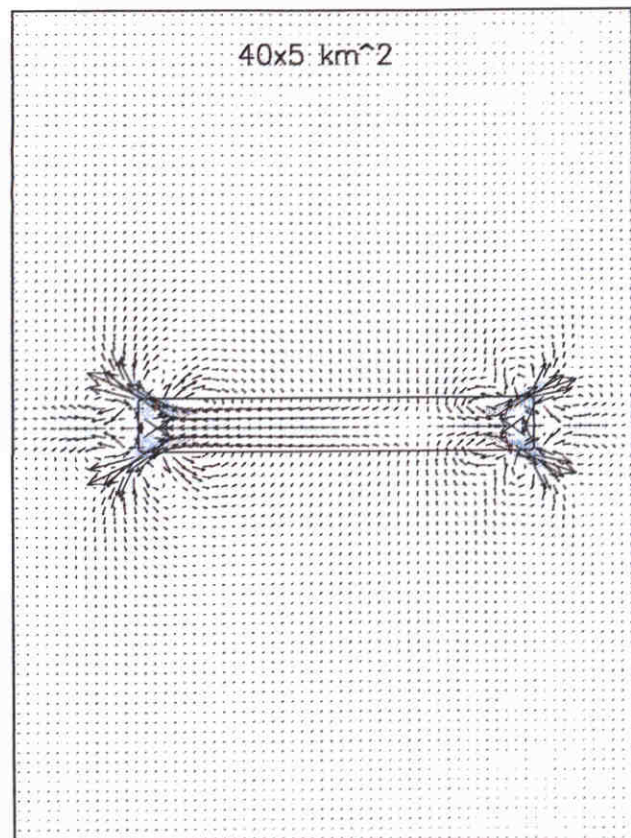


<0.01	<0.03	<0.05	<0.07	<0.09	>0.10
<0.02	<0.04	<0.06	<0.08	<0.10	$\rightarrow 0.050\text{m/s}$

Tide-averaged current velocities [m/s]

Influence of the tidal amplitude and the width on the tide-averaged current pattern

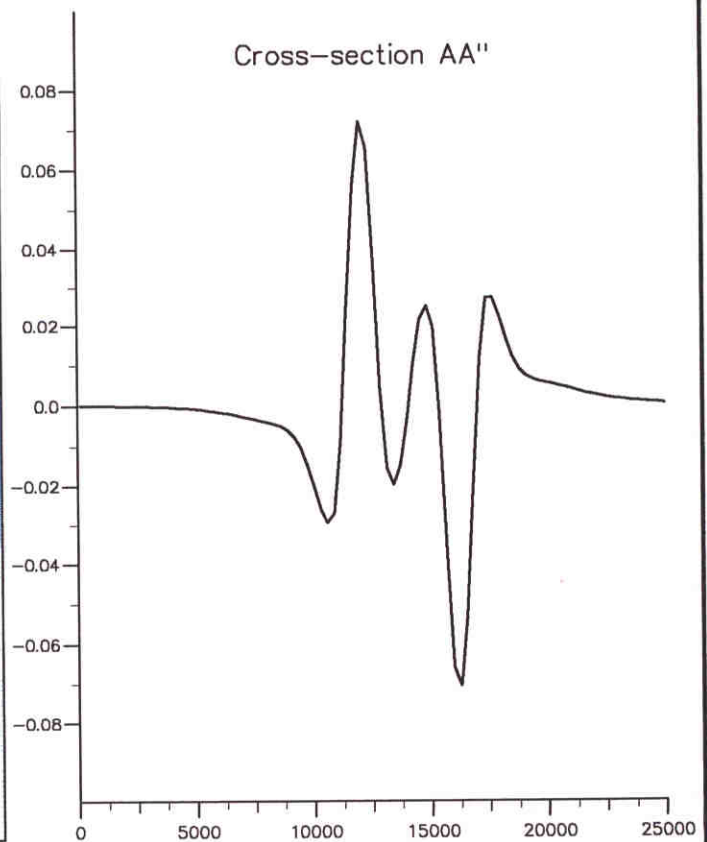
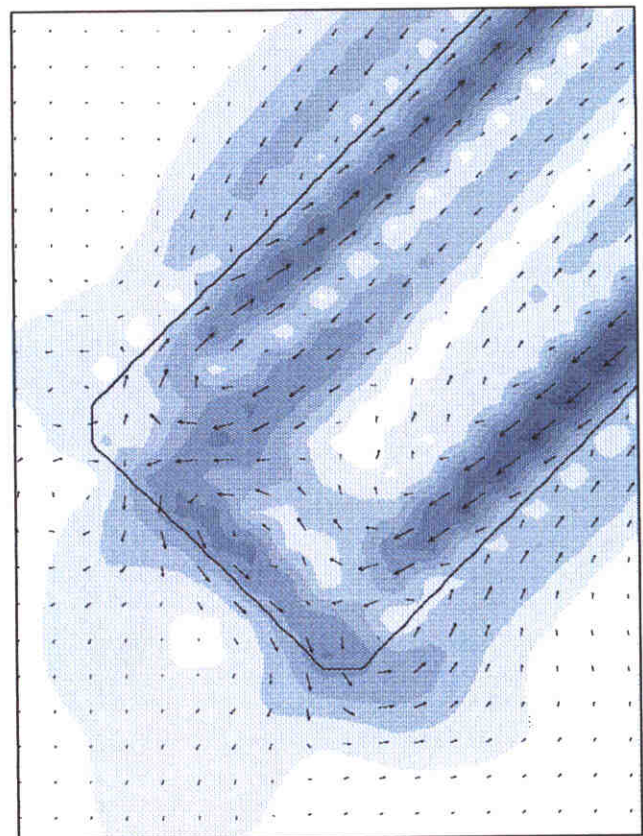
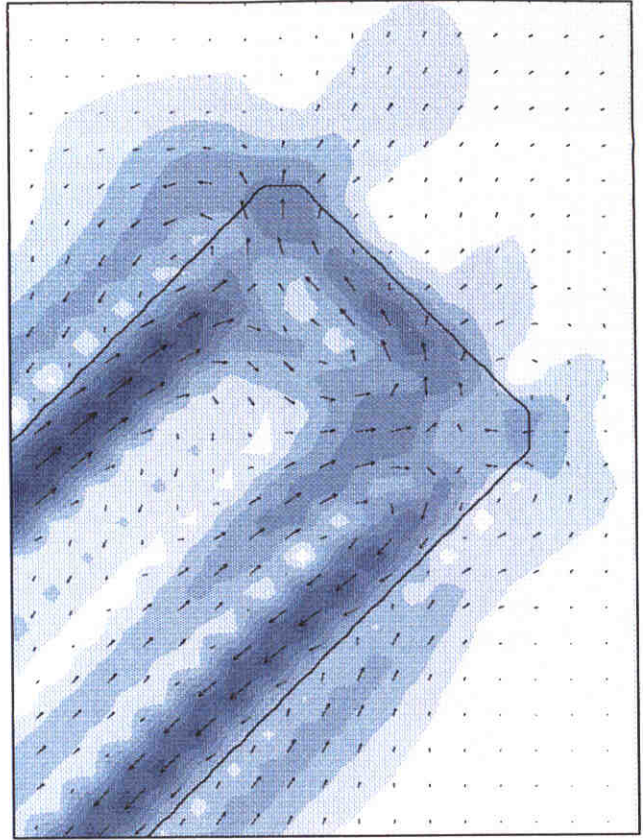
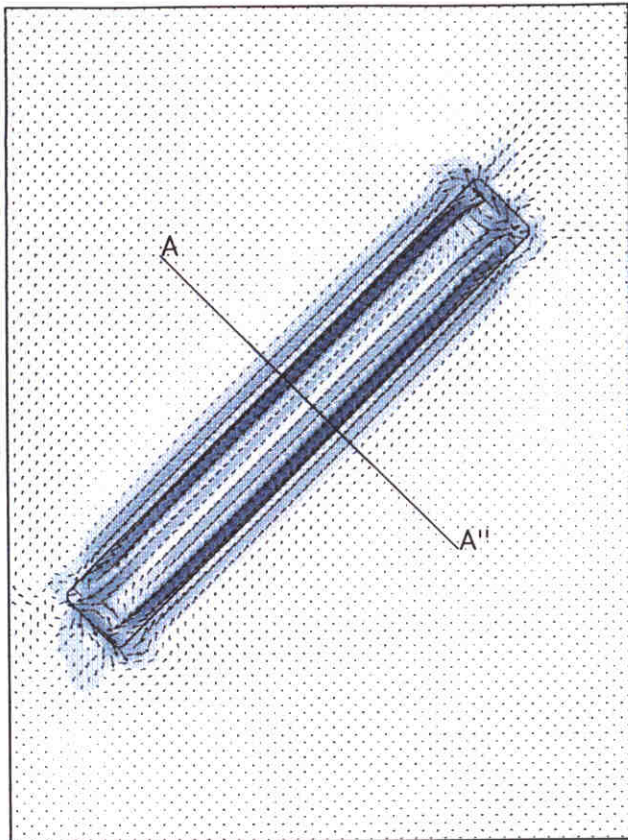
Tidal boundary conditions



Tide-averaged current velocities [m/s]

Influence of the length on the tide-averaged current pattern

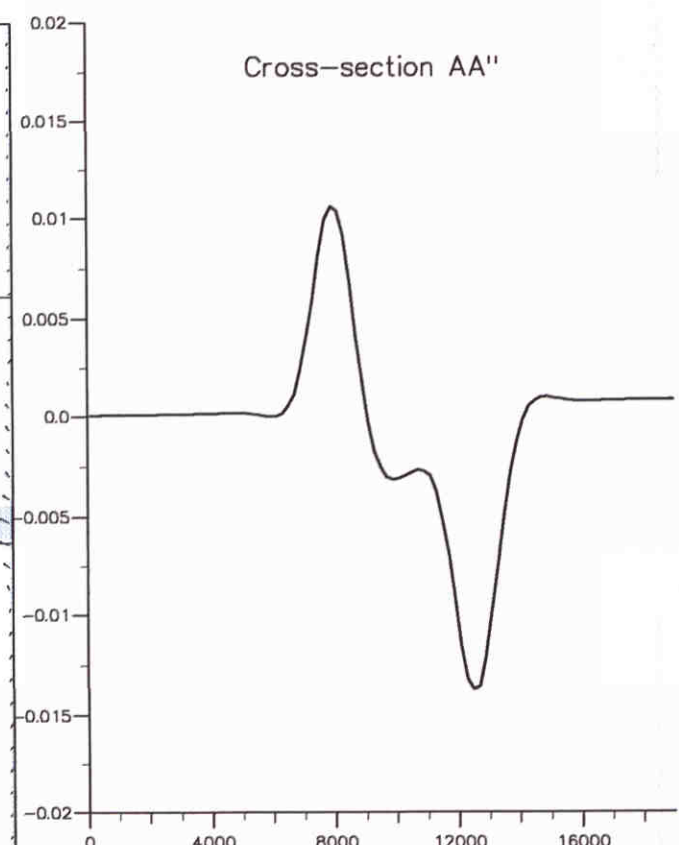
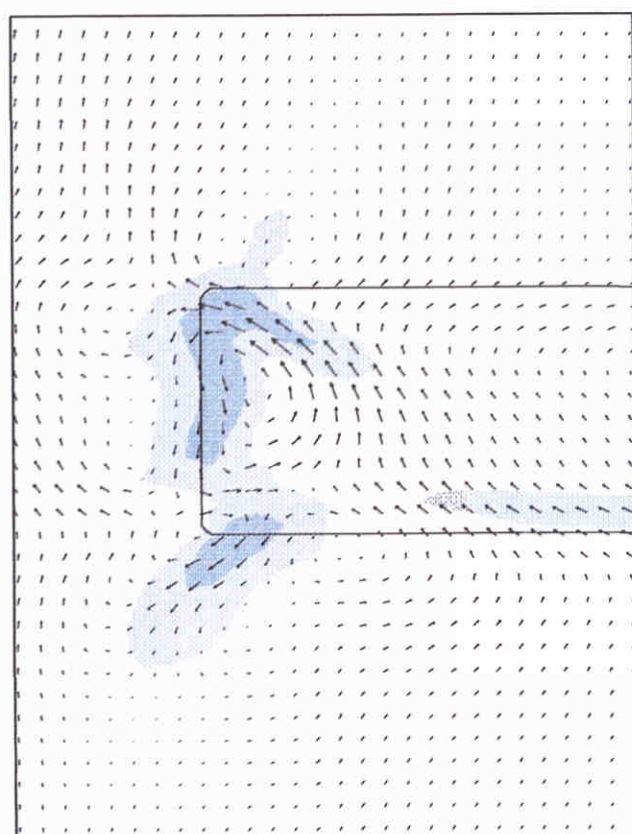
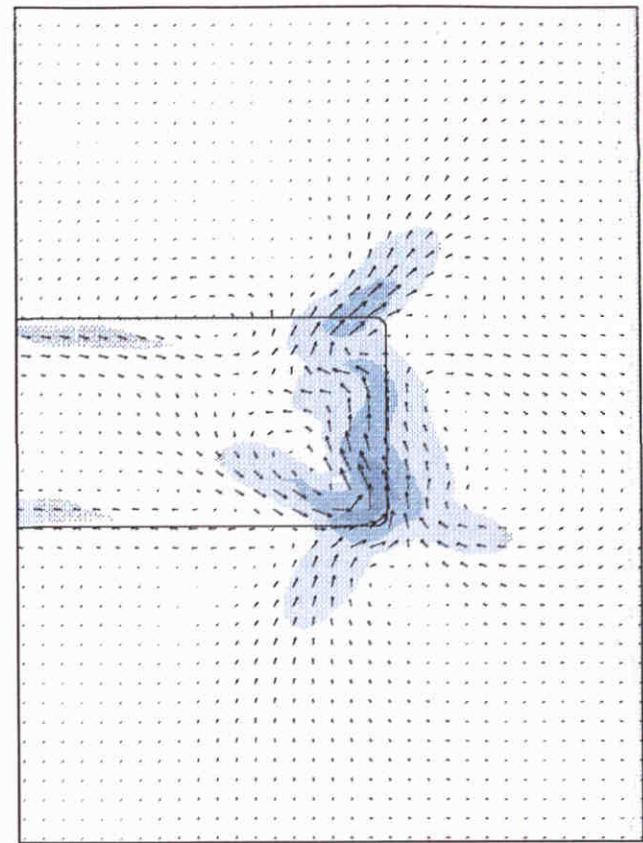
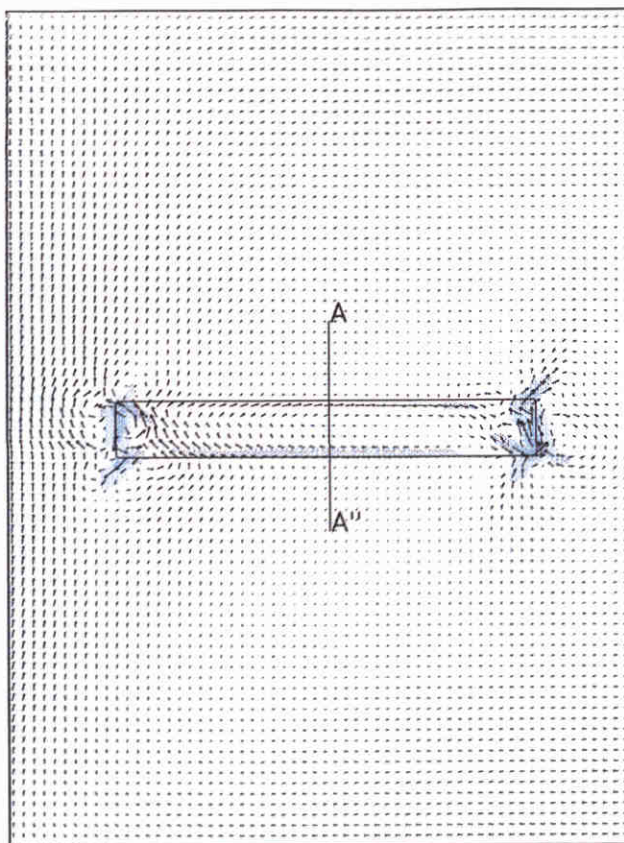
Tidal boundary conditions



Tide-averaged current velocities [m/s]

Tide-averaged current pattern and tide-averaged velocities in cross-section AA''

Tidal boundary conditions including Coriolis

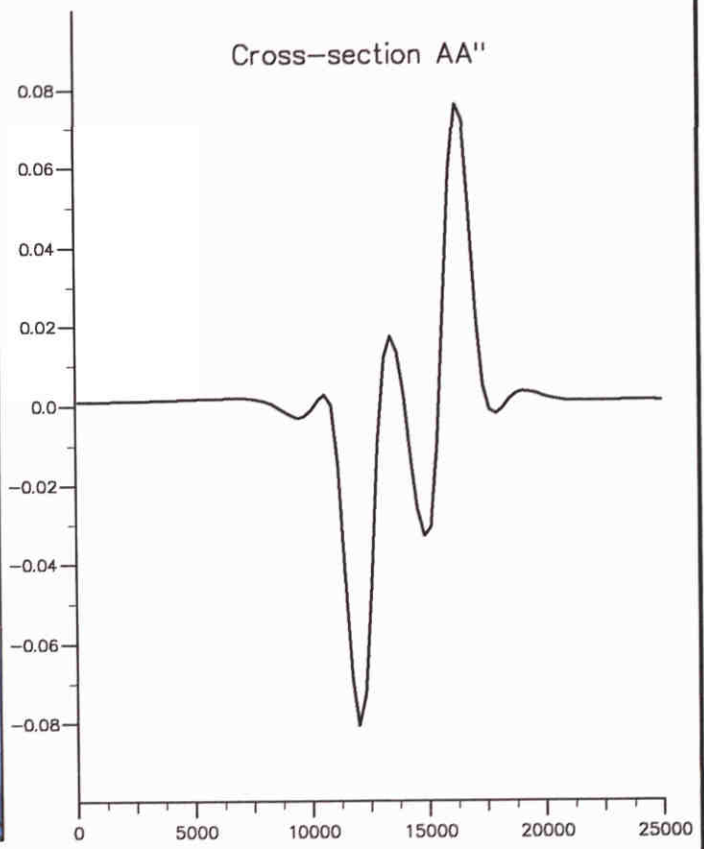
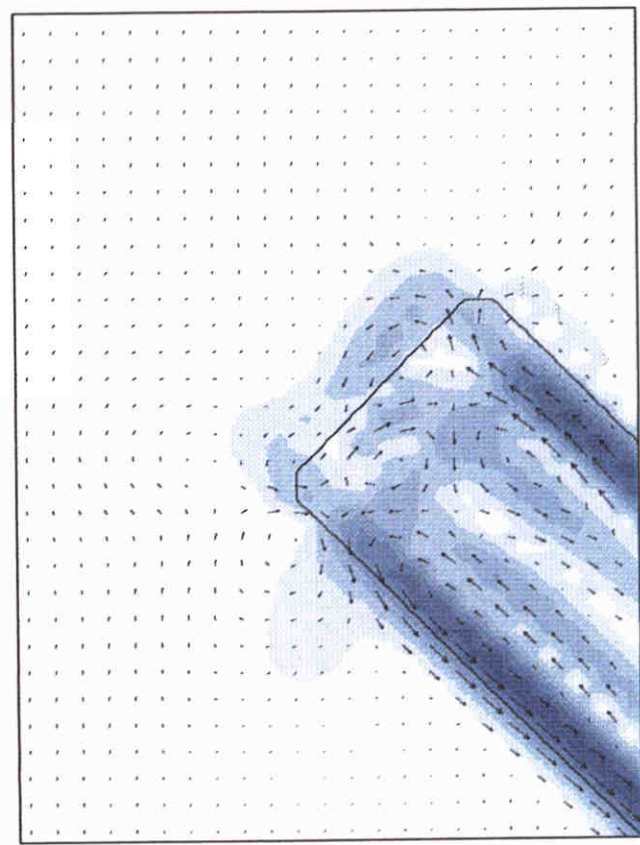
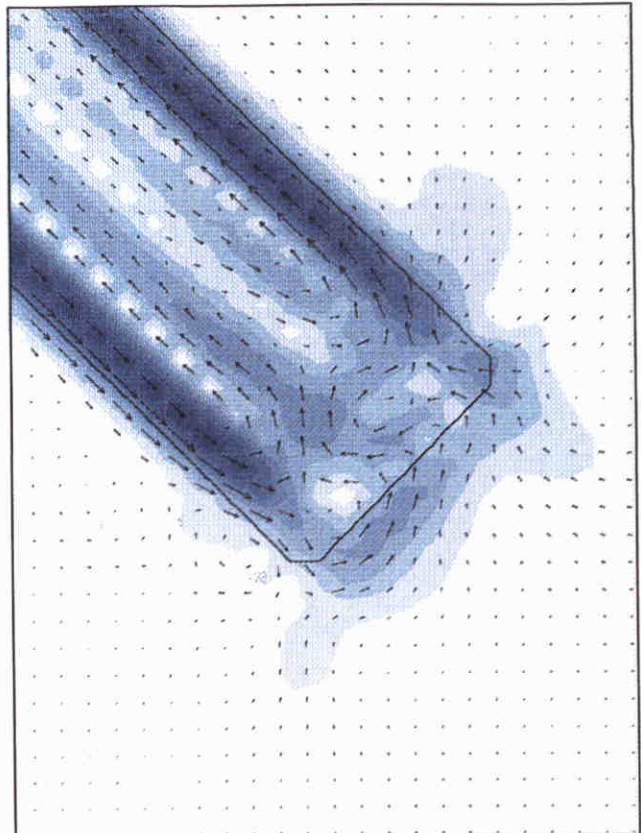
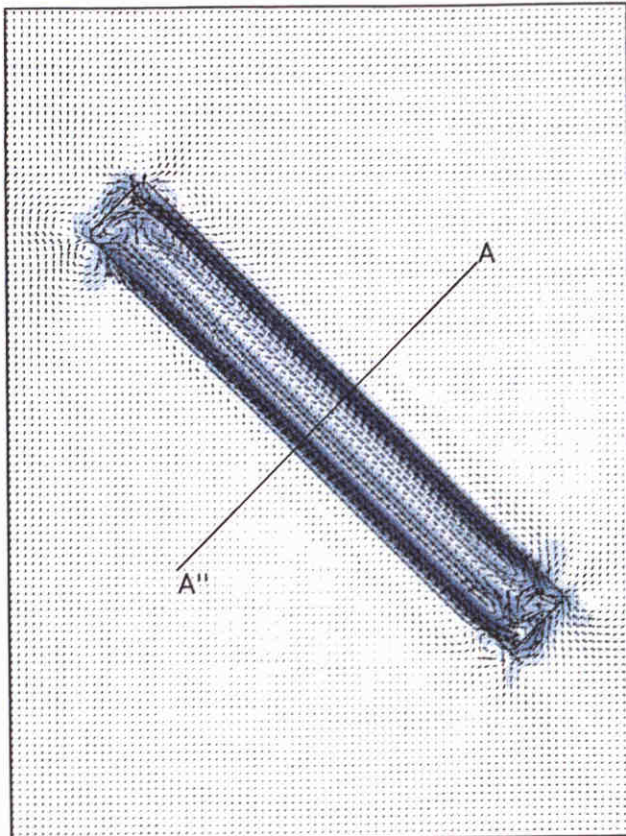


<0.01	<0.03	<0.05	<0.07	<0.09	>0.10
<0.02	<0.04	<0.06	<0.08	<0.10	$\rightarrow 0.050\text{m/s}$

Tide-averaged current velocities [m/s]

Tide-averaged current pattern and tide-averaged velocities in cross-section AA''

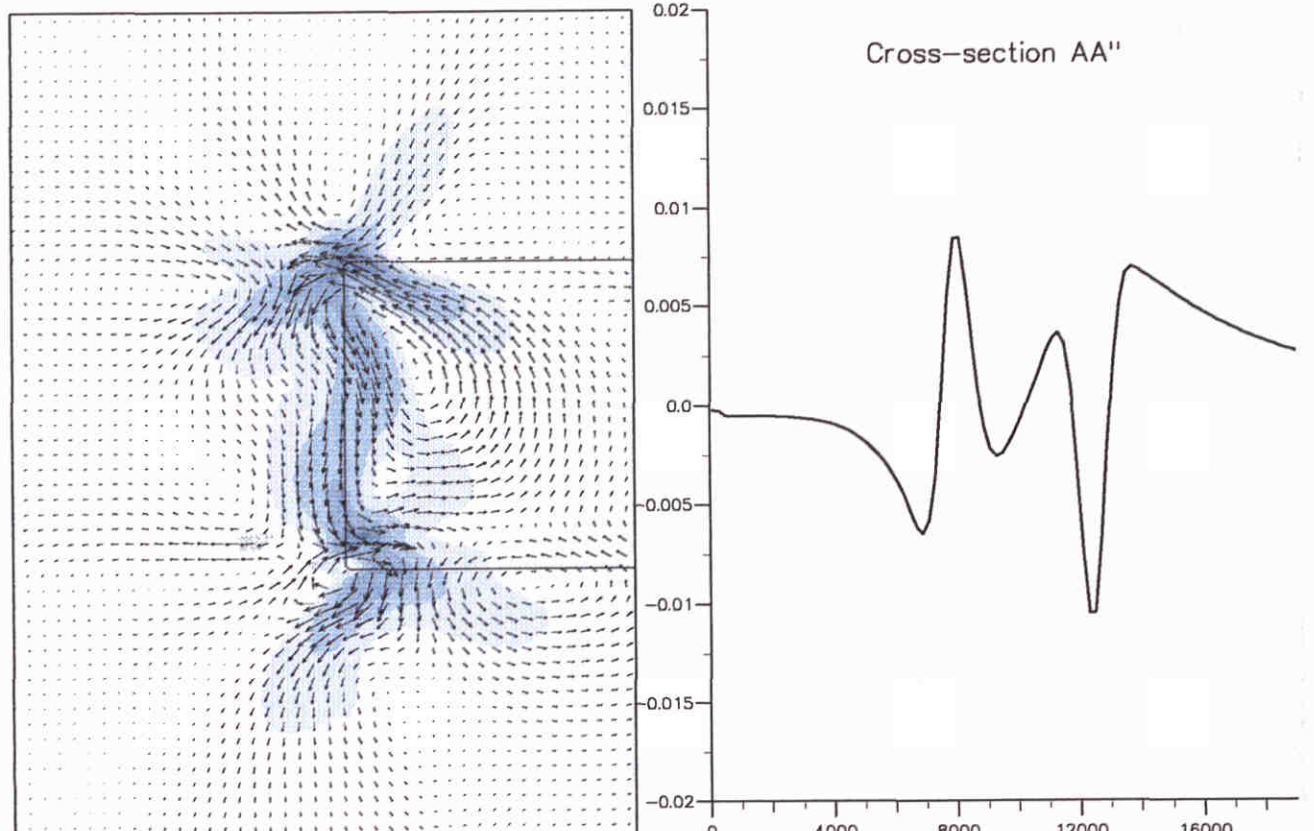
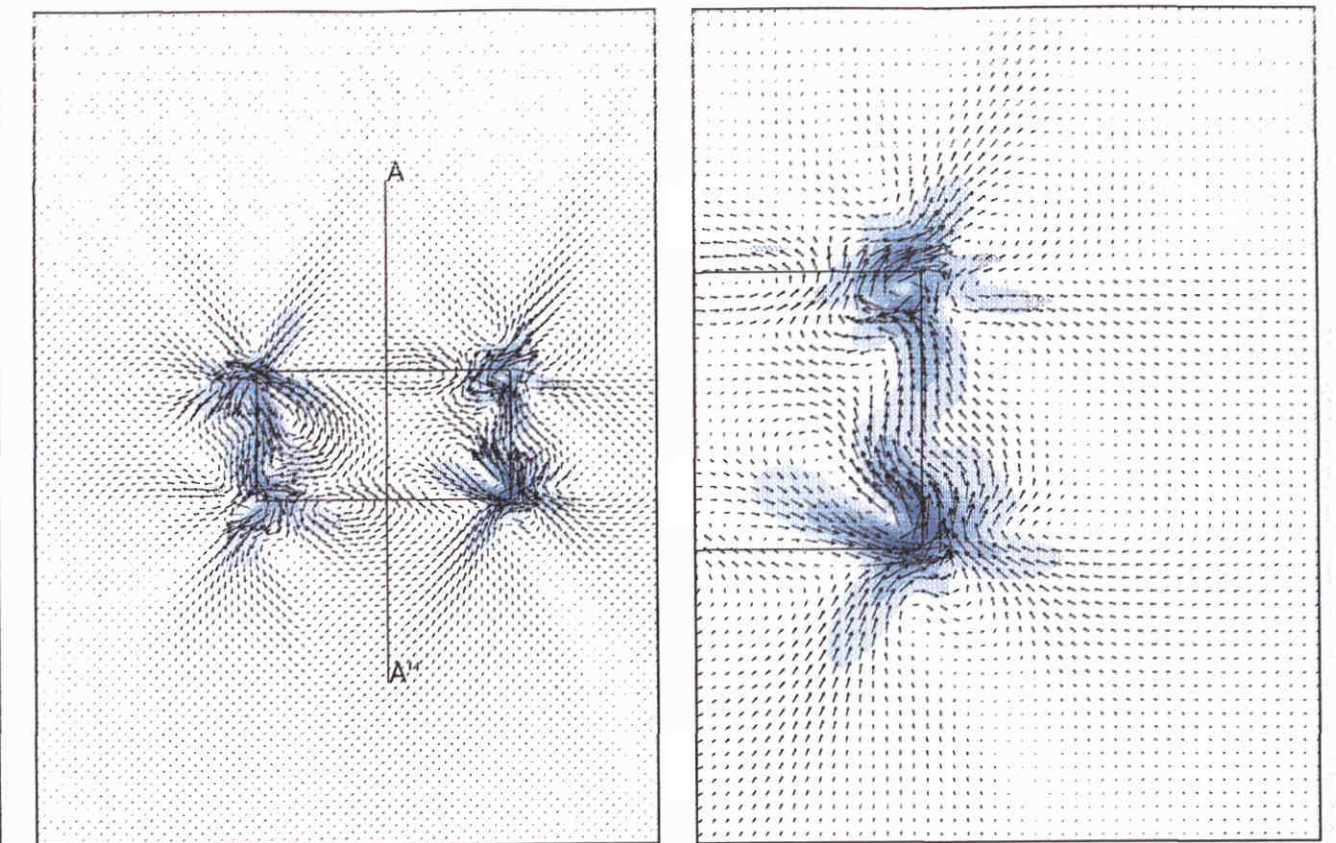
Tidal boundary conditions including Coriolis



Tide-averaged current velocities [m/s]

Tide-averaged current pattern and tide-averaged velocities in cross-section AA''

Tidal boundary conditions including Coriolis

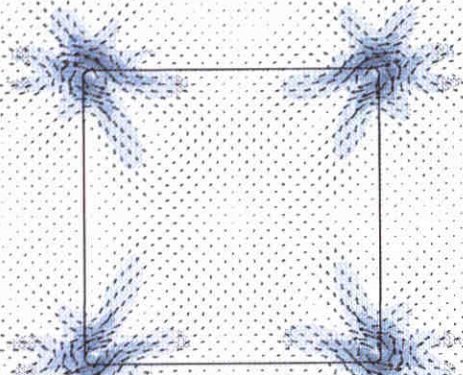


Tide-averaged current velocities [m/s]

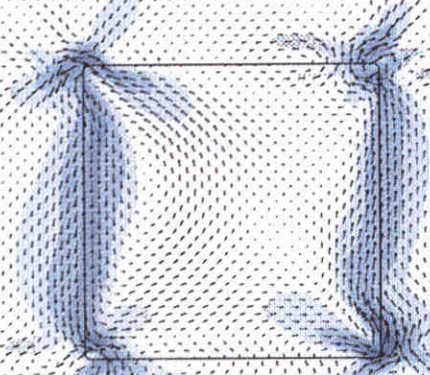
Tide-averaged current pattern and tide-averaged velocities in cross-section AA''

Tidal boundary conditions including Coriolis

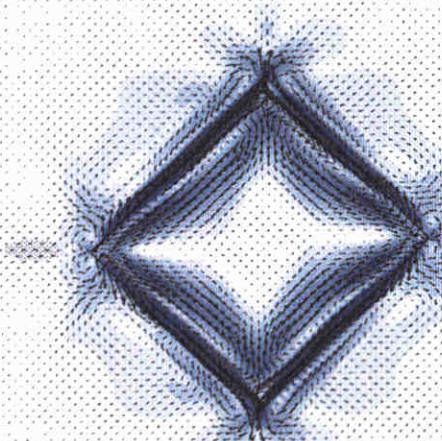
10x10 km²; no Coriolis



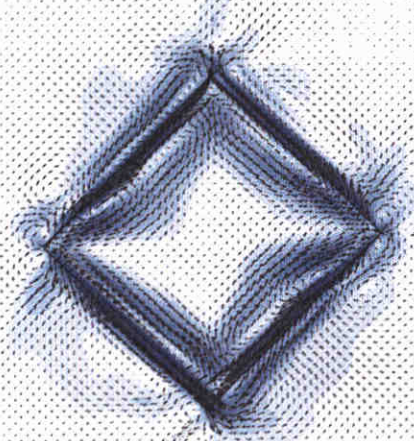
10x10 km²; including Coriolis



10x10 km²; no Coriolis



10x10 km²; including Coriolis



<0.01 <0.03 <0.05 <0.07
<0.02 <0.04 <0.06 <0.08

<0.09 >0.10
<0.10 → 0.050m/s

Tide-averaged current velocities [m/s]

Tide-averaged current pattern

Tidal boundary conditions with and without Coriolis

Figuur 8.2: Influence of the transport mode, while ALFABD is I



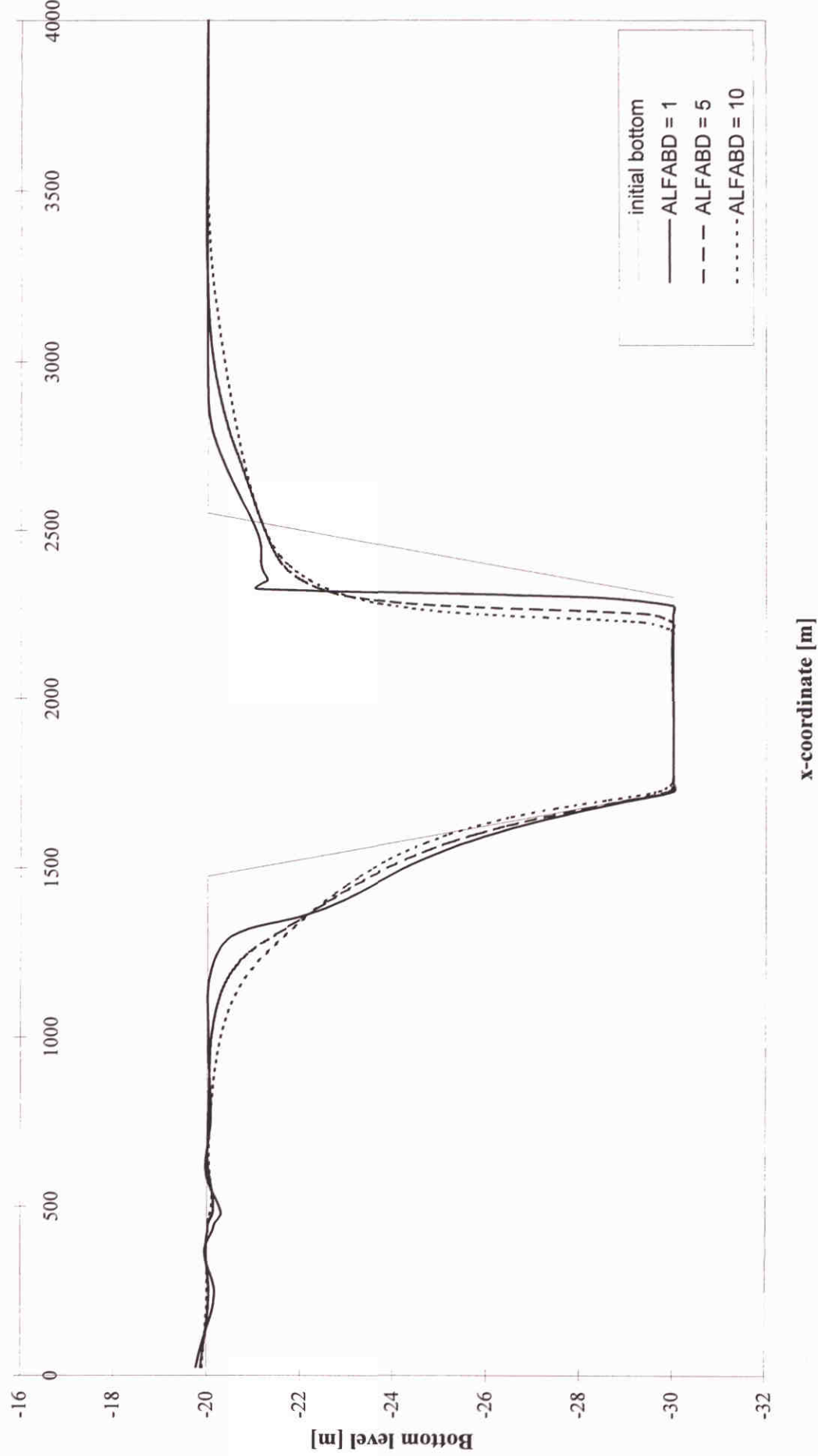
Figuur 8.3: Influence of the transport mode, while ALFABD is 5



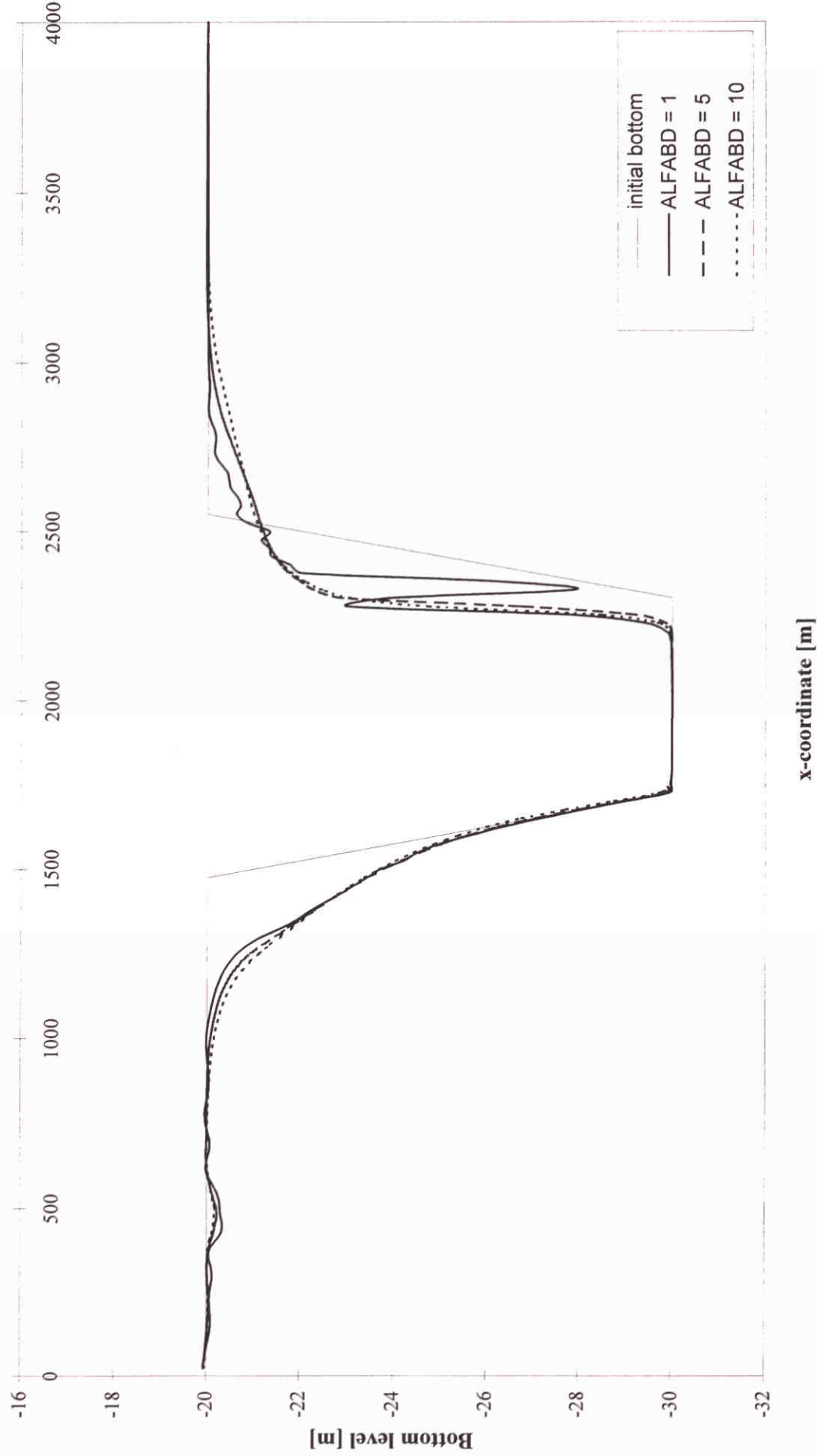
Figuur 8.4: Influence of the transport mode, while ALFABD is 10



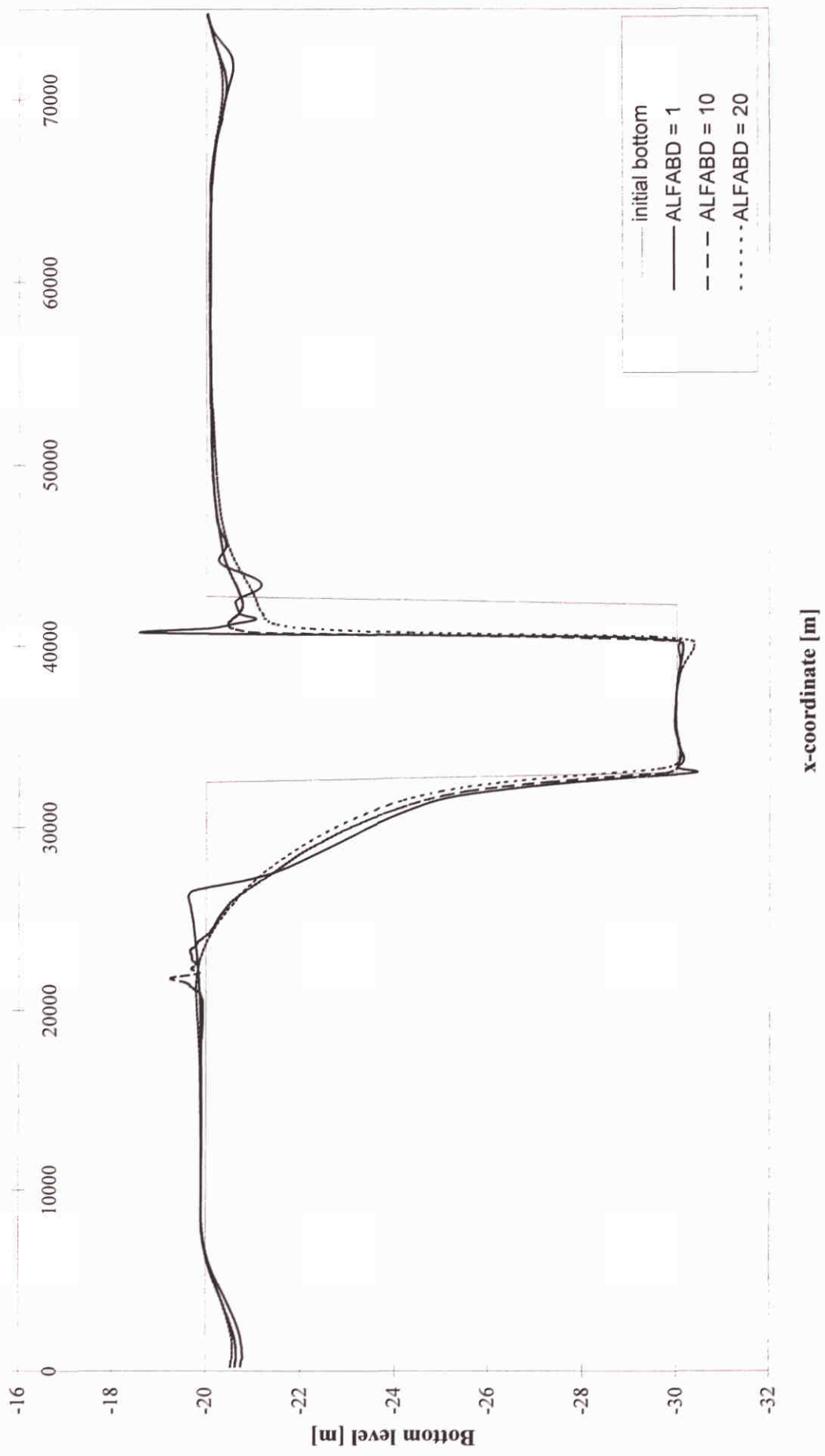
Figuur 8.5: Influence of ALFABD on the results of the total transport mode



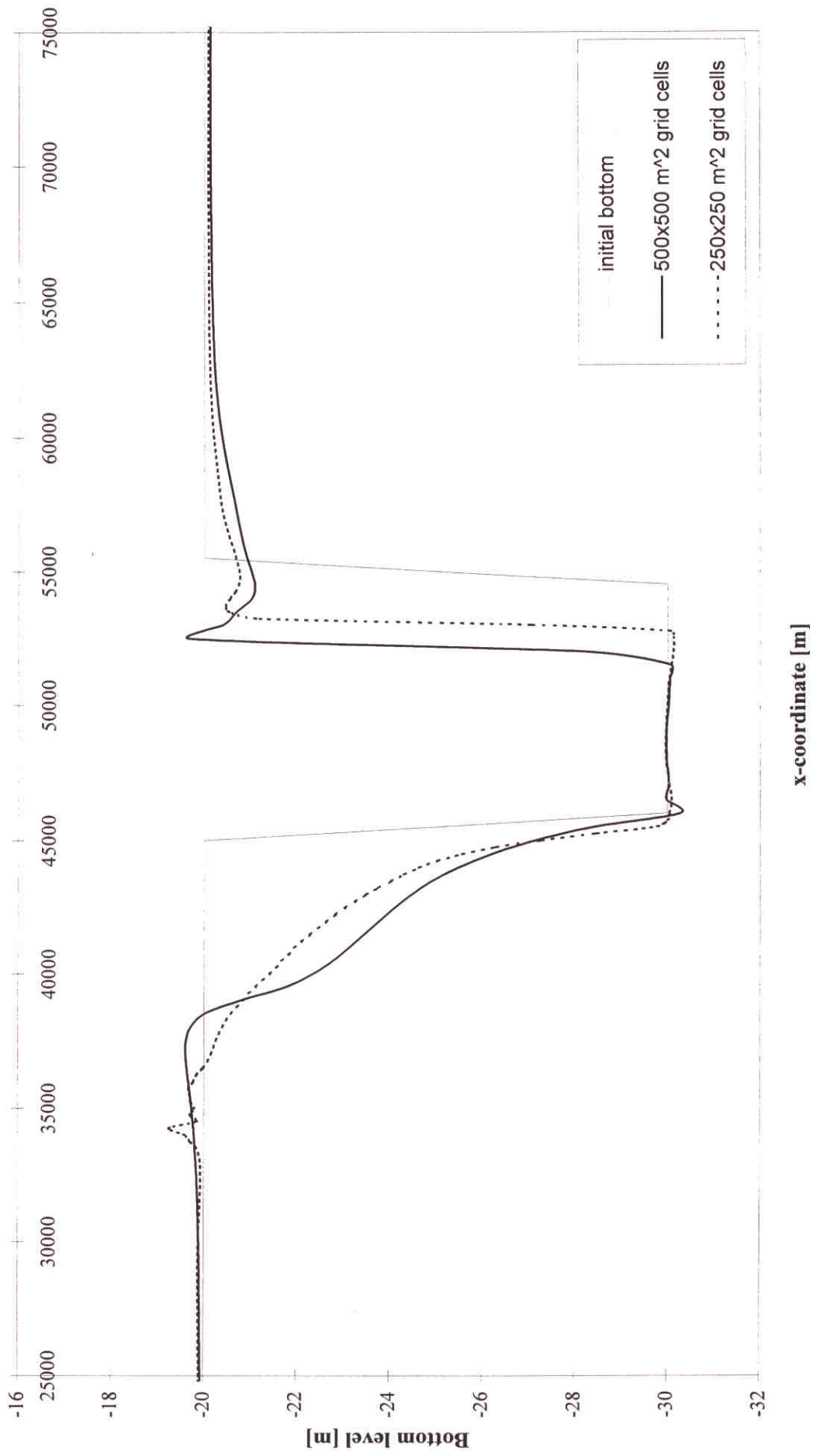
Figuur 8.6: Influence of ALFABD on the results of the bed and suspended transport mode



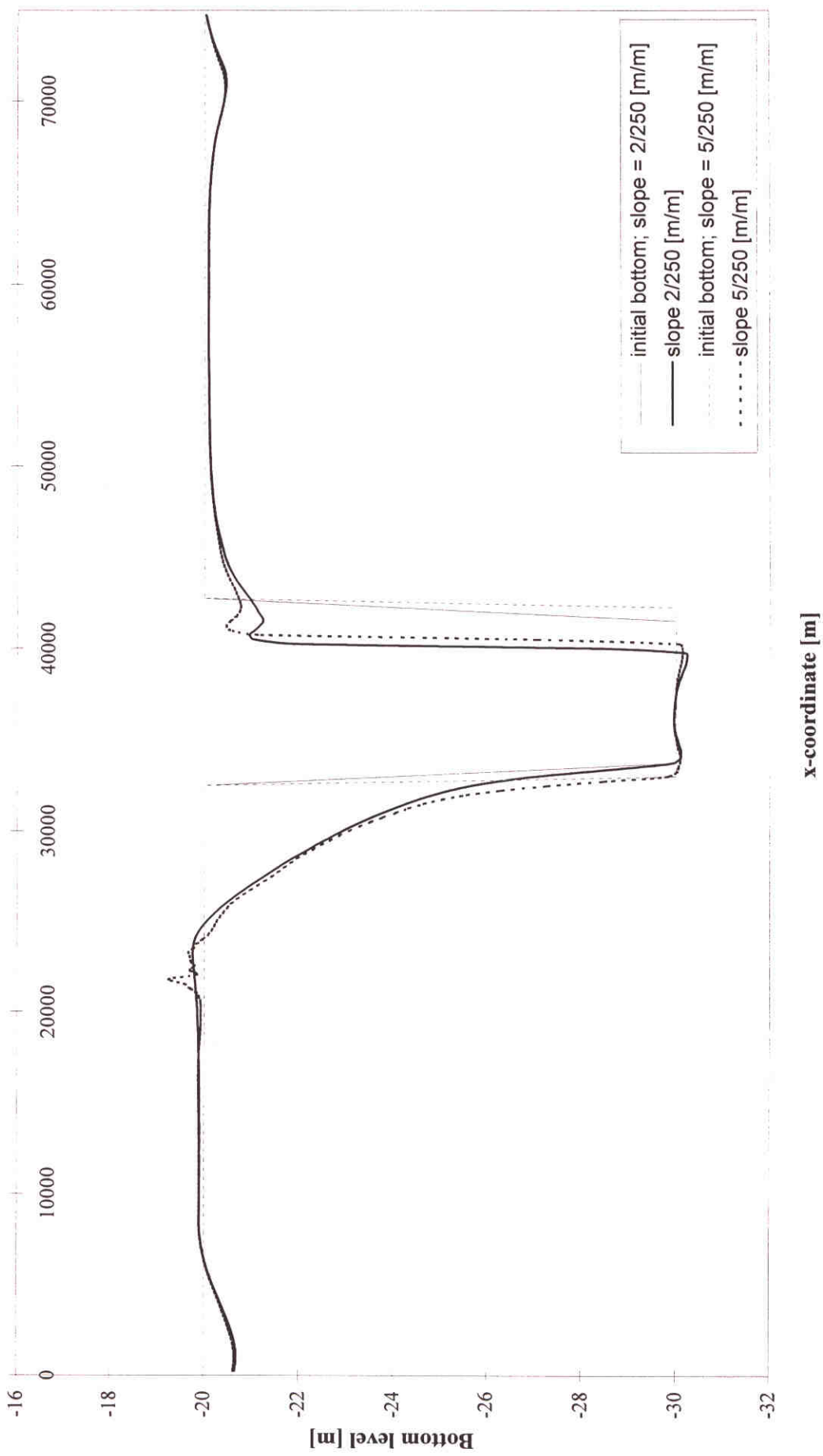
Figuur 8.7: Influence of ALFABD on a $10 \times 10 \text{ km}^2$ sandpit with total transport



Figuur 8.8: Influence of the grid cell size on the morphological results



Figuur 8.9: Influence of the slope of the sandpit on the morphological results



Figuur 8.10: Influence of the number of bottom computations per flow computation

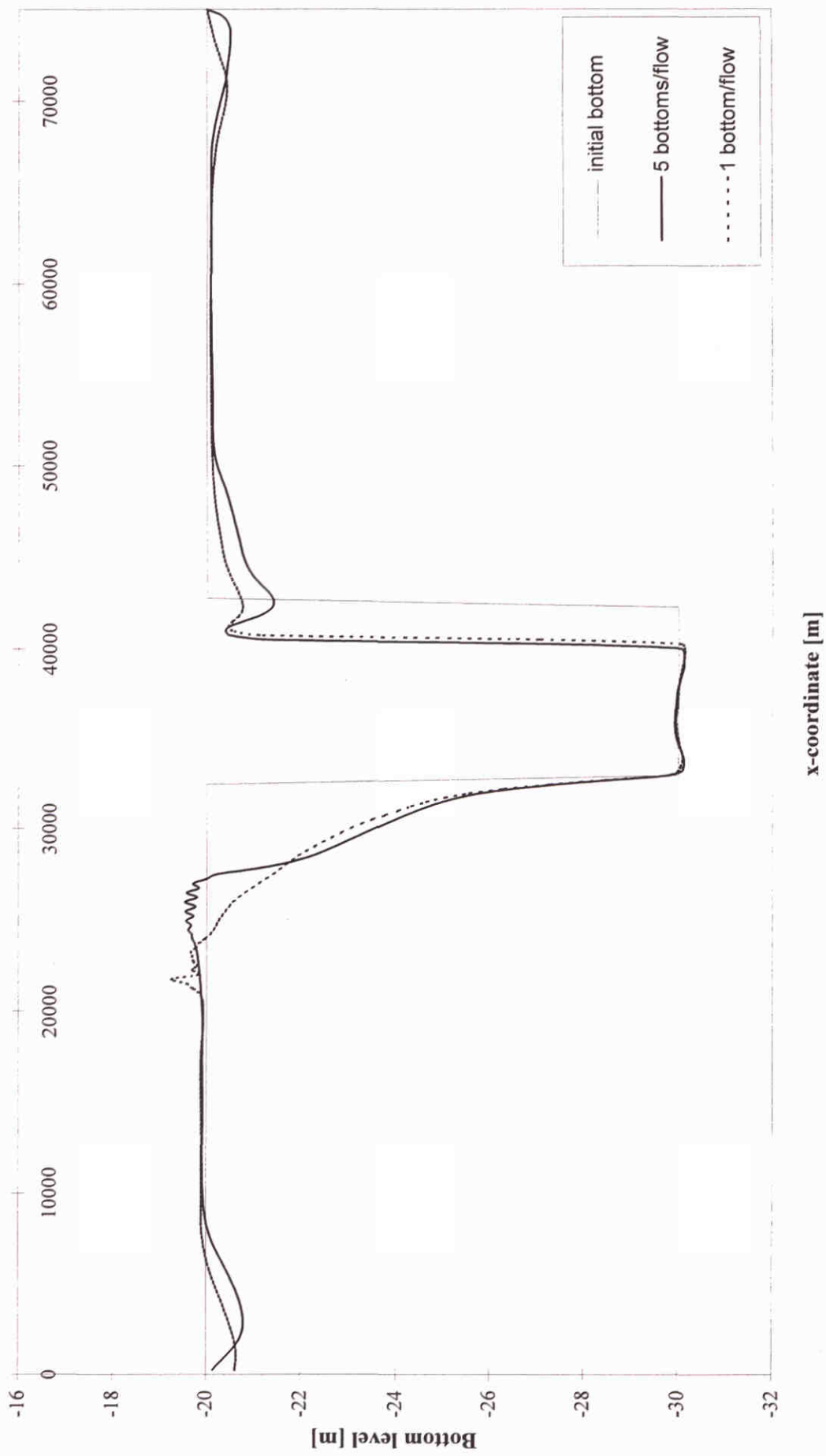


Figure 8.11: Data points for tide analysis

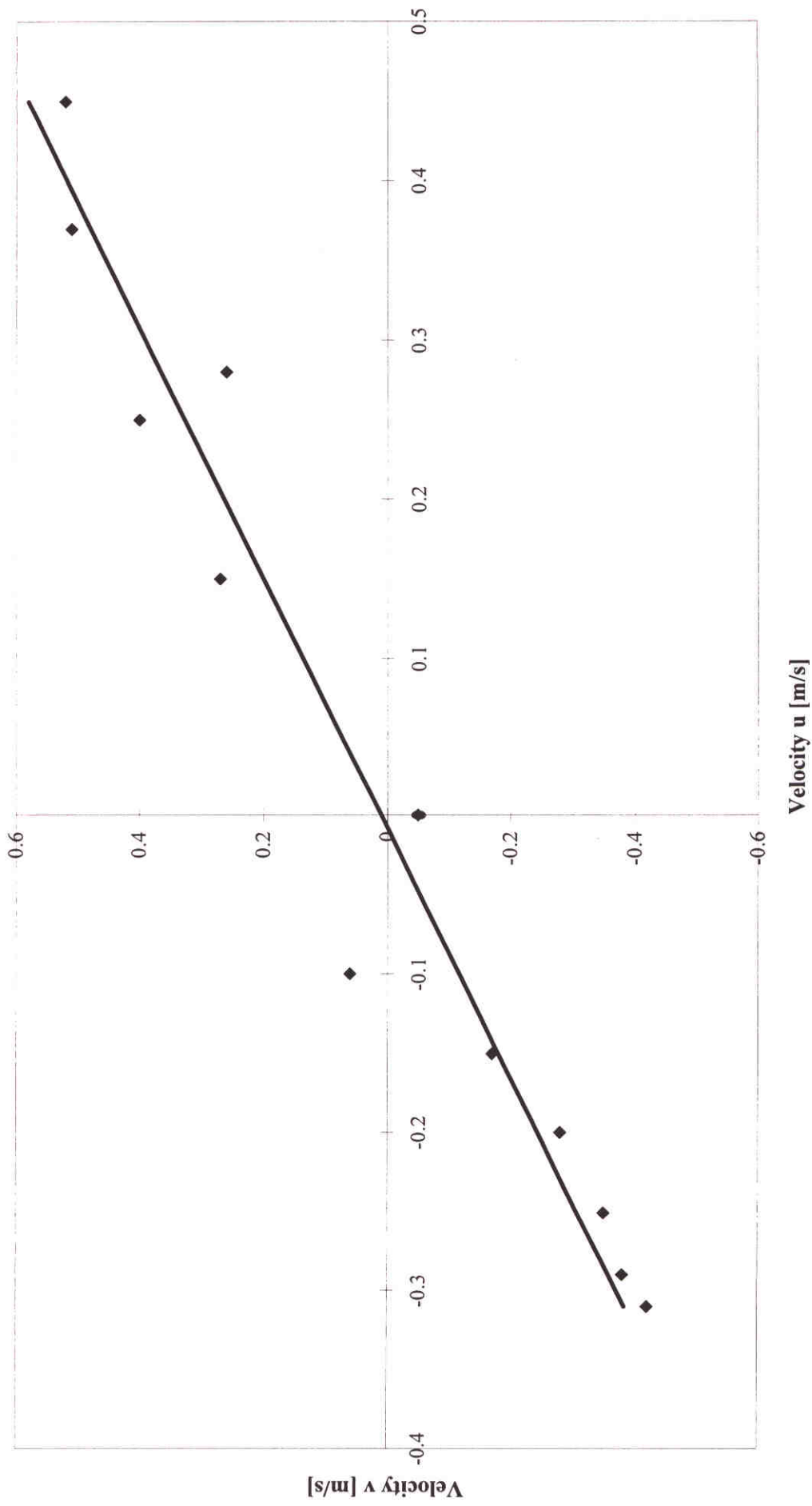
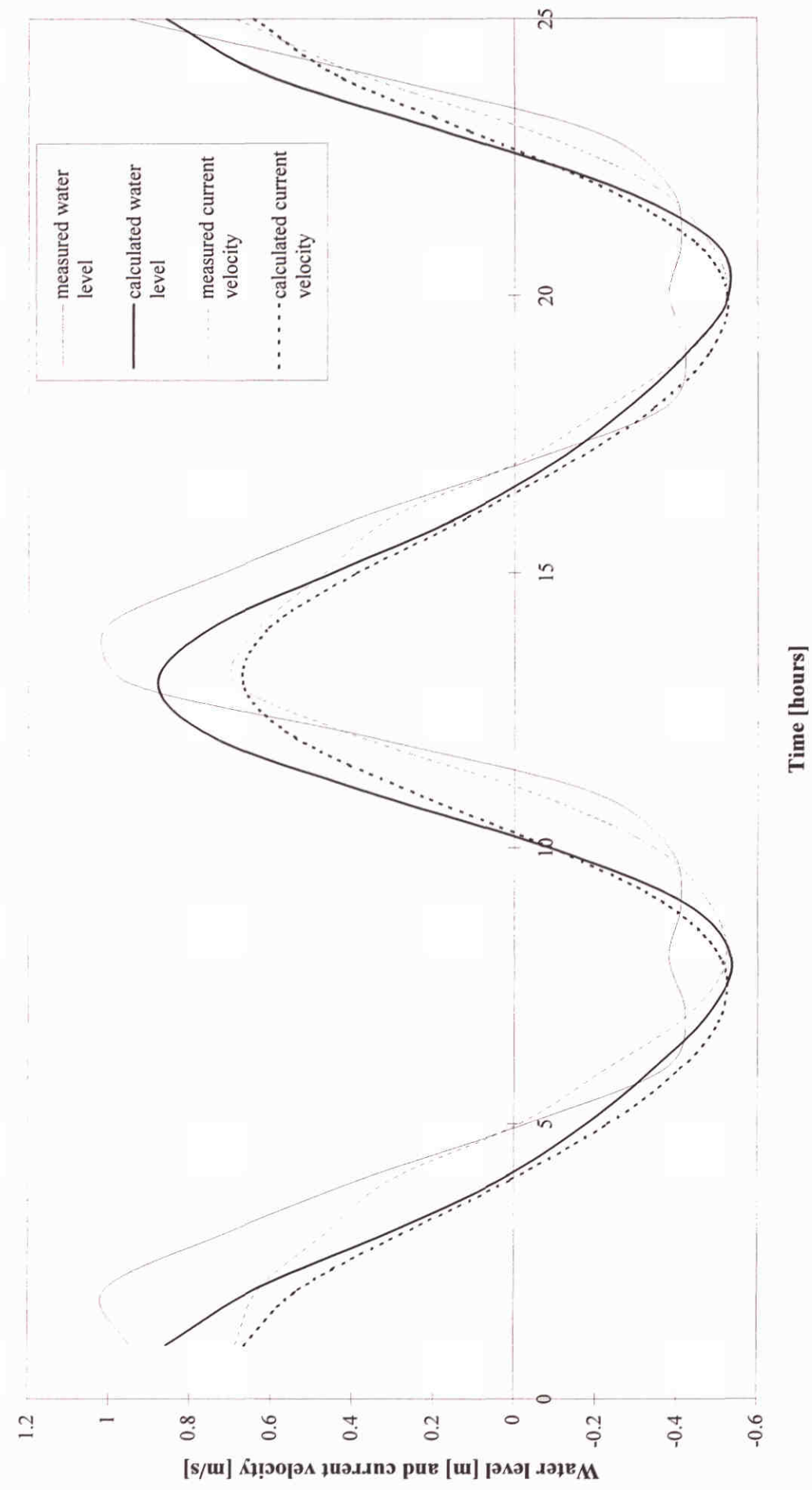
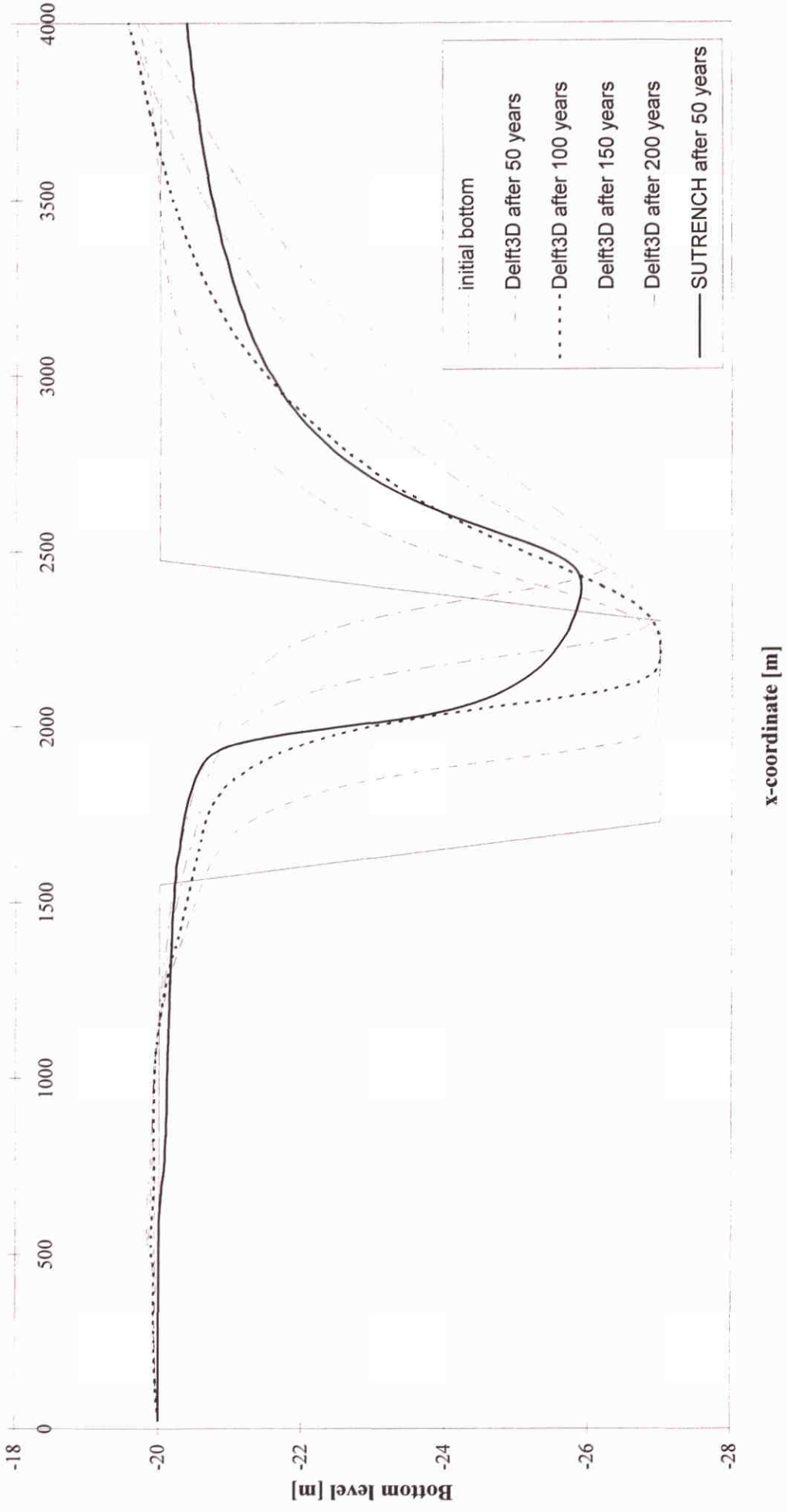


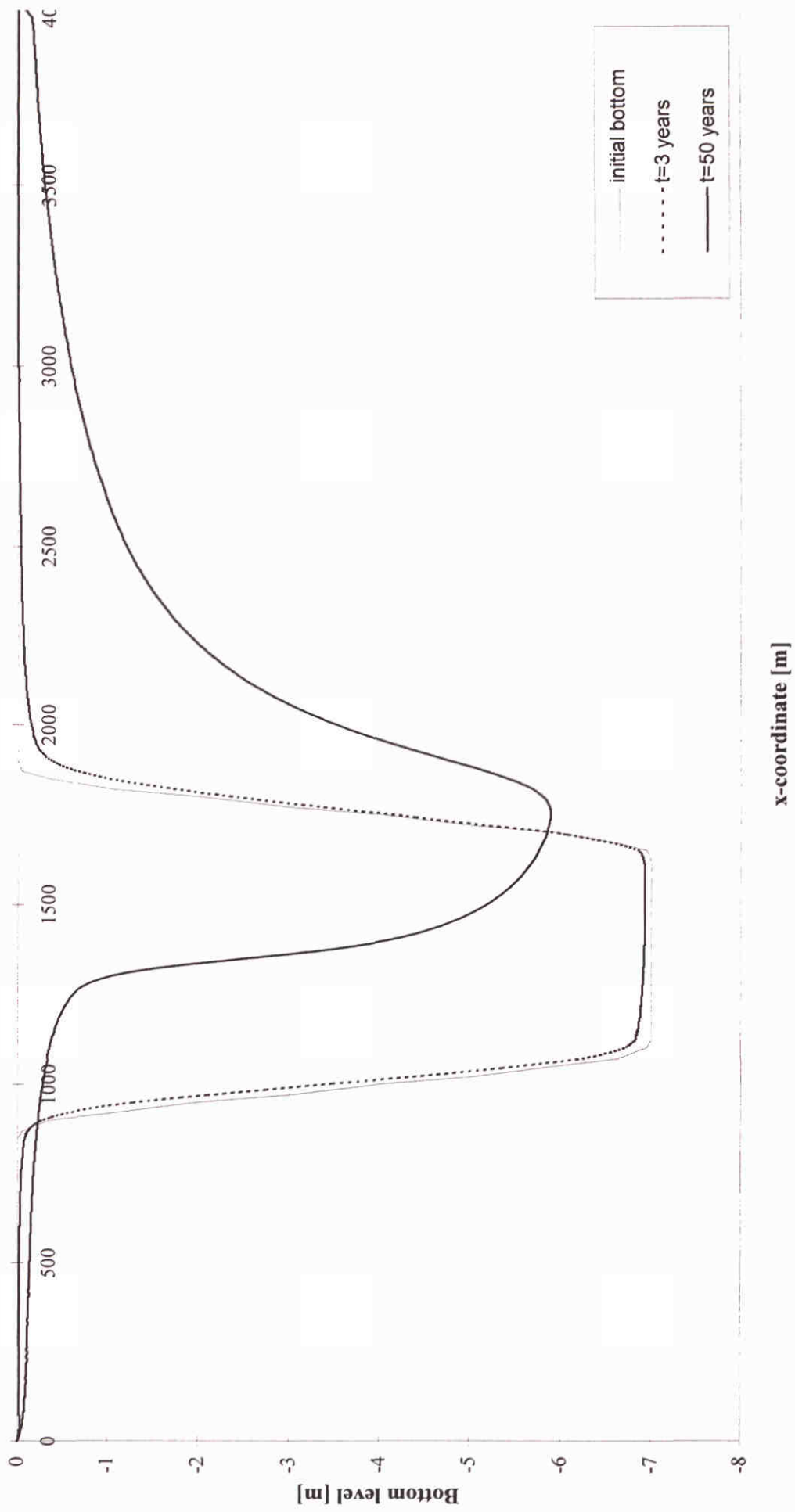
Figure 8.12: Results of the tide analysis

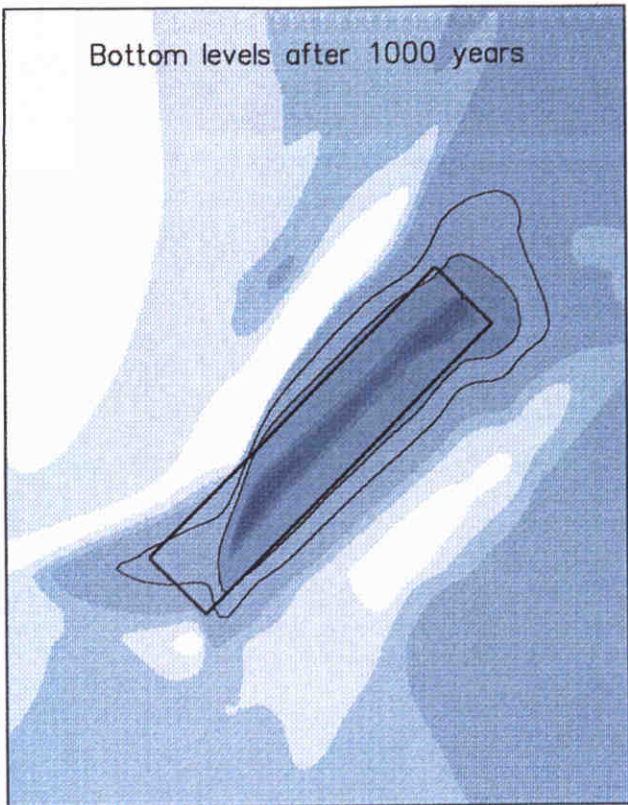


Figuur 8.13: SUTRENCH and Delft3D results of a reference trench

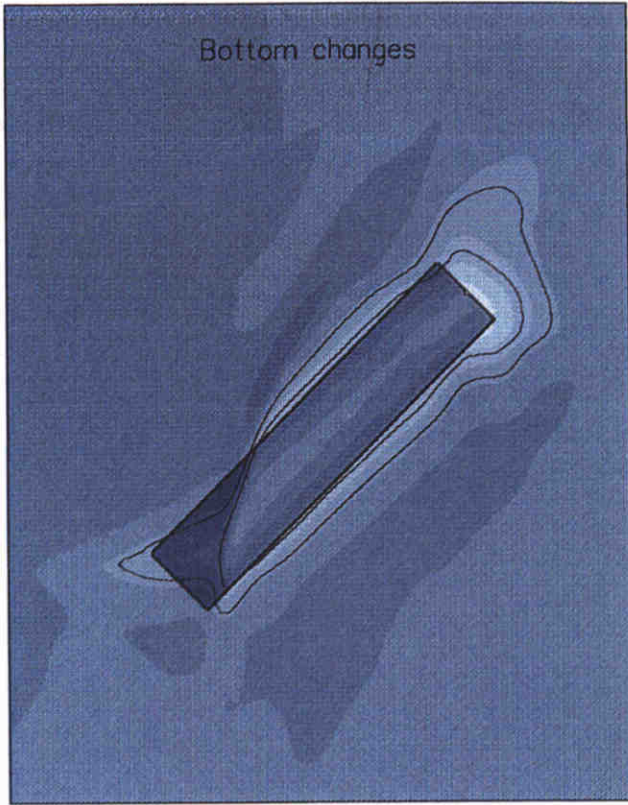


Figuur 8.14: SUTRENCH results of Walstra (1998)

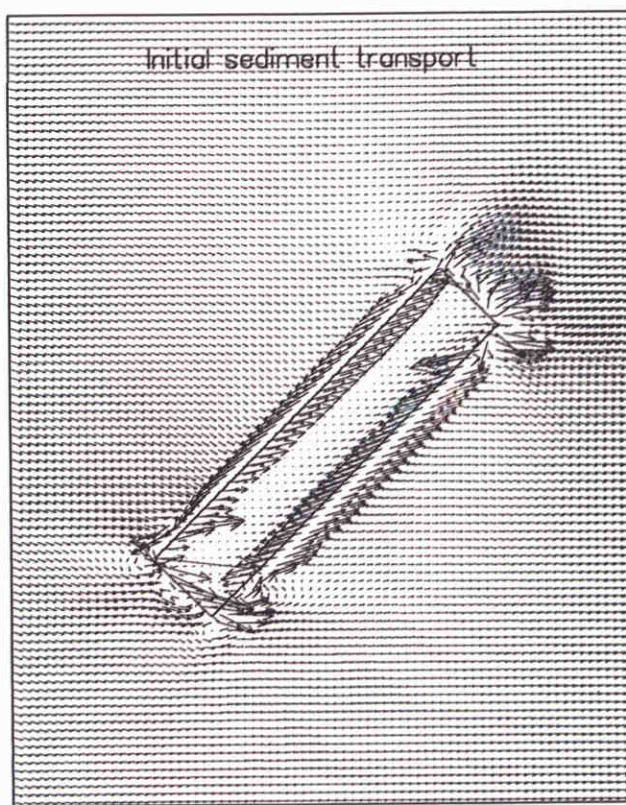




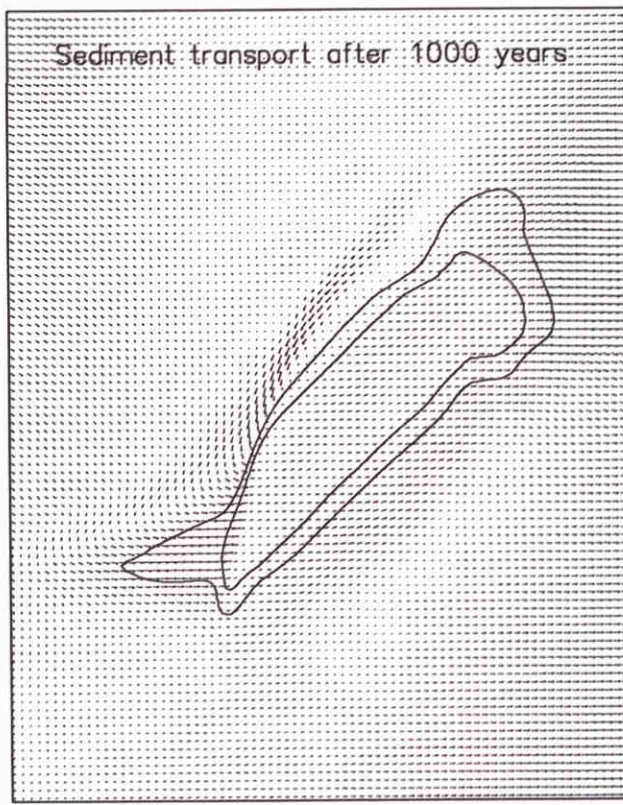
<19.5	<20.5	<29.5	<30.5
≤ 20.0	≤ 25.0	≤ 30.0	>30.5



<-10.0	<-8.0	<-6.0	<-4.0	<-2.0	<0.0	>2.0	>4.0	>6.0	>8.0	>10.0
----------	---------	---------	---------	---------	--------	--------	--------	--------	--------	---------



→ $2.0 \times 10^{-8} \text{ m}^2/\text{s}$



Bottom levels and changes [m]; sediment transport [m^2/s]

+45 degrees rotated 25x5 km² sandpit

Morphological results after 1000 years

Figure 8.15b: Bottom levels in the longitudinal section of a +45° rotated $25 \times 5 \text{ km}^2$ sandpit

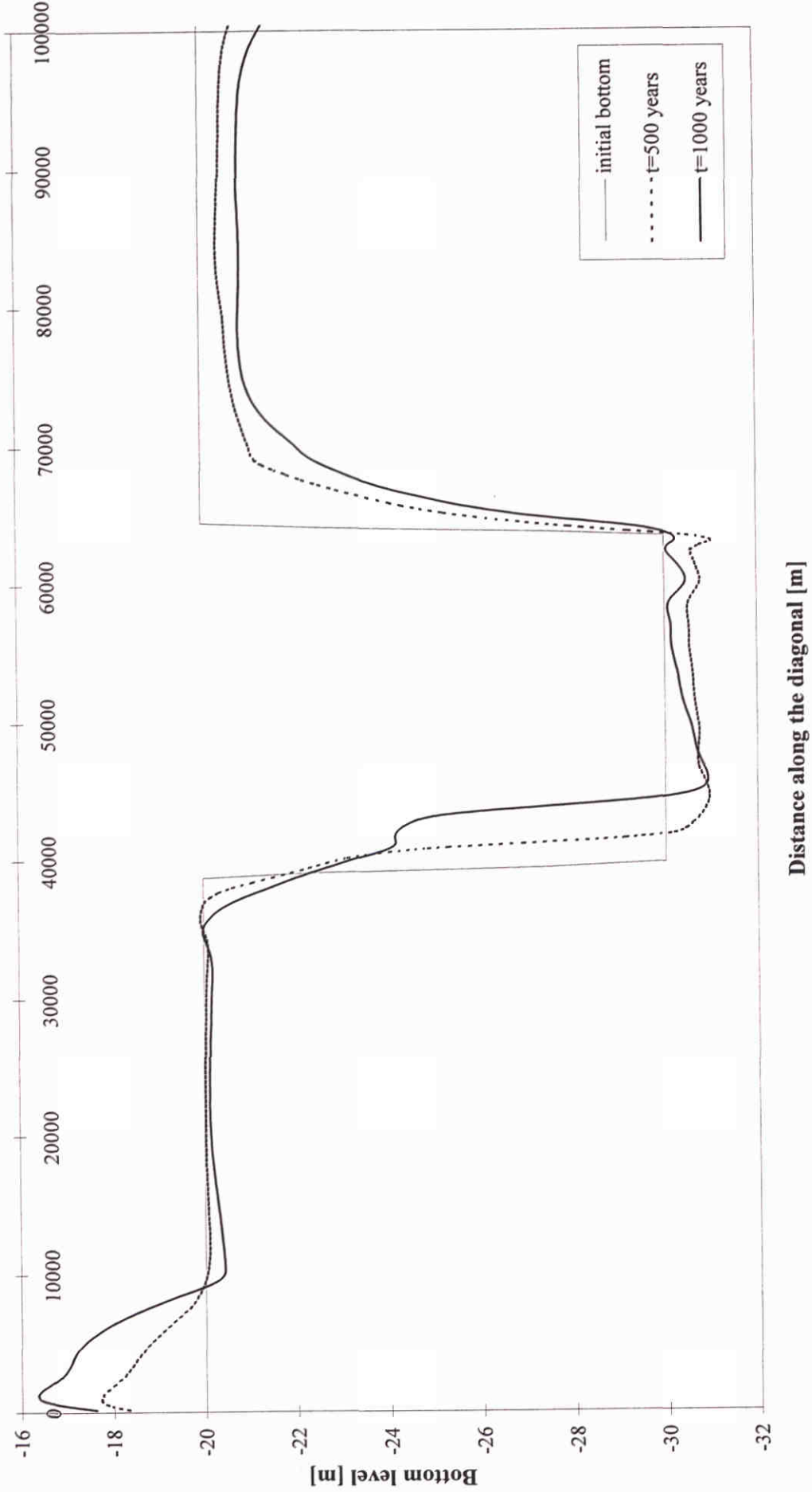
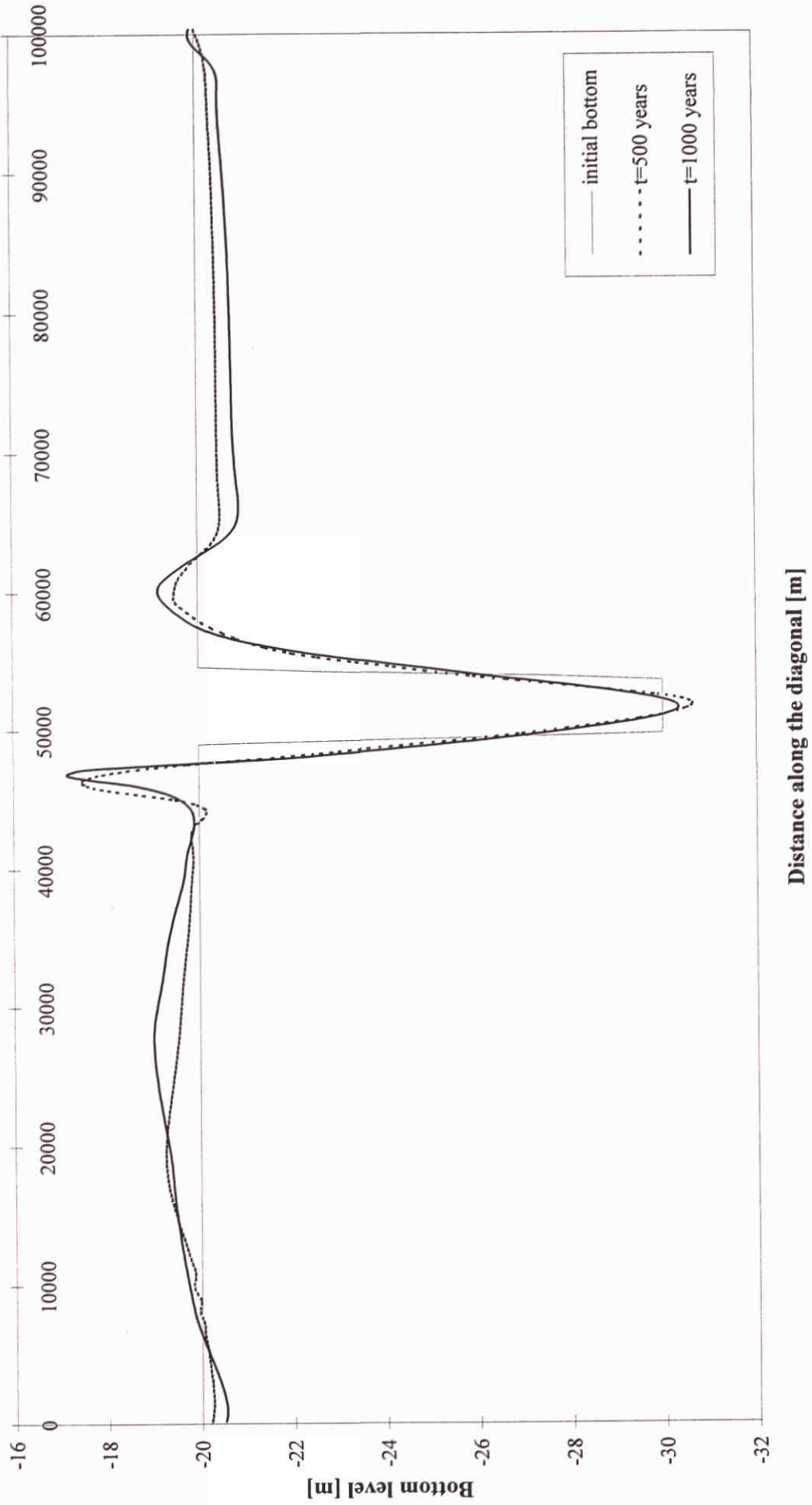
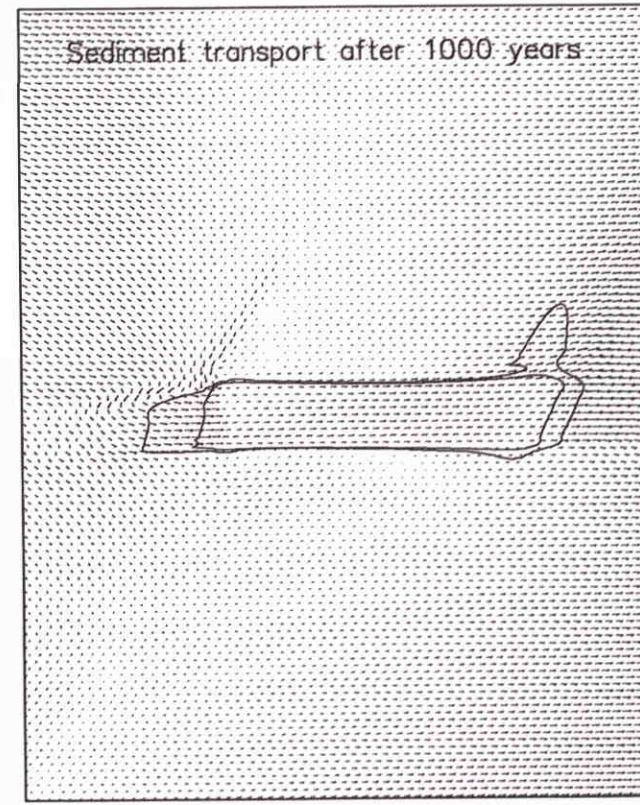
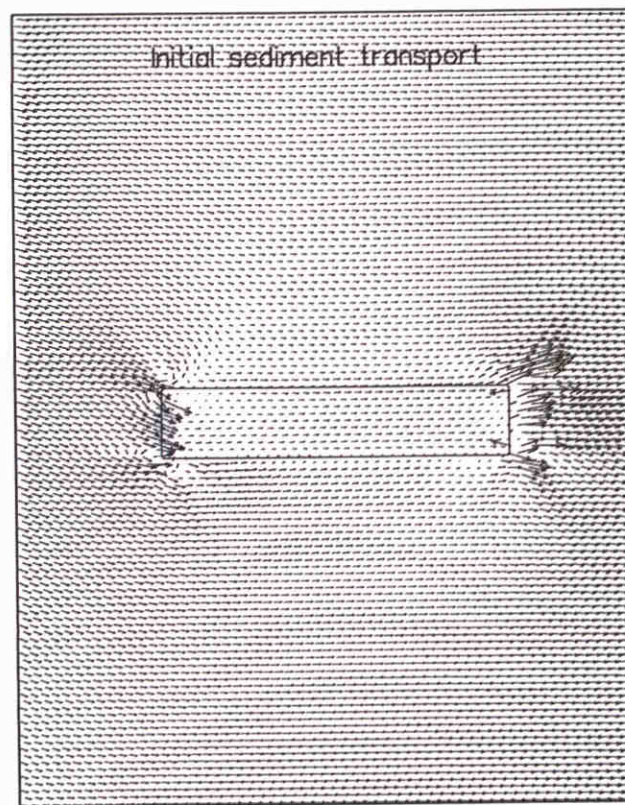
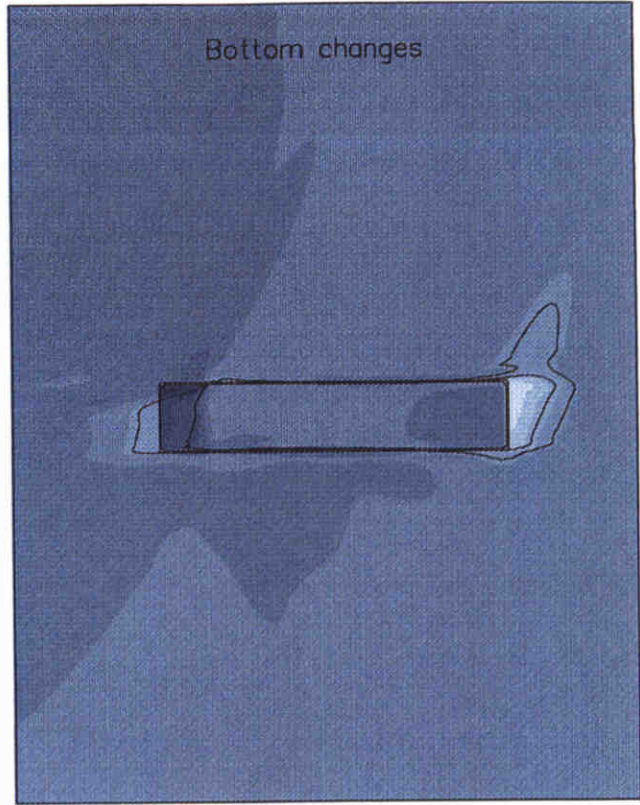
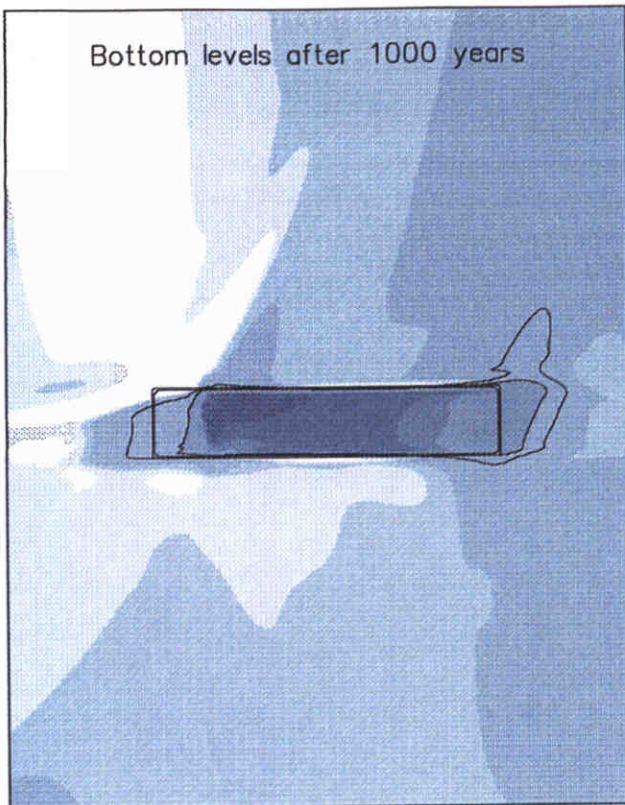


Figure 8.15c: Bottom levels in the center cross-section of a +45° rotated 25x5 km² sandpit



Distance along the diagonal [m]



→ $2.0 \times 10^{-6} \text{ m}^2/\text{s}$

Bottom levels and changes [m]; sediment transport [m^2/s]

Parallel 25x5 km^2 sandpit

Morphological results after 1000 years

Figuur 8.16b: Bottom levels in the center longitudinal section of a parallel $25 \times 5 \text{ km}^2$ sandpit

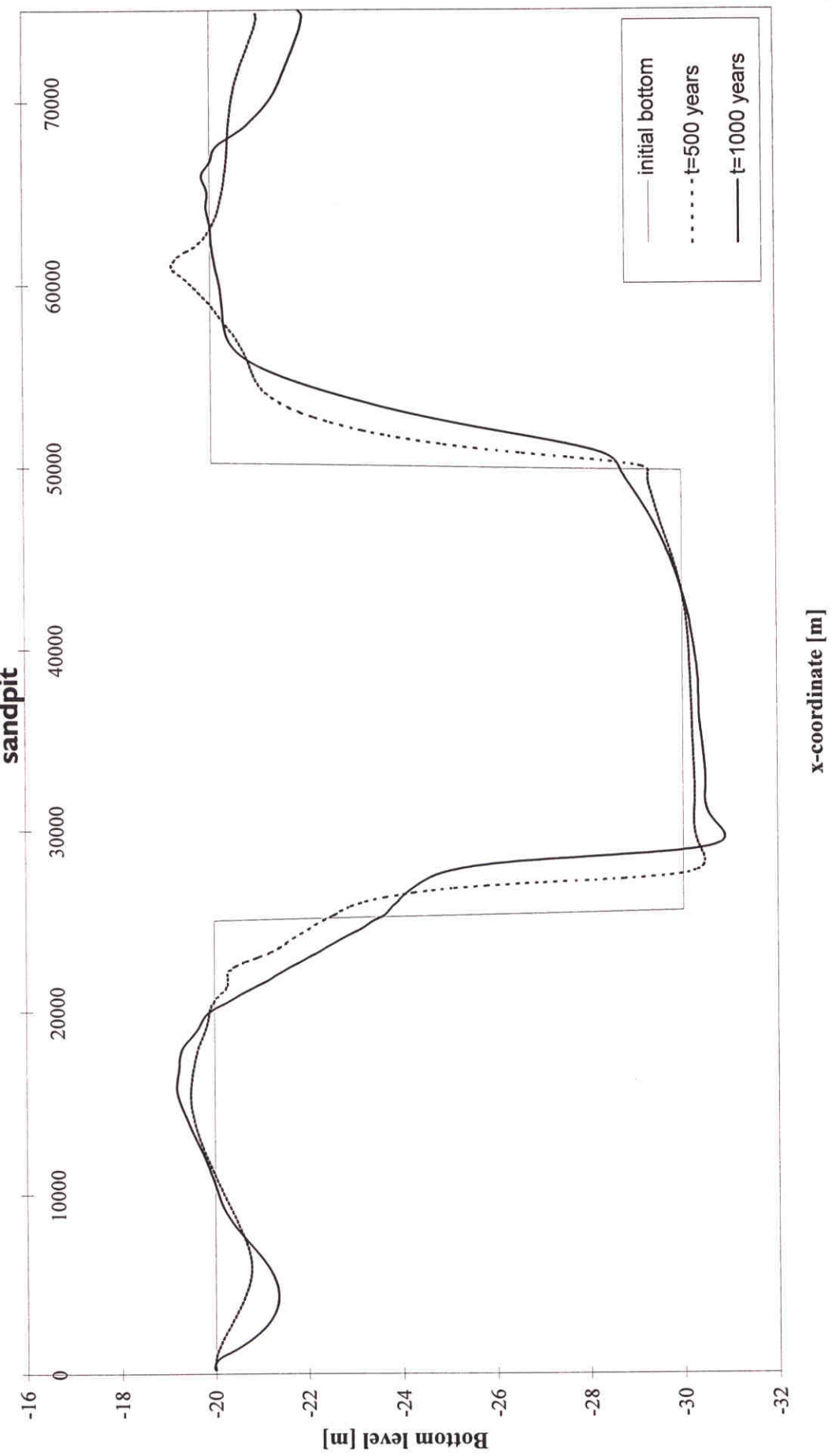
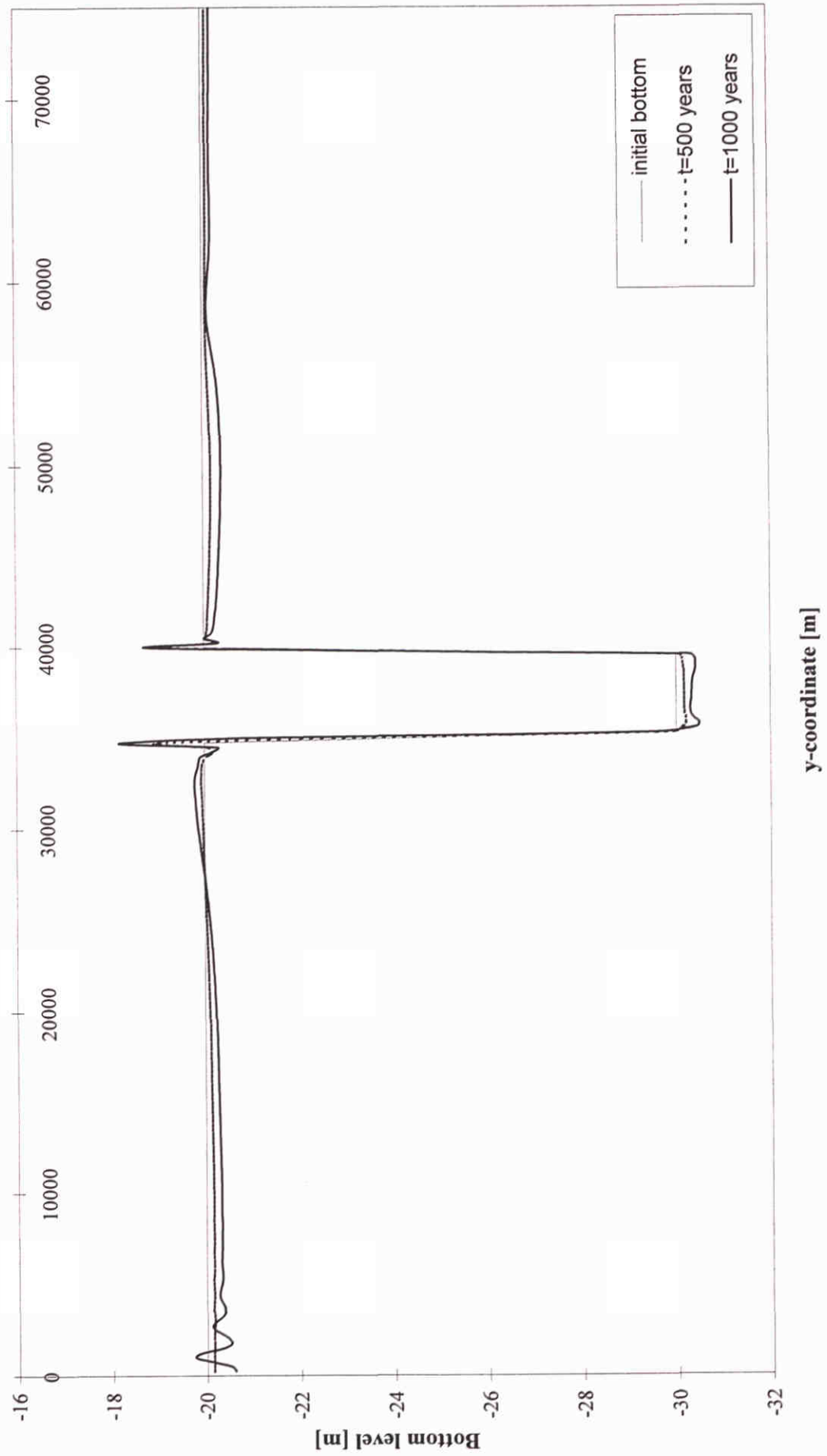
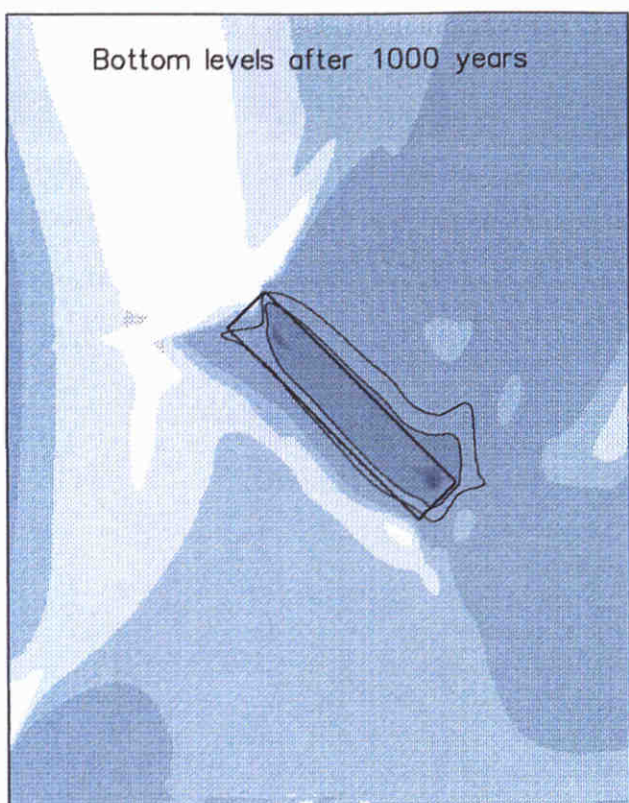
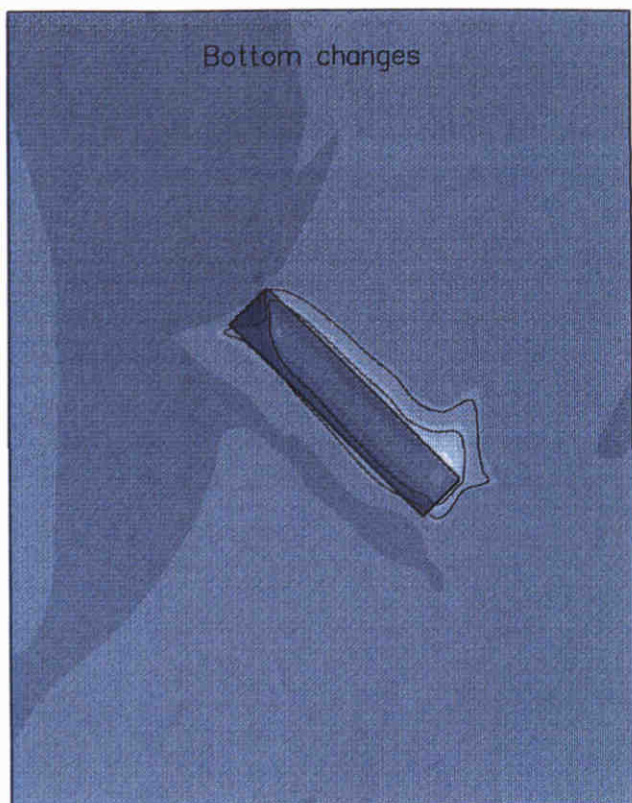


Figure 8.16c: Bottom levels in the center cross-section of a parallel 25×5 km \wedge 2 sandpit

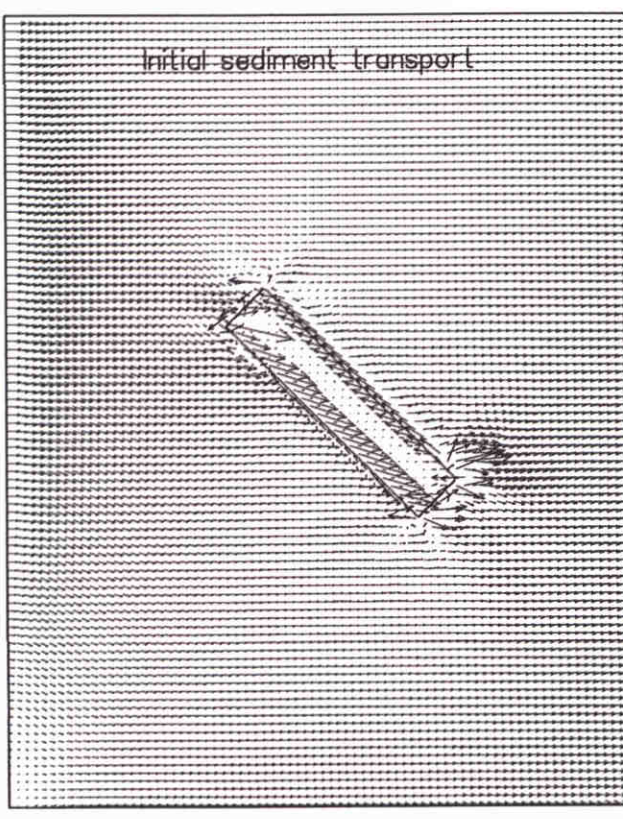




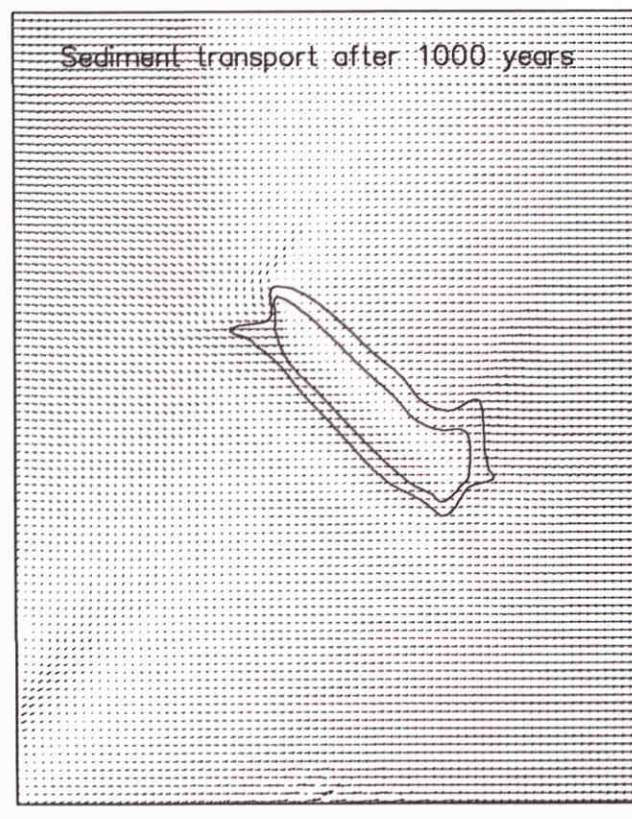
<input type="checkbox"/> <19.5	<input type="checkbox"/> <20.5	<input type="checkbox"/> <29.5	<input type="checkbox"/> <30.5
<input checked="" type="checkbox"/> <20.0	<input type="checkbox"/> <25.0	<input type="checkbox"/> <30.0	<input type="checkbox"/> >30.5



<input type="checkbox"/> <-10.0	<input type="checkbox"/> <-4.0	<input type="checkbox"/> <2.0	<input type="checkbox"/> <8.0
<input type="checkbox"/> <-8.0	<input type="checkbox"/> <-2.0	<input type="checkbox"/> <4.0	<input type="checkbox"/> <10.0
<input type="checkbox"/> <-6.0	<input type="checkbox"/> <0.0	<input type="checkbox"/> <6.0	<input type="checkbox"/> >10.0



→ $2.0 \times 10^{-8} \text{ m}^2/\text{s}$



Bottom levels and changes [m]; sediment transport [m^2/s]

-45 degrees rotated 25x5 km² sandpit

Morphological results after 1000 years

Figure 8.I7b: Bottom levels in the center longitudinal section of a -45° rotated $25 \times 5 \text{ km}^2$ sandpit

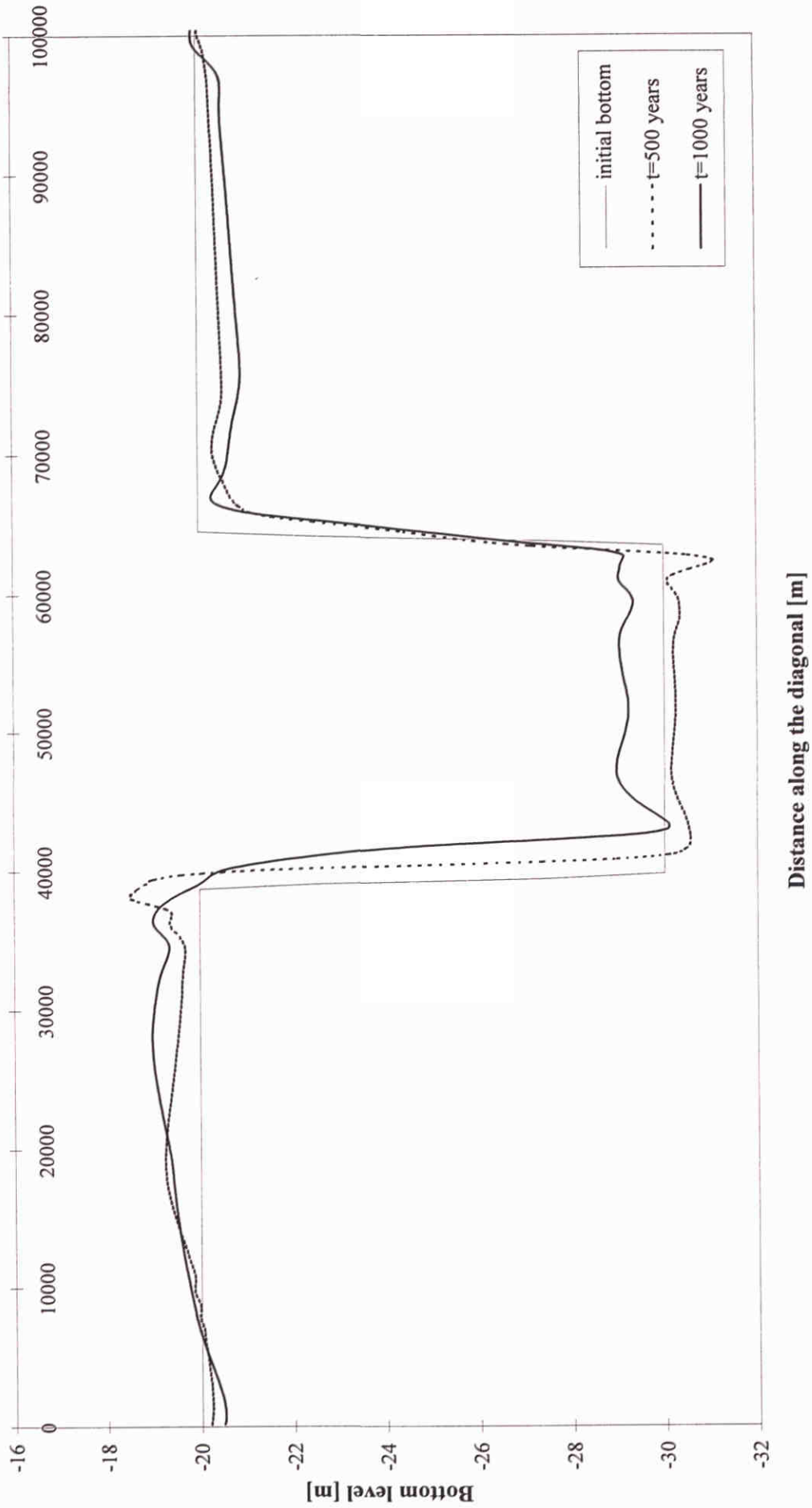
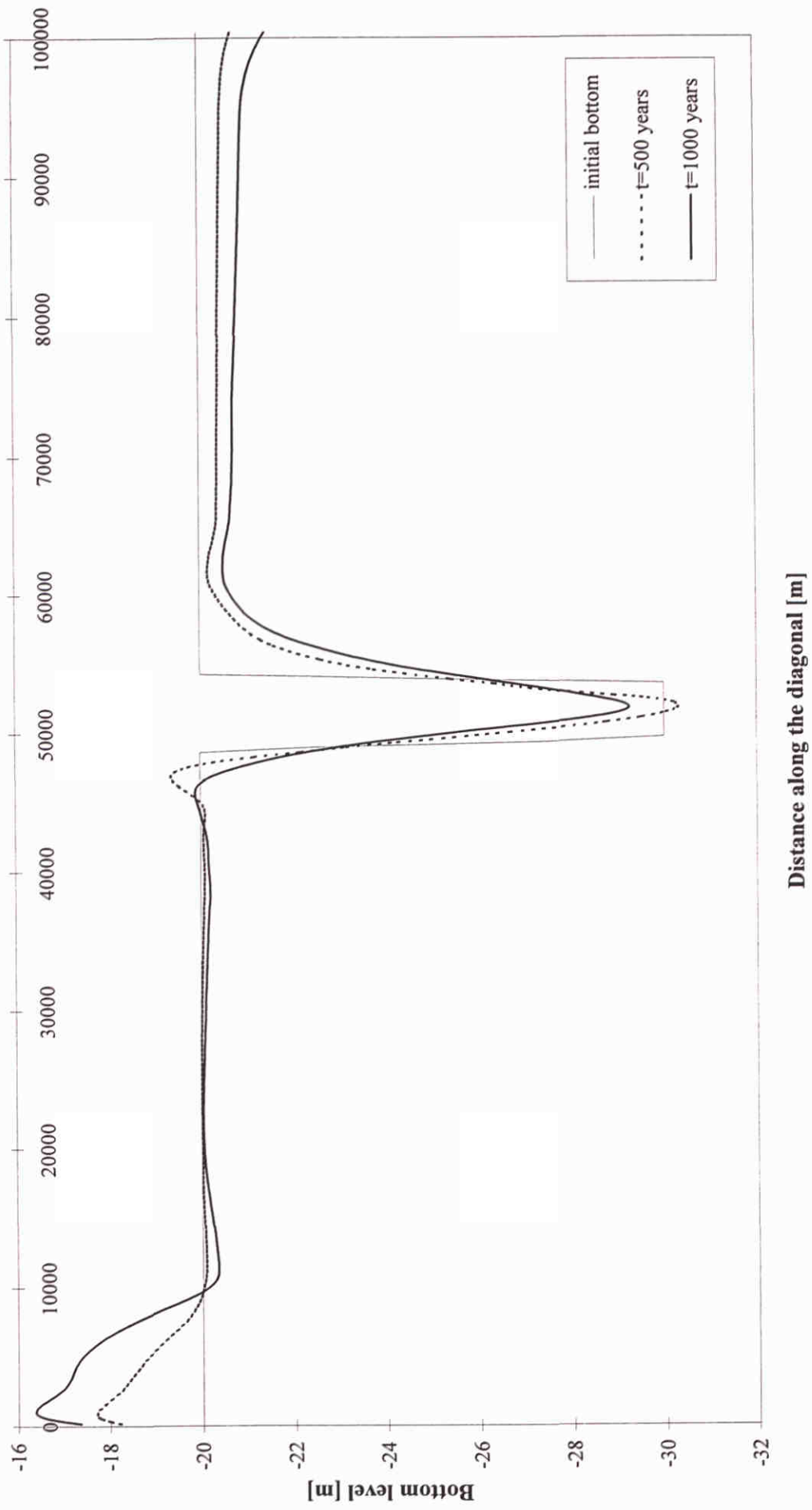
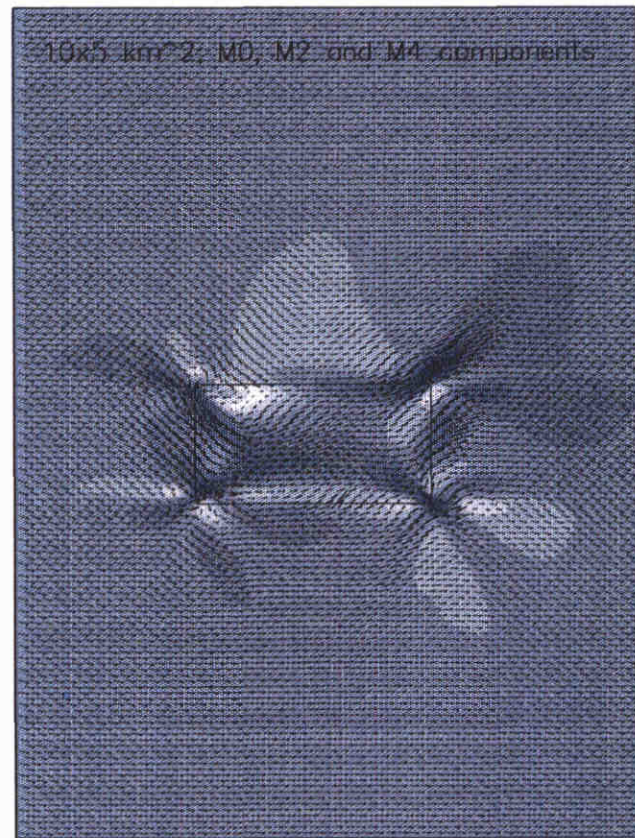
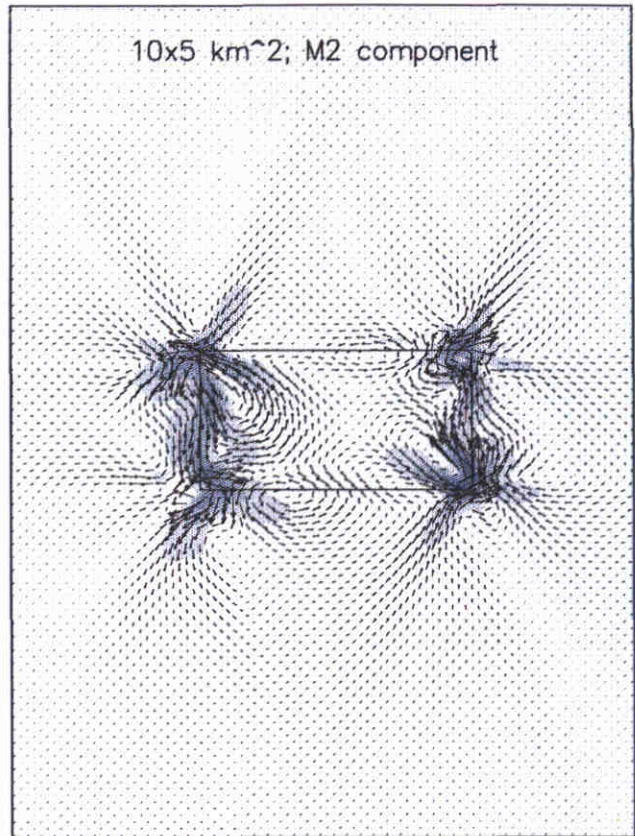
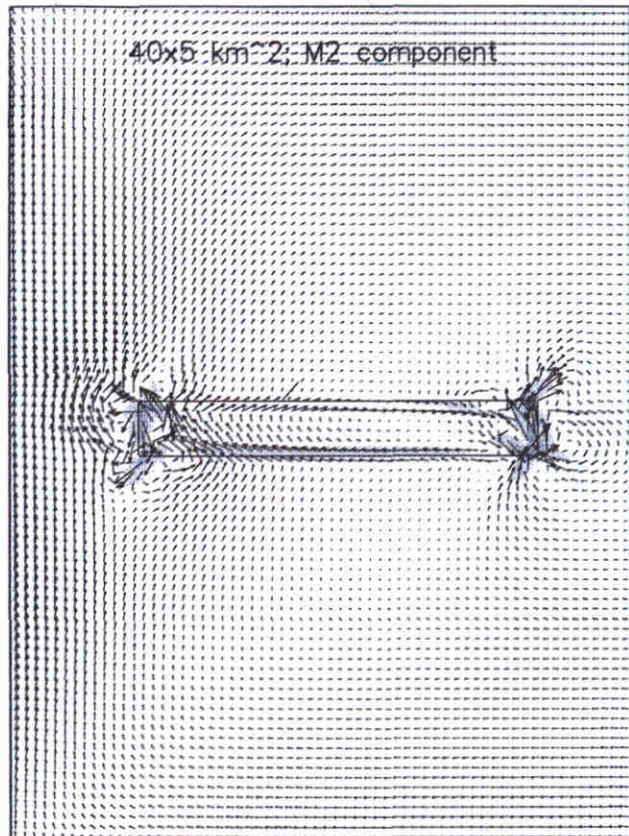


Figure 8.17c: Bottom levels in the center cross-section of a -45° rotated 25x5 km² sandpit



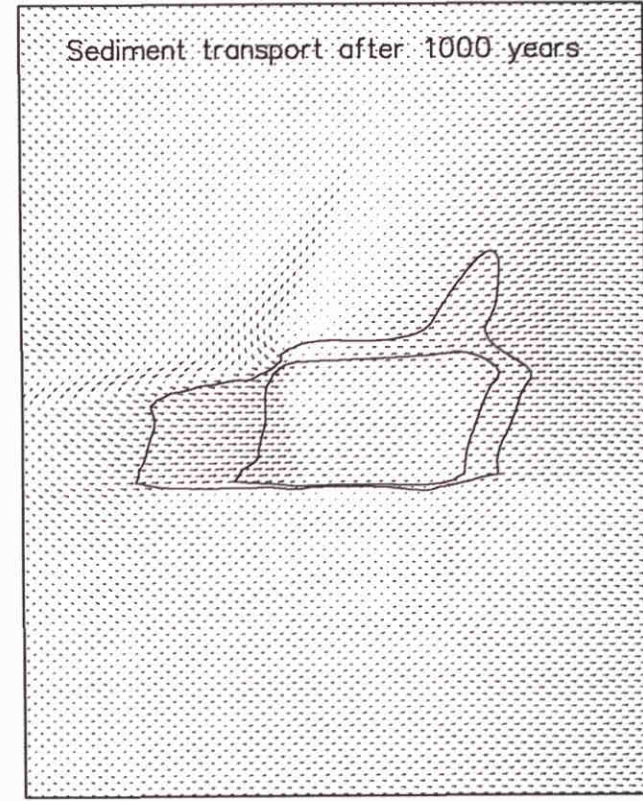
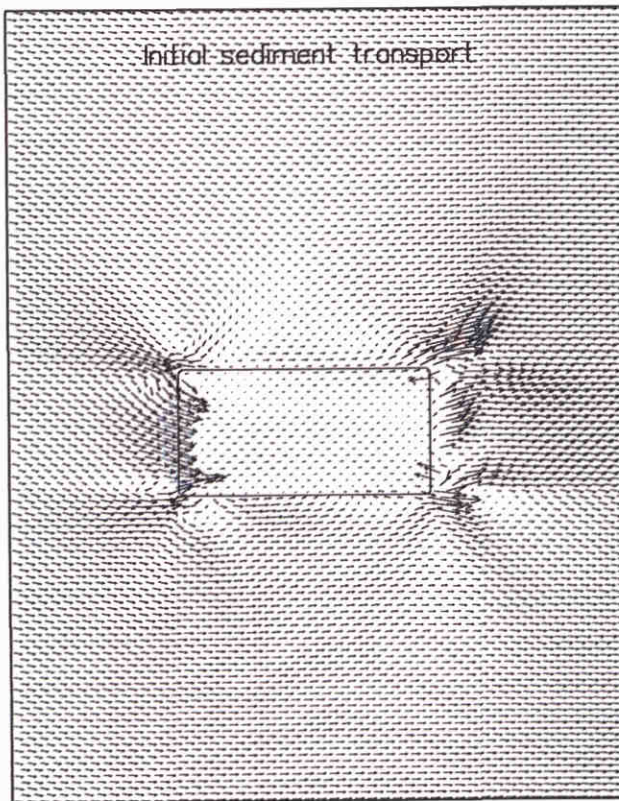
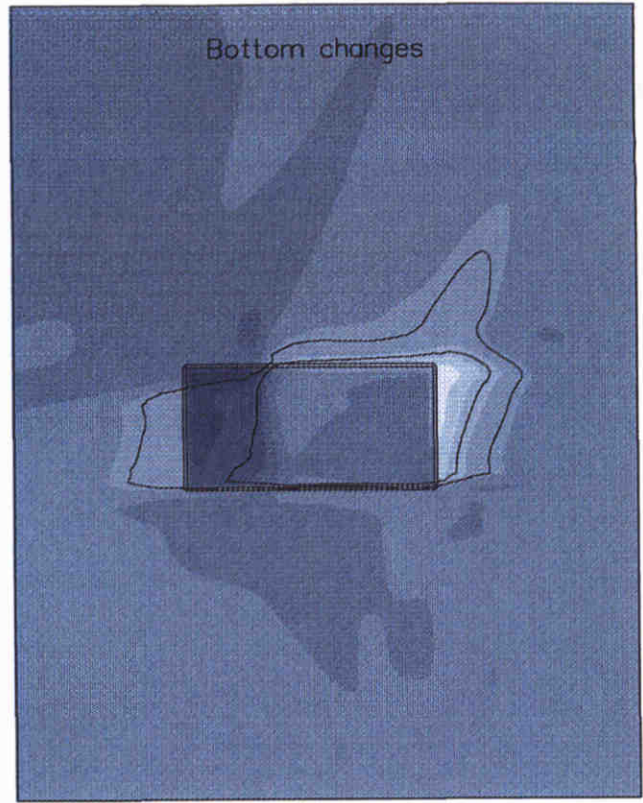
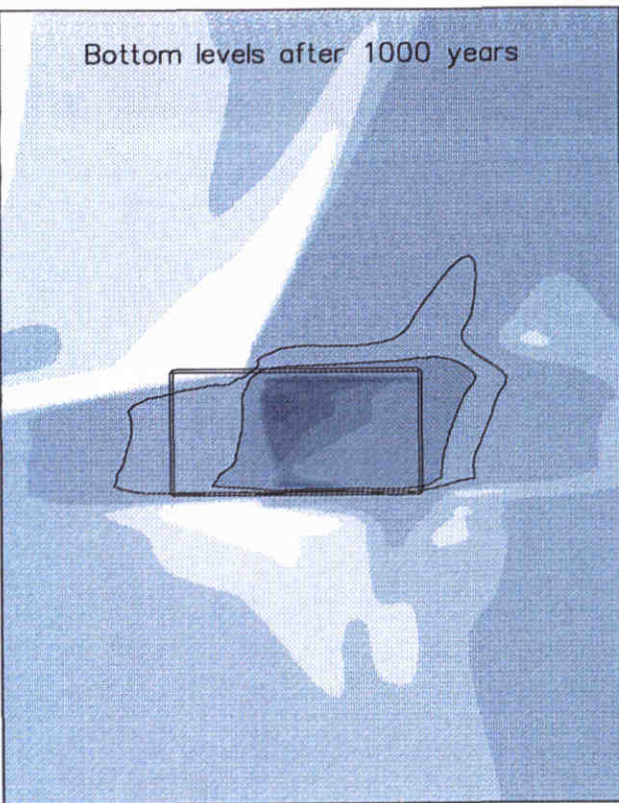
Distance along the diagonal [m]



Tide-averaged current velocities [m/s]

Influence of the tidal motion and the length on the averaged current pattern

Tidal boundary conditions including



Bottom levels and changes [m]; sediment transport [m^2/s]

Parallel 10x5 km^2 sandpit

Morphological results after 1000 years

Figure 8.19b: Bottom levels in the longitudinal section of a parallel $10 \times 5 \text{ km}^2$ sandpit

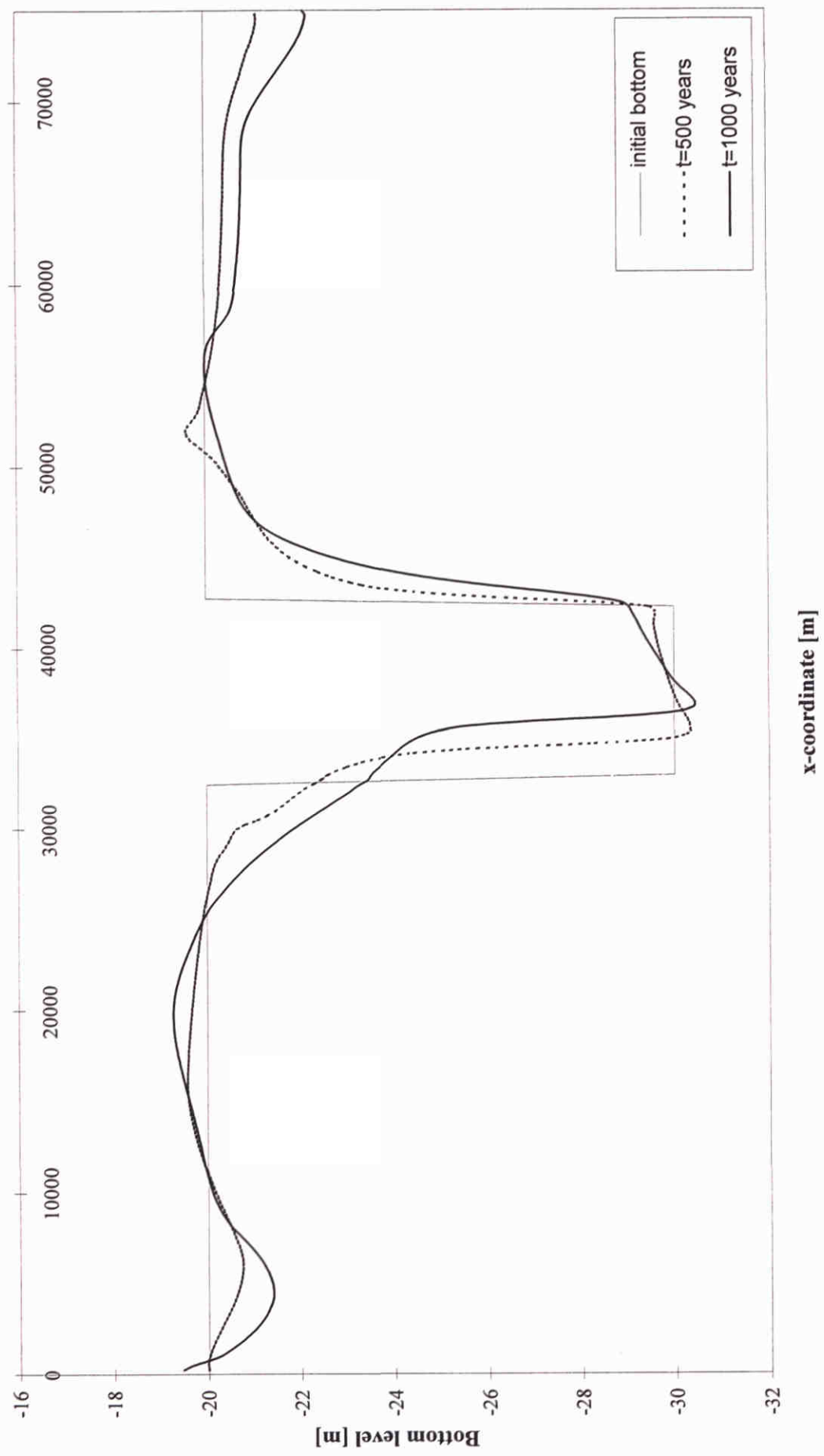
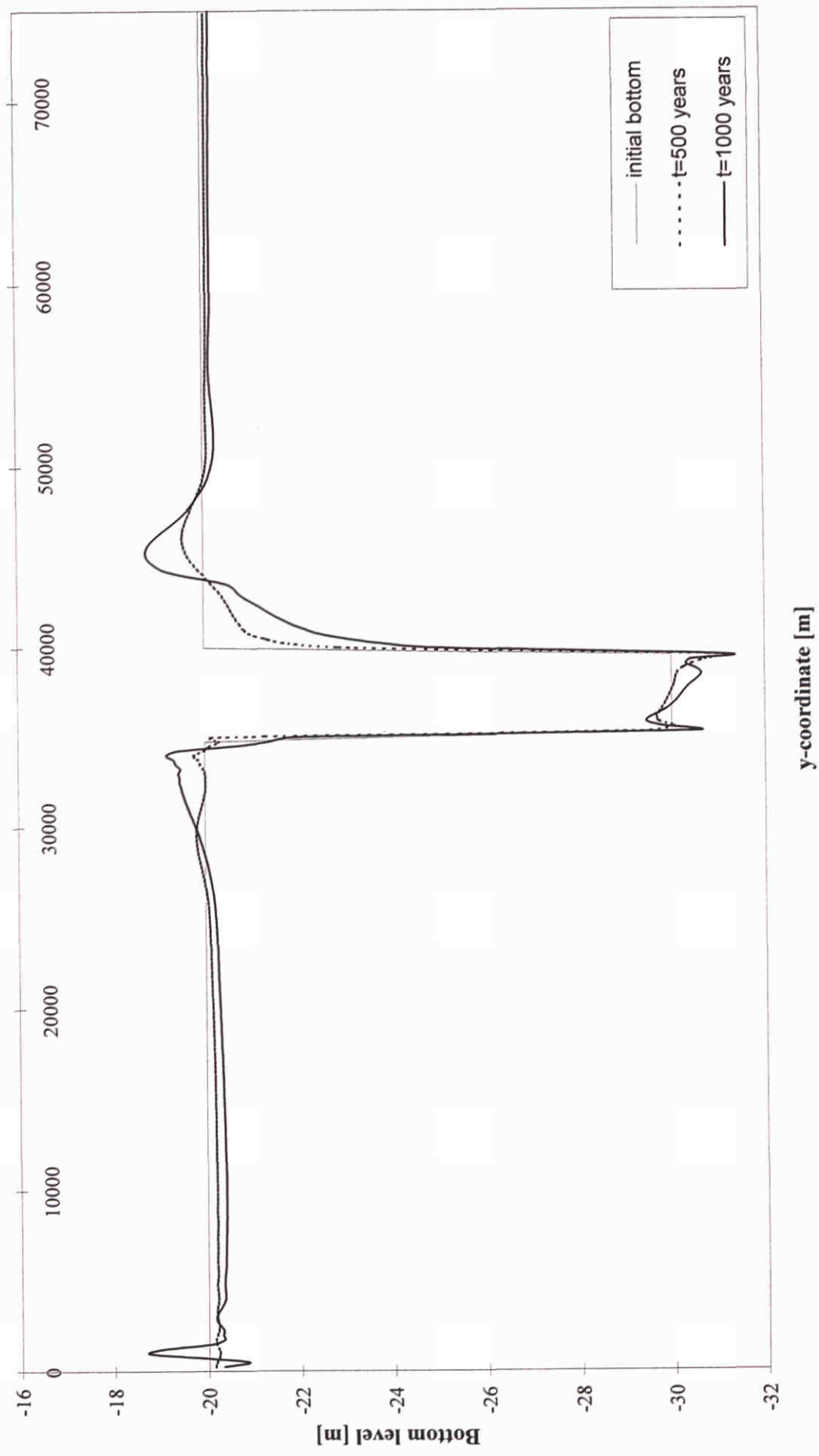
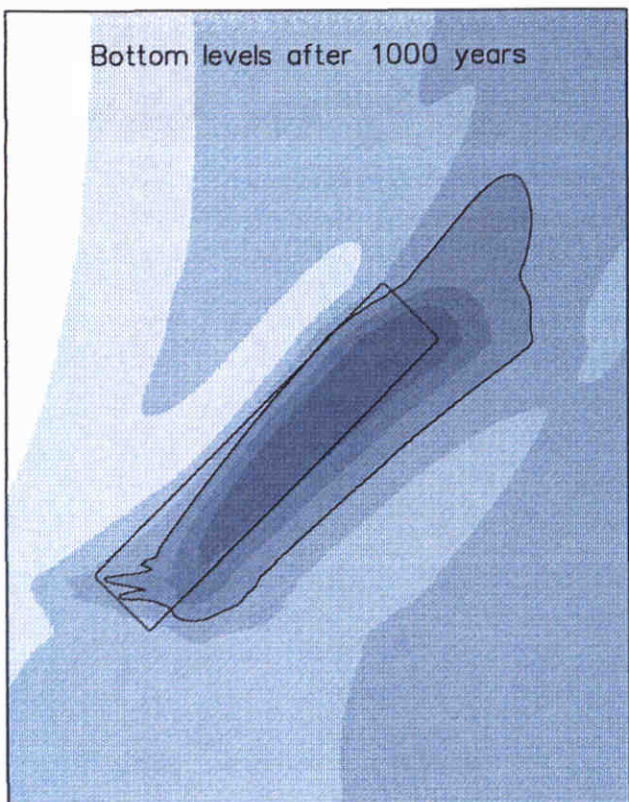
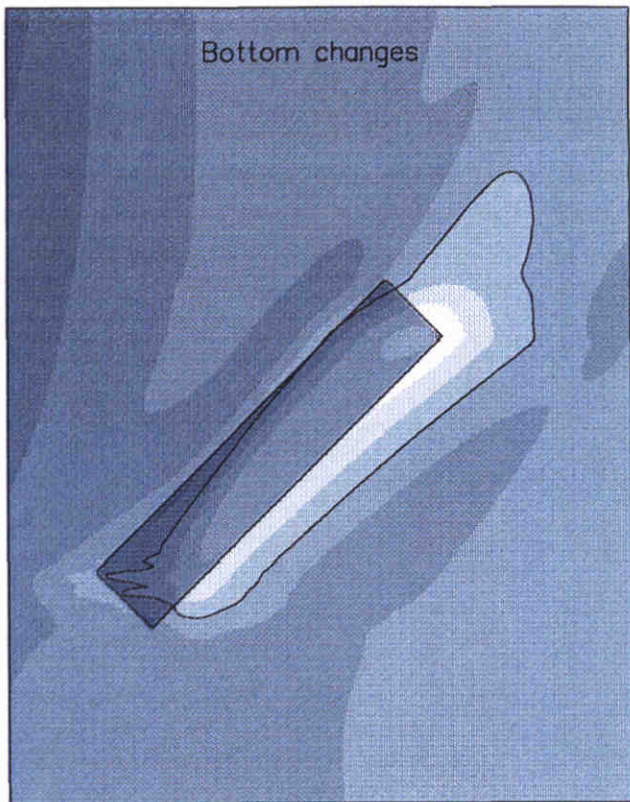


Figure 8.19c: Bottom levels in the center cross-section of a parallel $10 \times 5 \text{ km}^2$ sandpit

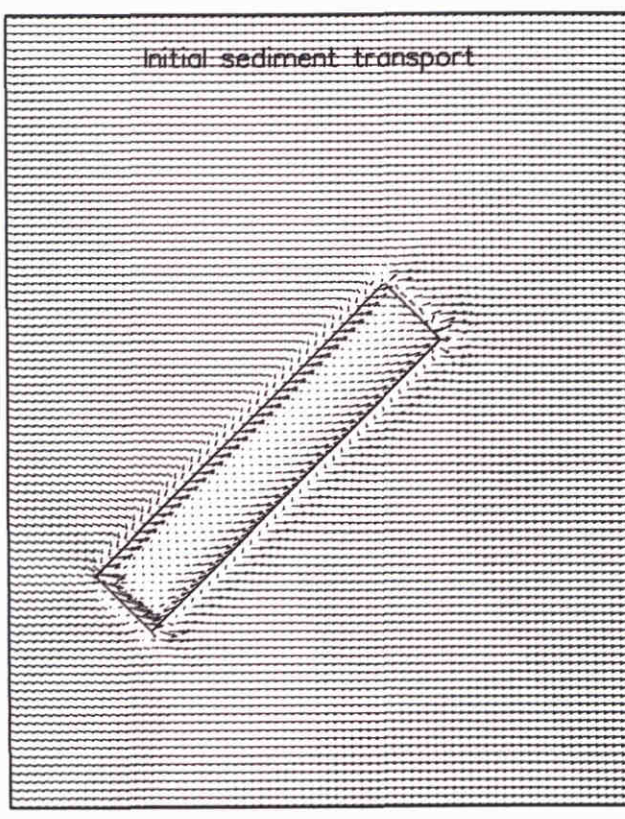




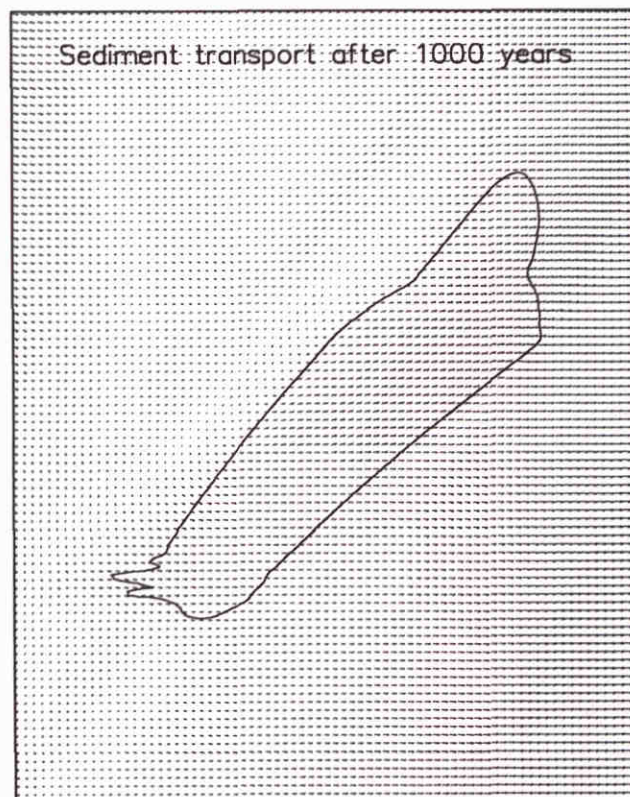
<19.5	<20.5	<21.5	>22.0
<20.0	<21.0	<22.0	



<-2.0	<-0.5	<1.0	>2.0
<-1.5	<0.0	<1.5	
<-1.0	<0.5	<2.0	



→ $2.0 \times 10^{-6} \text{ m}^2/\text{s}$



Bottom levels and changes [m]; sediment transport m^2/s
+45 degrees rotated, 22m deep $25 \times 5 \text{ km}^2$ sandpit
Morphological results after 1000 years

z2615

Figure 8.20a

Distance along the diagonal [m]

Figure 8.20b: Bottom levels in the center longitudinal section of a +45° rotated 25x5 km², 22m deep sandpit

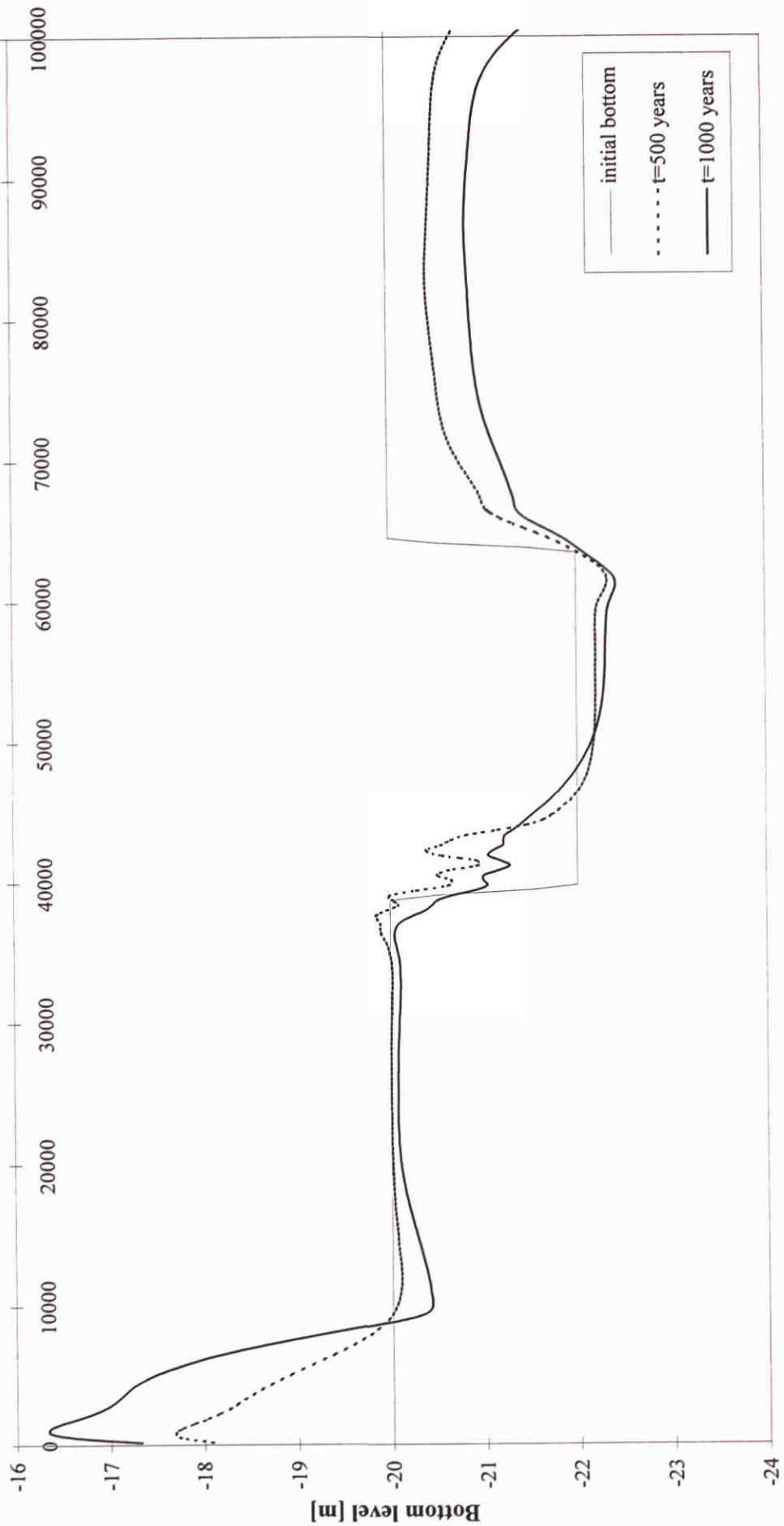
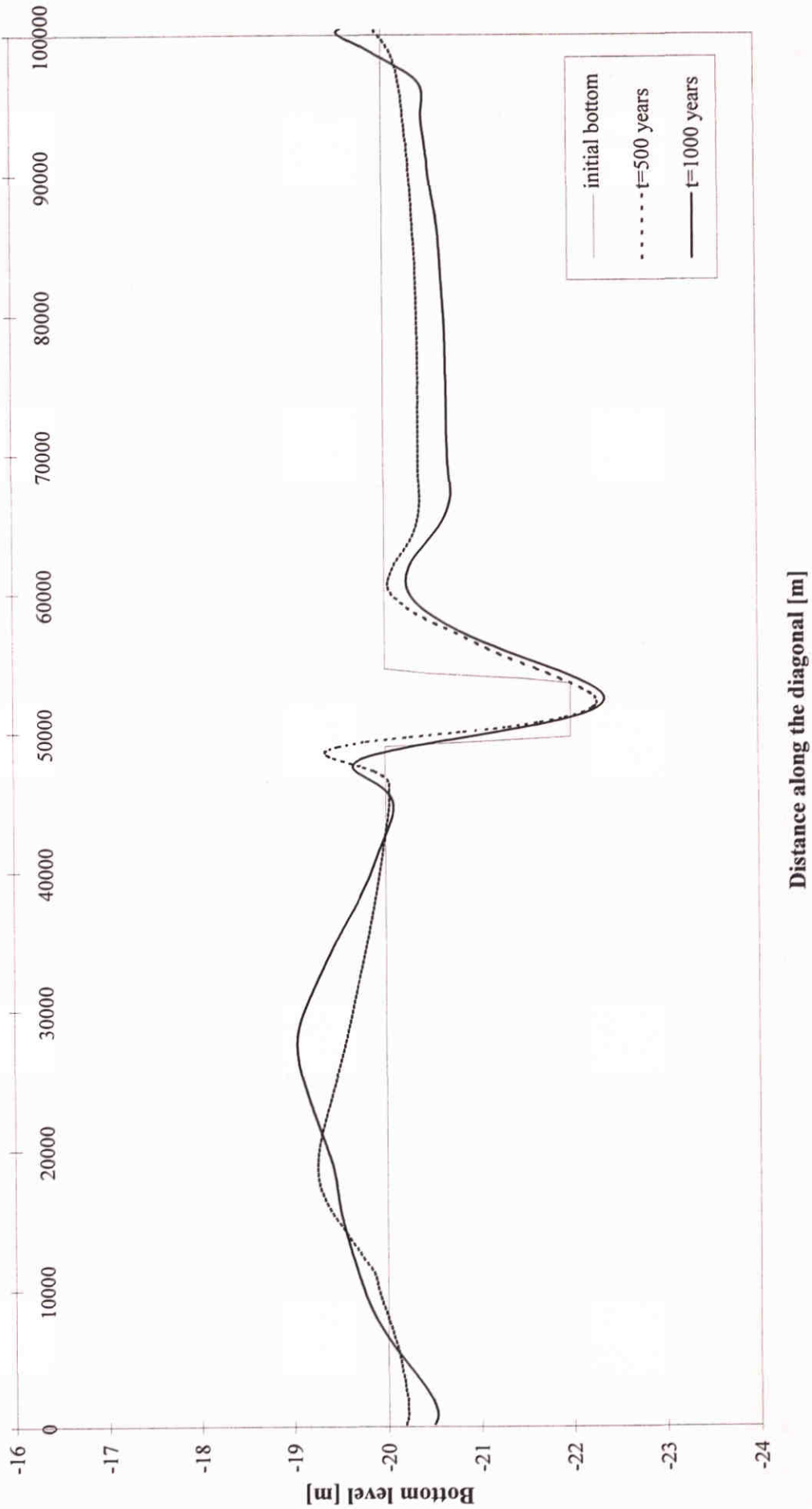
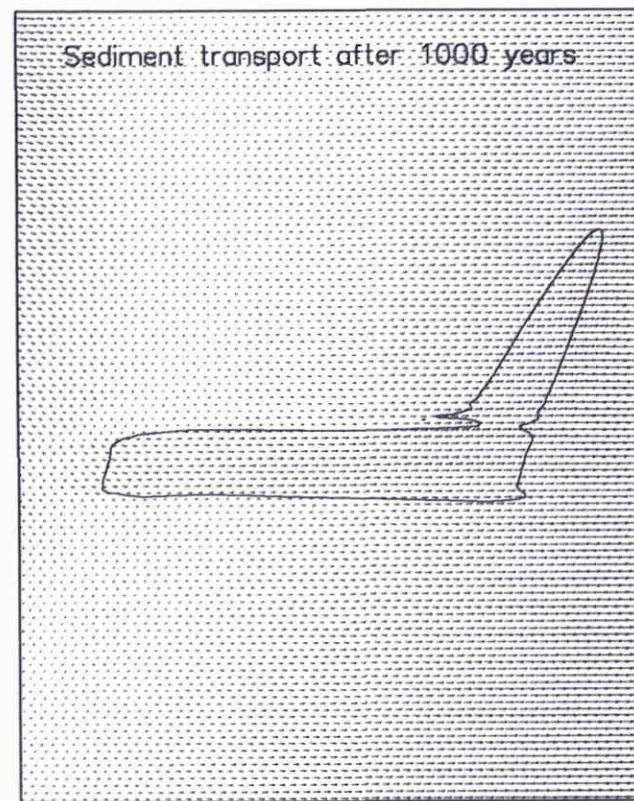
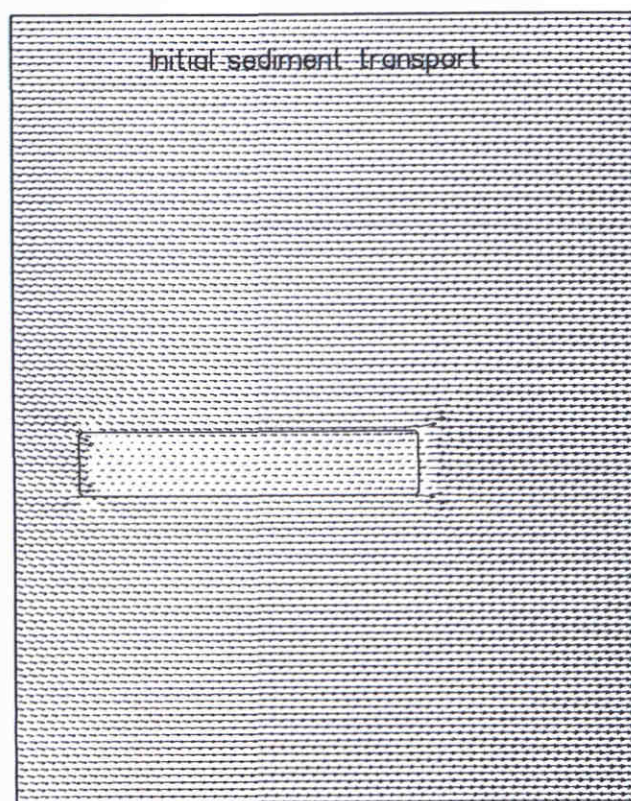
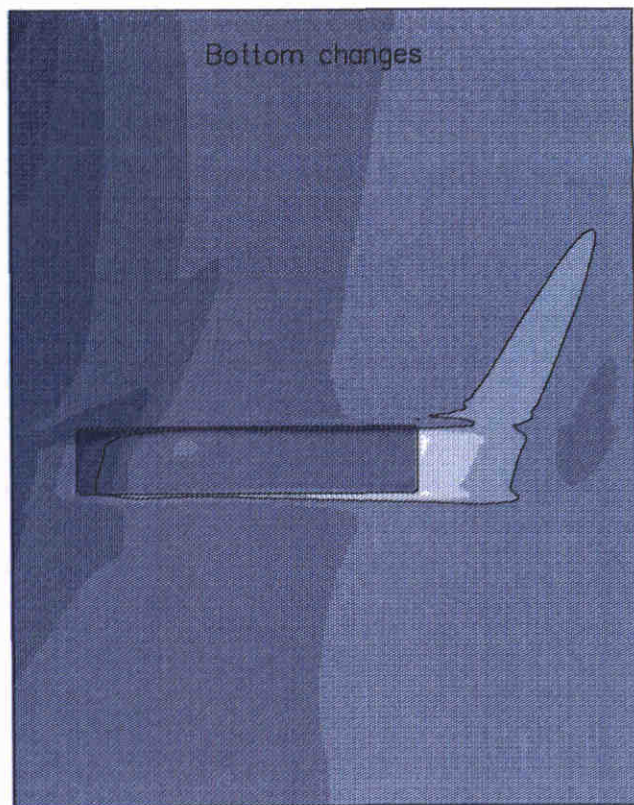
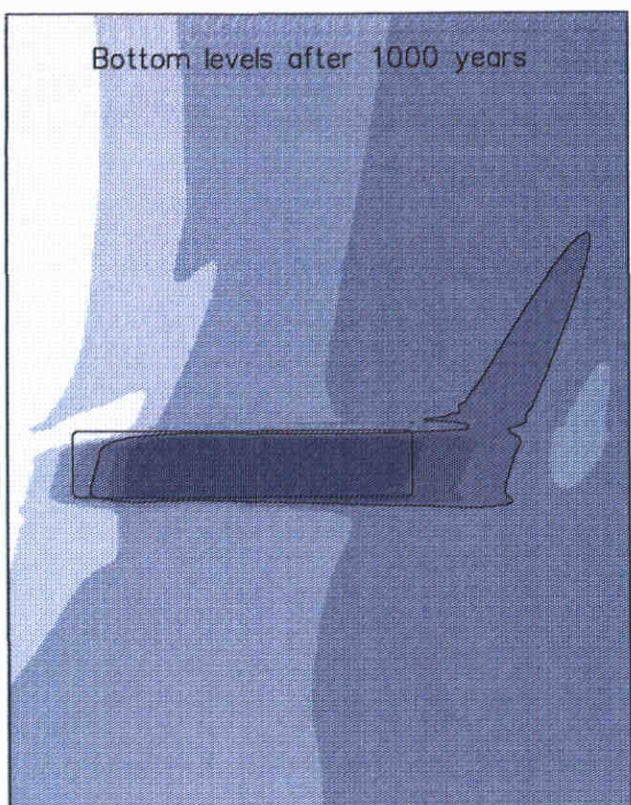


Figure 8.20c: Bottom levels in the center cross-section of a +45° rotated, 22 m deep 25x5 km² sandpit



Distance along the diagonal [m]



Bottom levels and changes [m]; sediment transport [m^2/s]

Parallel, 22 m deep 25x5 km²

Morphological results

Figure 8.21b: Bottom levels in the center longitudinal section of a parallel, 22 m deep, 25x5 km² sandpit

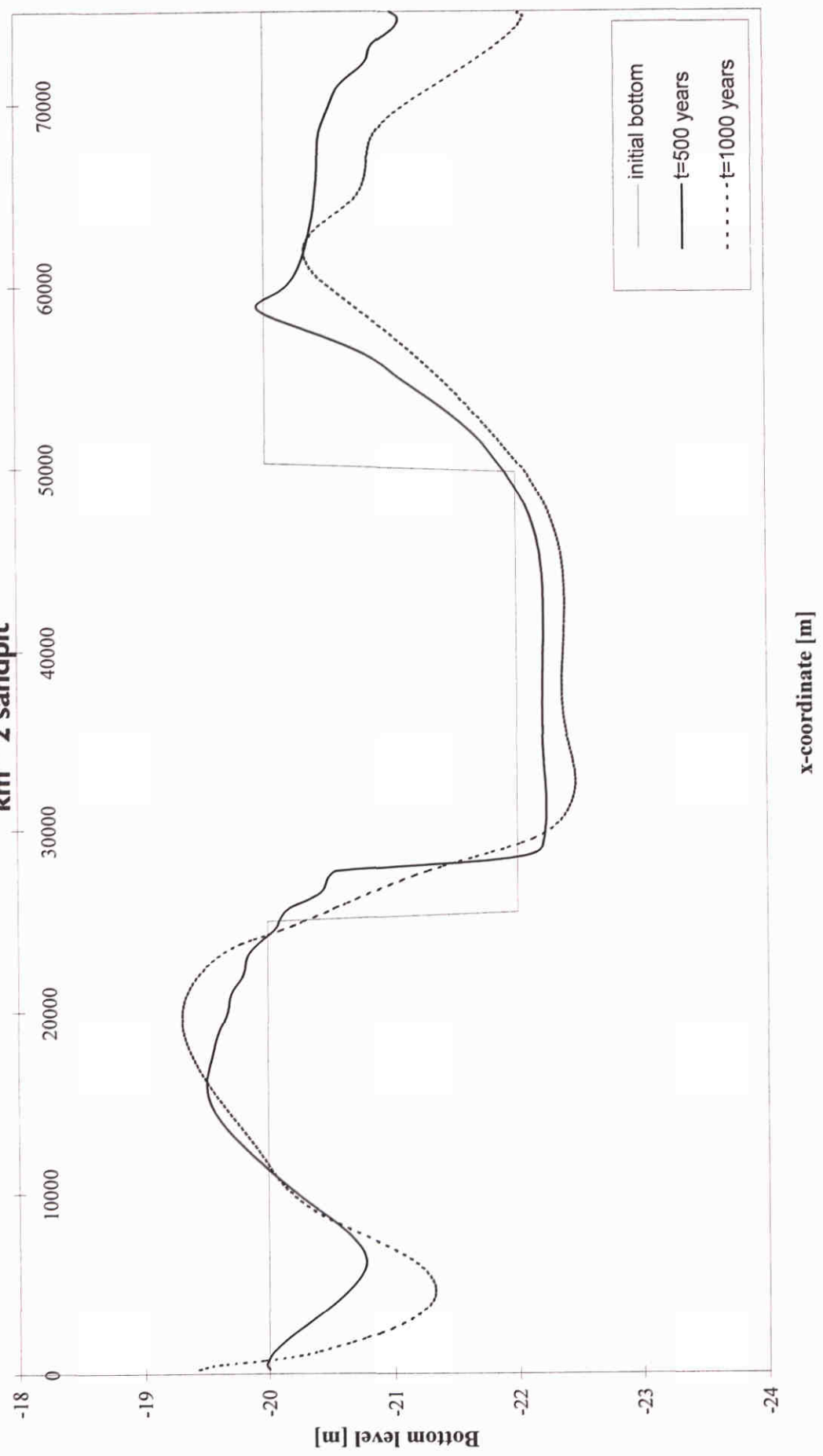
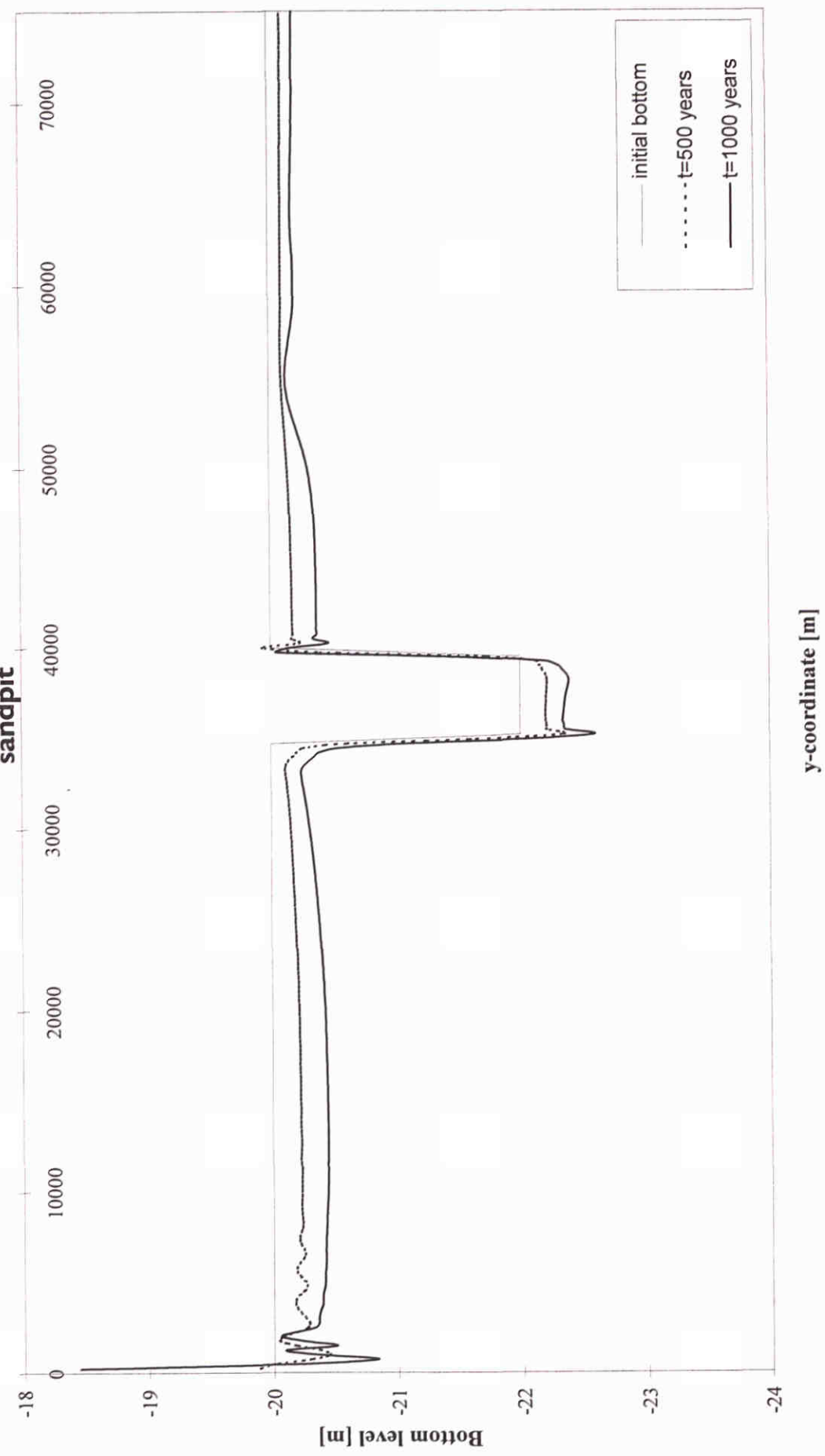
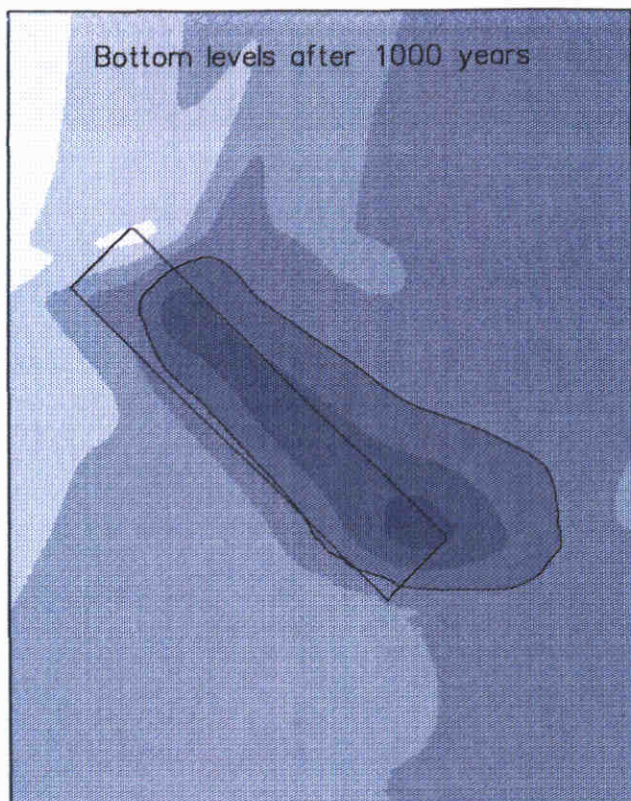
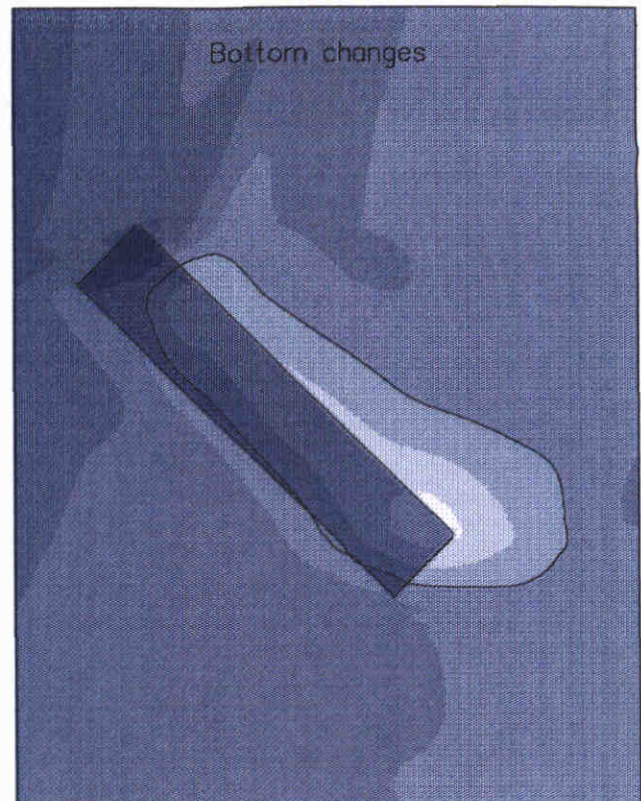


Figure 8.21c: Bottom levels in the center cross-section of a parallel, 22 m deep, $25 \times 5 \text{ km}^2$ sandpit

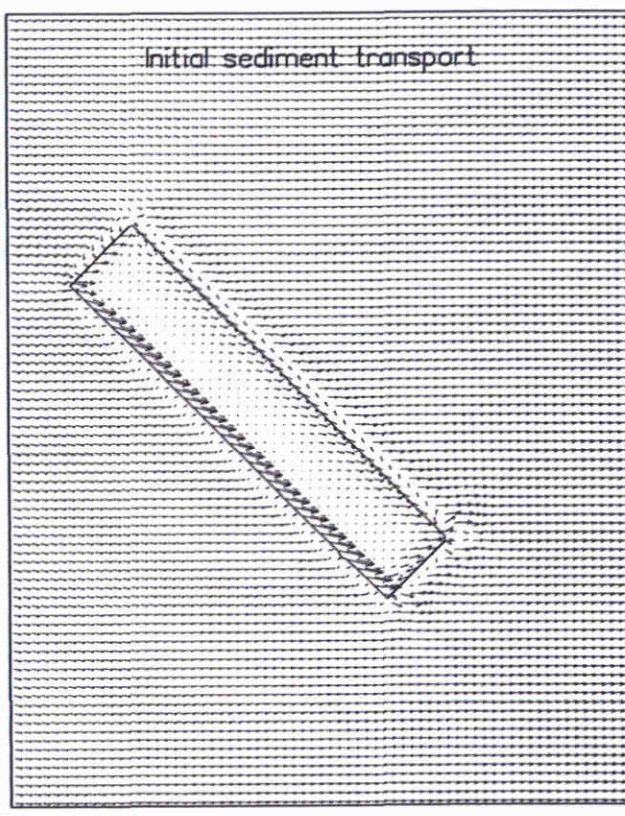




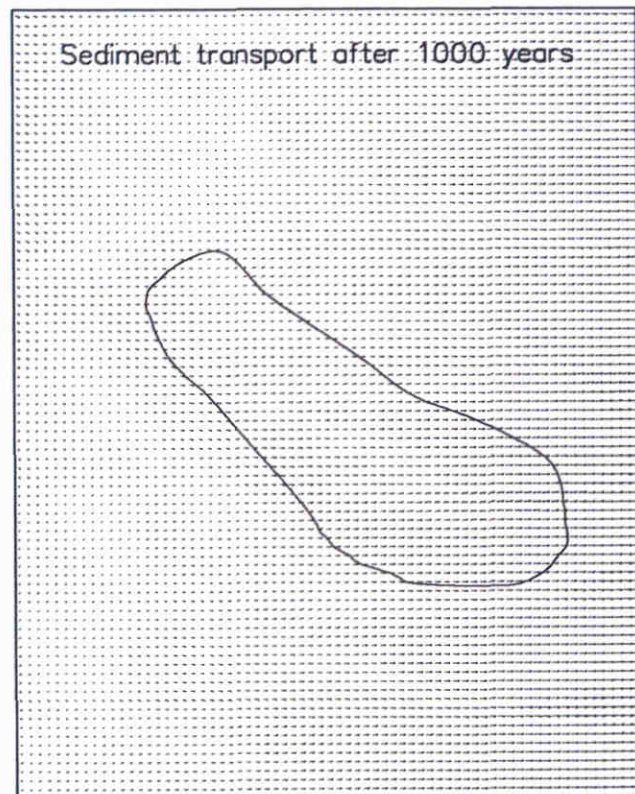
<19.5	<20.5	<21.5	>22.0
<20.0	<21.0	<22.0	



<-2.0	<-0.5	<1.0	>2.0
<-1.5	<0.0	<1.5	
<-1.0	<0.5	<2.0	



→ $2.0 \times 10^{-6} \text{ m}^2/\text{s}$



Bottom levels and changes [m]; sediment transport [m^2/s]

-45 degrees rotated, 22m deep $25 \times 5 \text{ km}^2$ sandpit

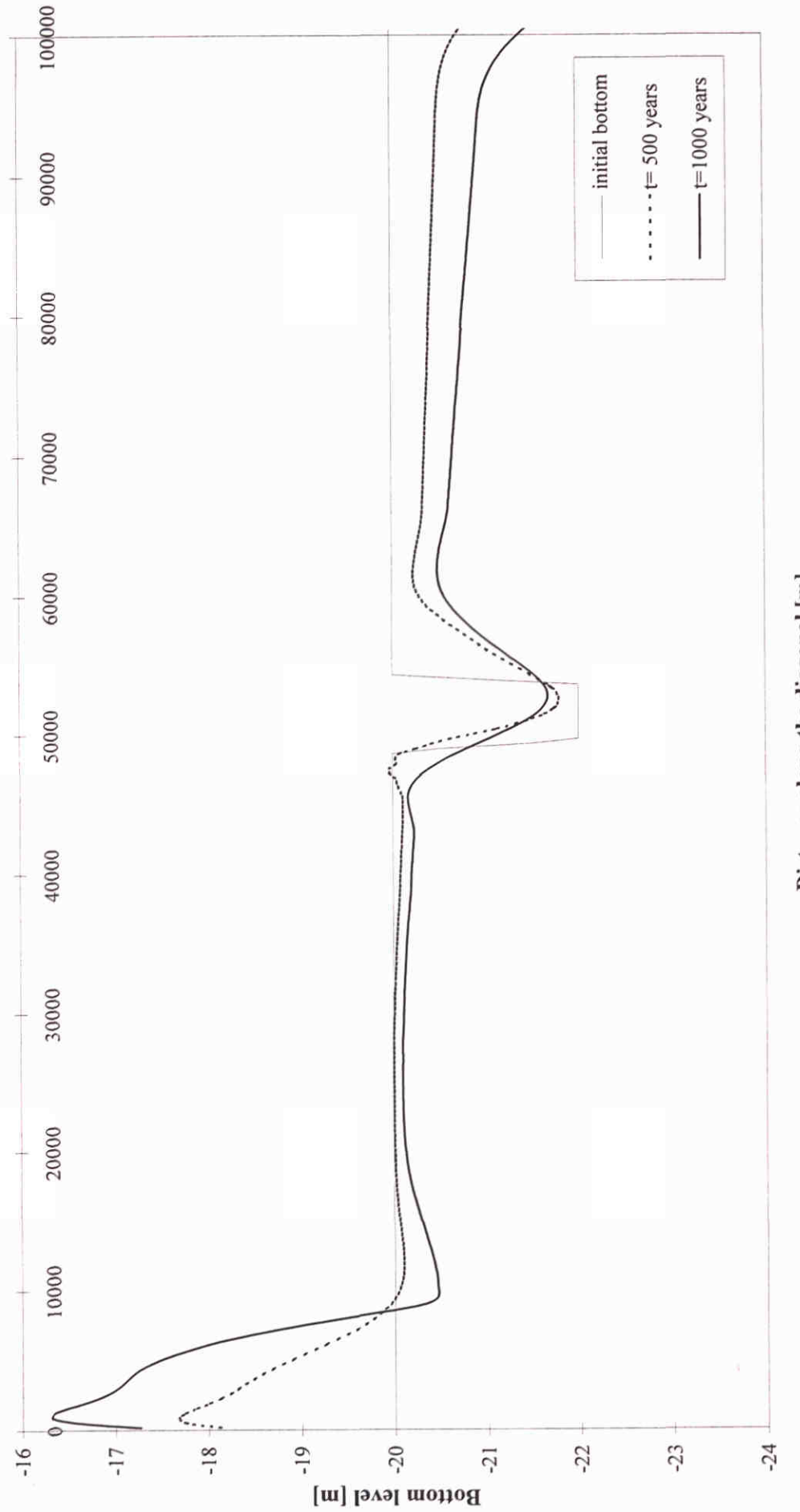
Morphological results after 1000 years

Figure 8.22b: Bottom levels in the longitudinal section of a +45° rotated, 22 m deep 25x5 km \wedge 2 sandpit

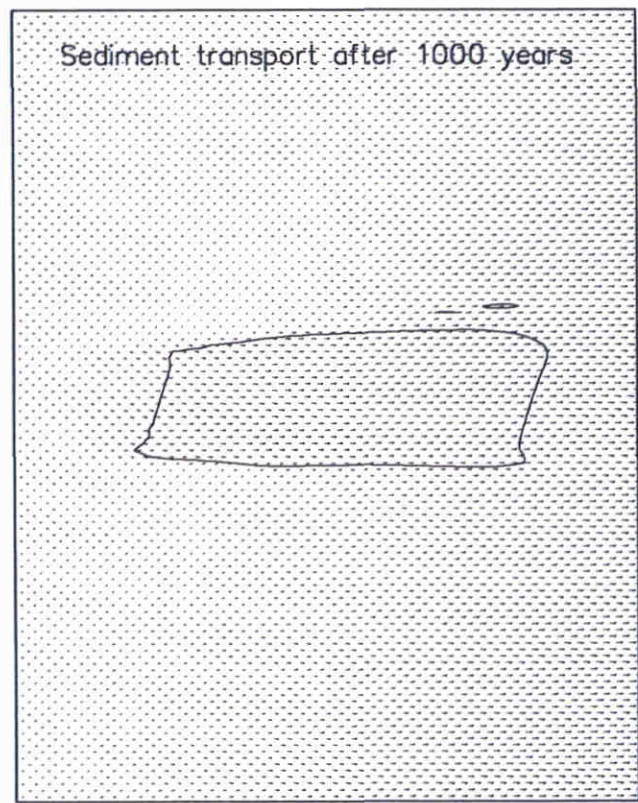
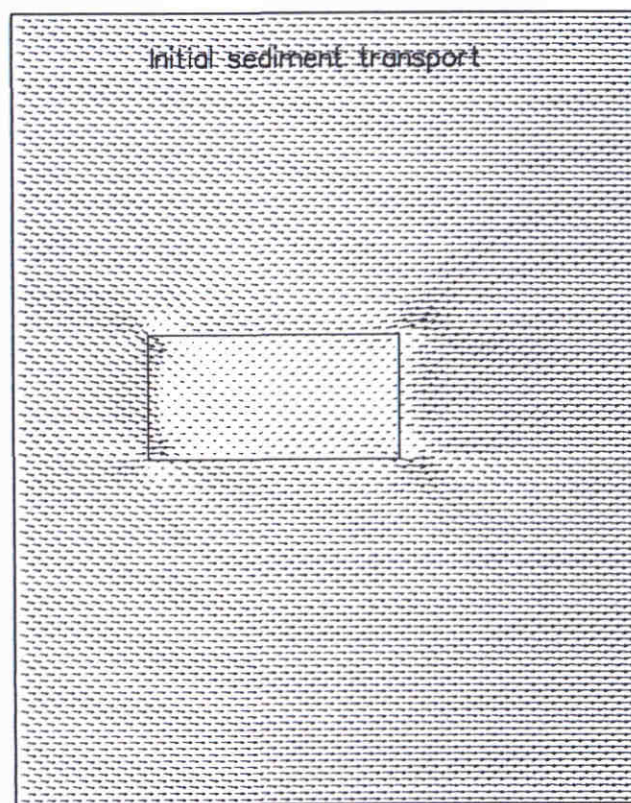
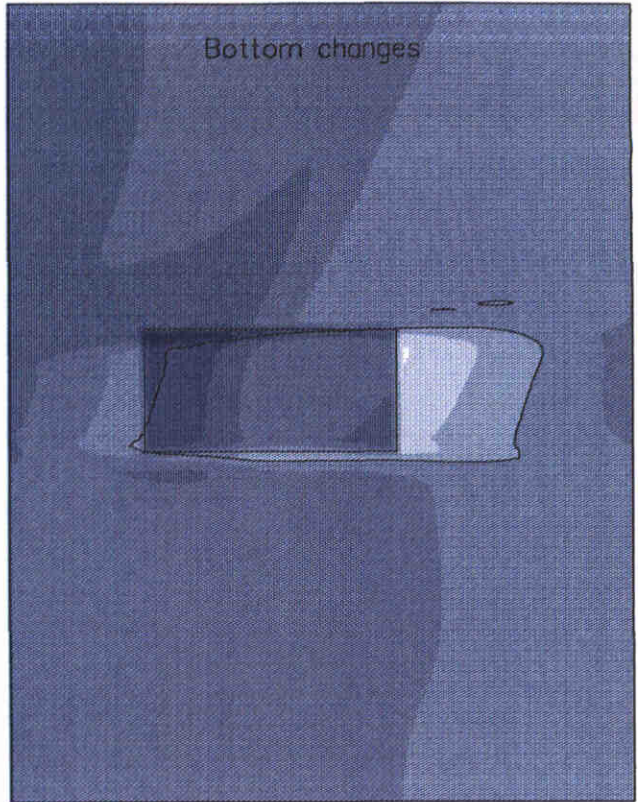
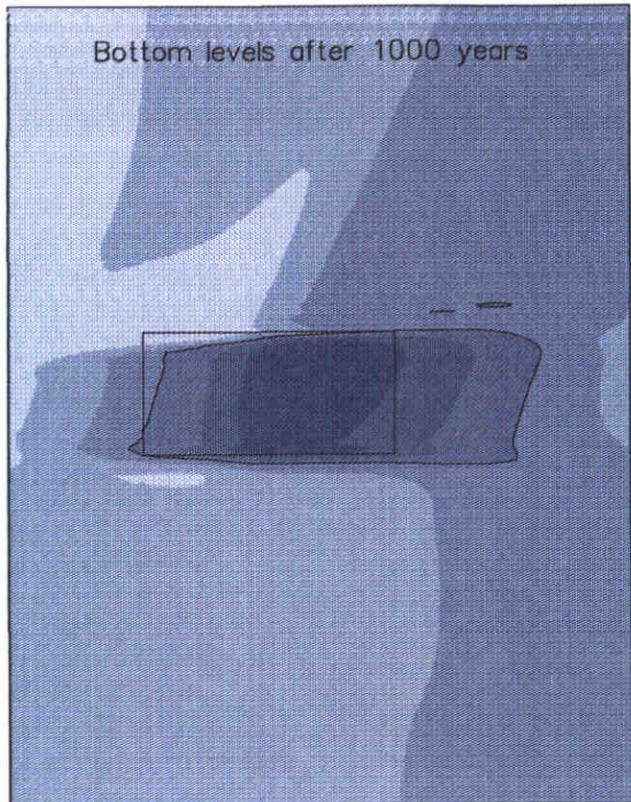


Distance along the diagonal [m]

Figure 8.22c: Bottom levels in the center cross-section of a -45° rotated, 22m deep 25x5 km² sandpit



Distance along the diagonal [m]

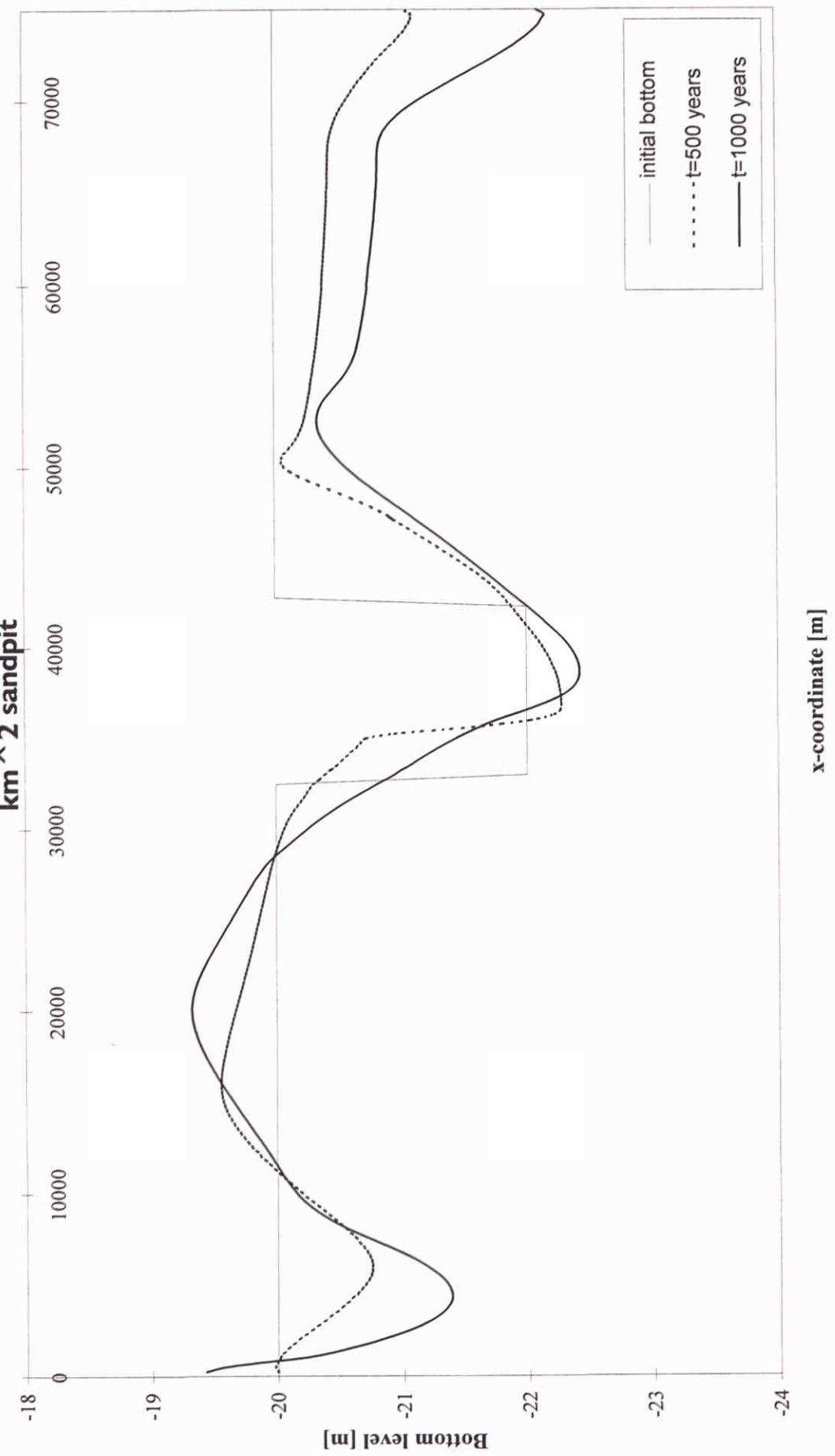


Bottom levels and changes [m]; sediment transport [m^2/s]

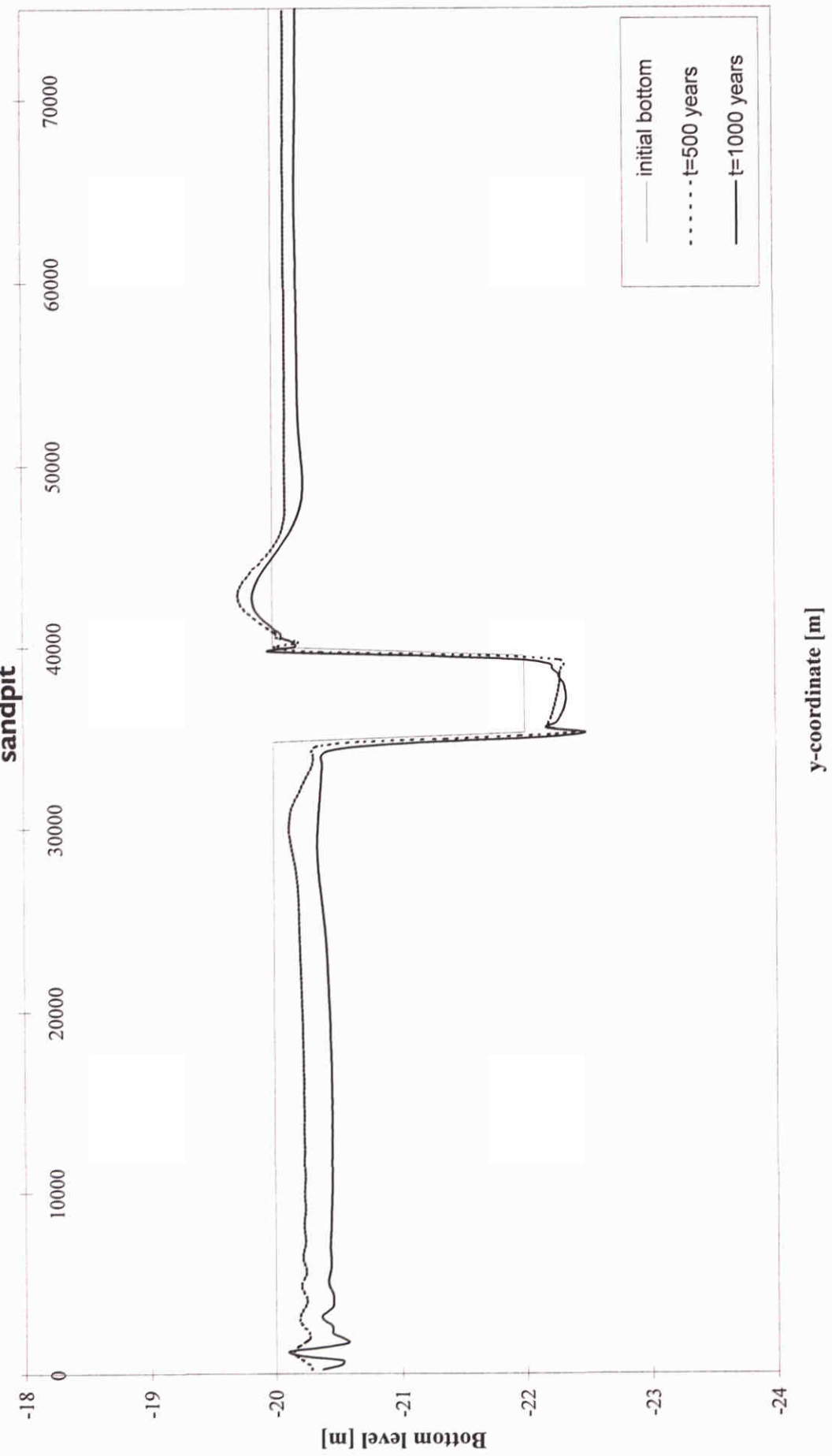
Parallel, 22 m deep 10x5 km² sandpit

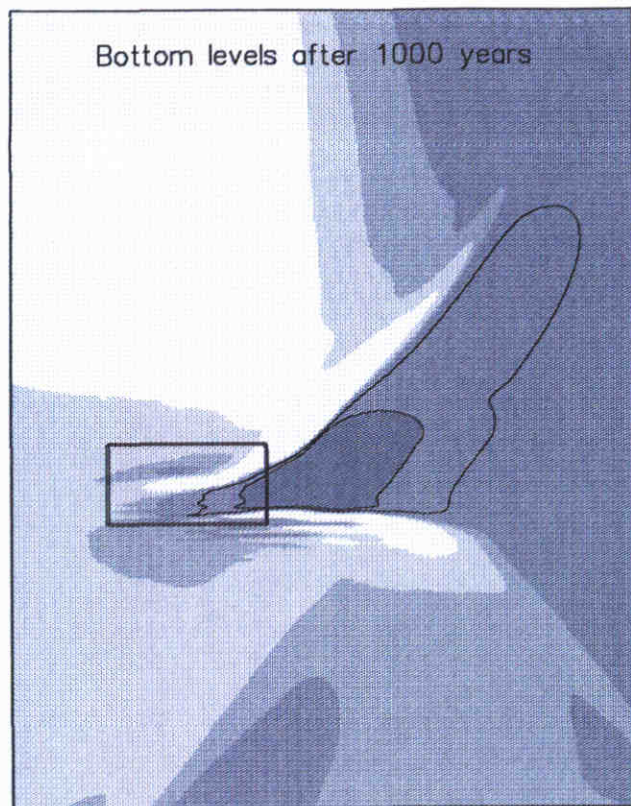
Morphological results after 1000 years

Figuur 8.23b: Bottom levels in the center longitudinal section of parallel, 22 m deep 10x5 km \sim 2 sandpit

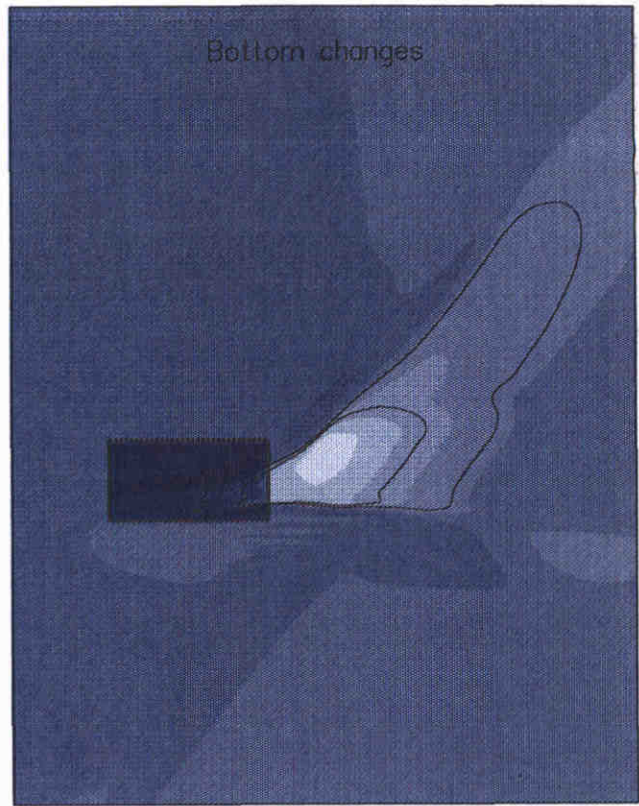


Figuur 8.23c: Bottom levels in the center cross-section of parallel, 22 m deep $10 \times 5 \text{ km}^2$ sandpit

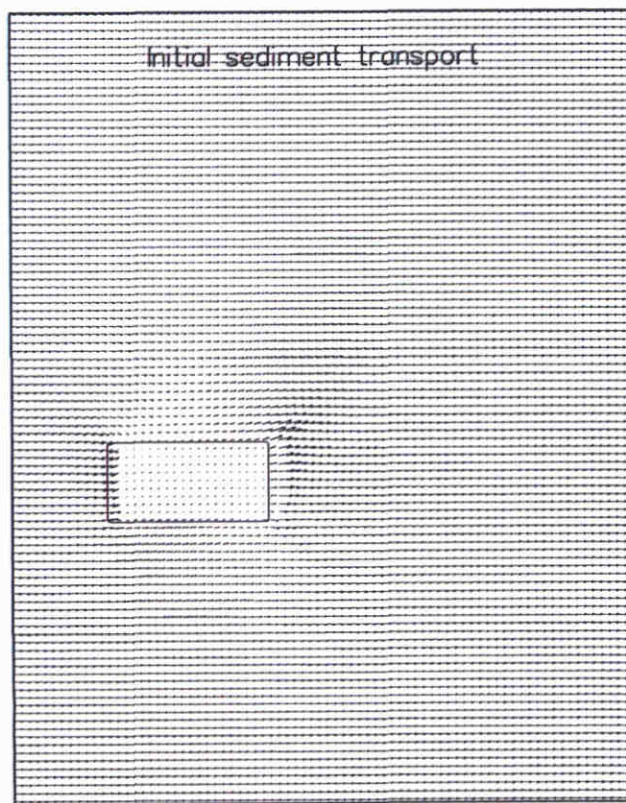




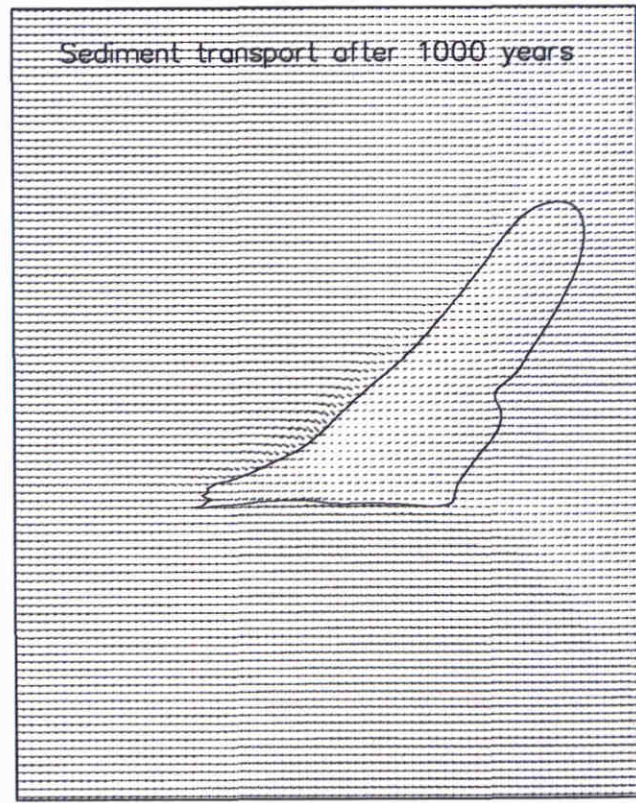
<19.5	<20.5	<29.5	<30.5
>20.0	>25.0	>30.0	>30.5



<-10.0	<-4.0	<2.0	<8.0
<-8.0	<-2.0	<4.0	<10.0
<-6.0	<0.0	<6.0	>10.0



→ $1.0 \times 10^{-5} \text{ m}^2/\text{s}$



Bottom levels and changes [m]; sediment transport [m^2/s]

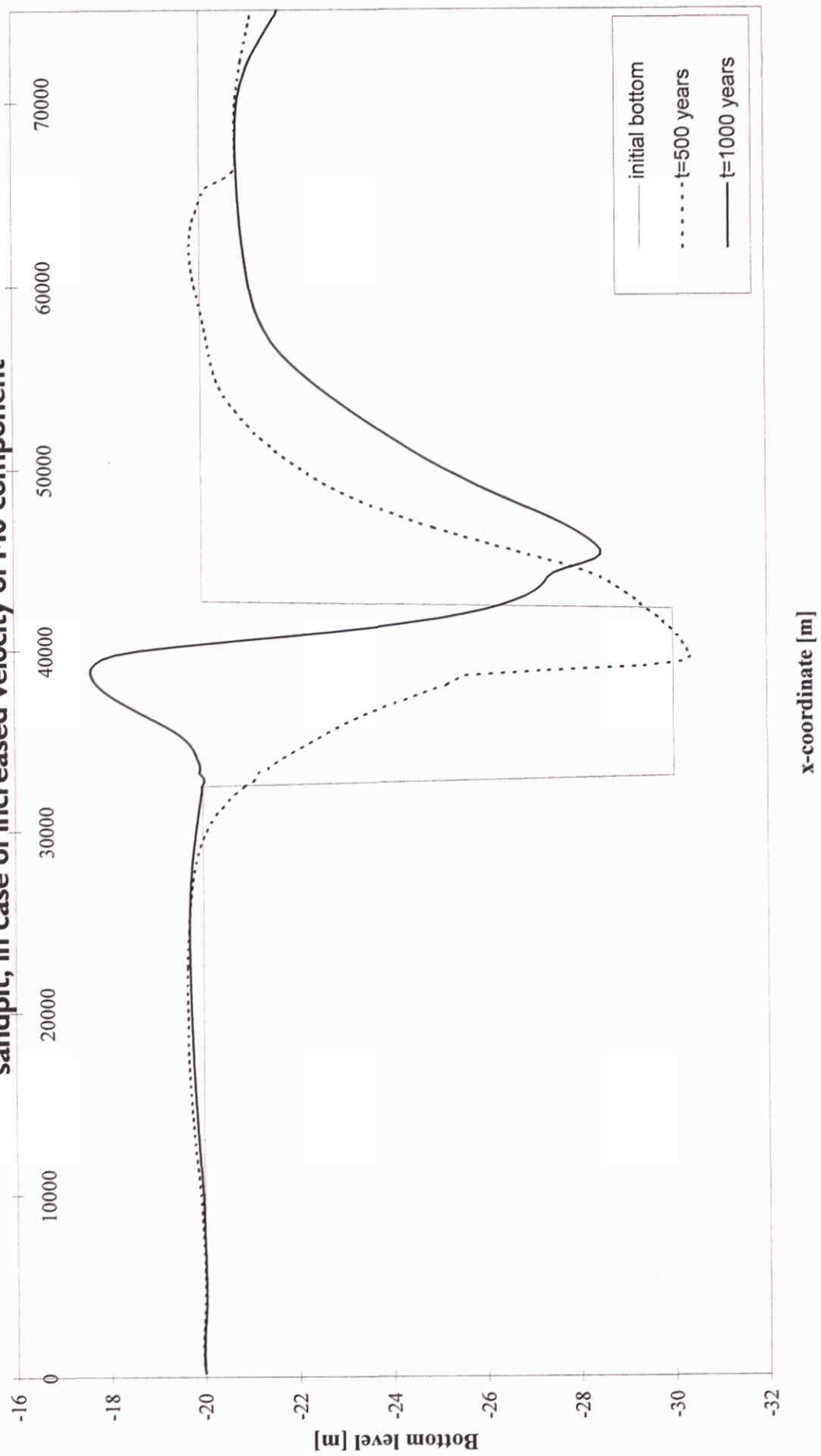
Parallel 10x5 km² sandpit; variant with increased MO velocity

Morphological results after 1000 years

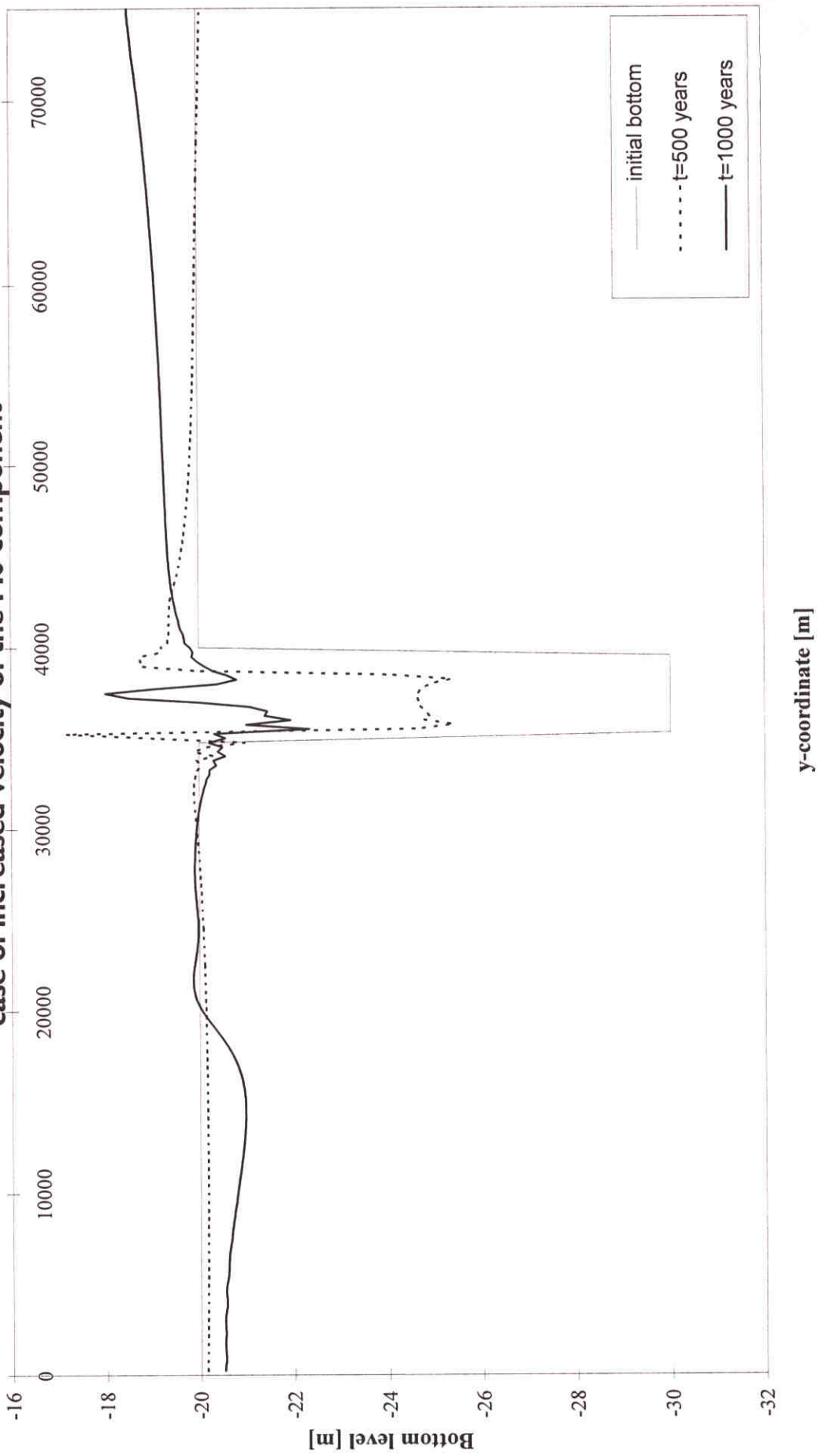
z2615

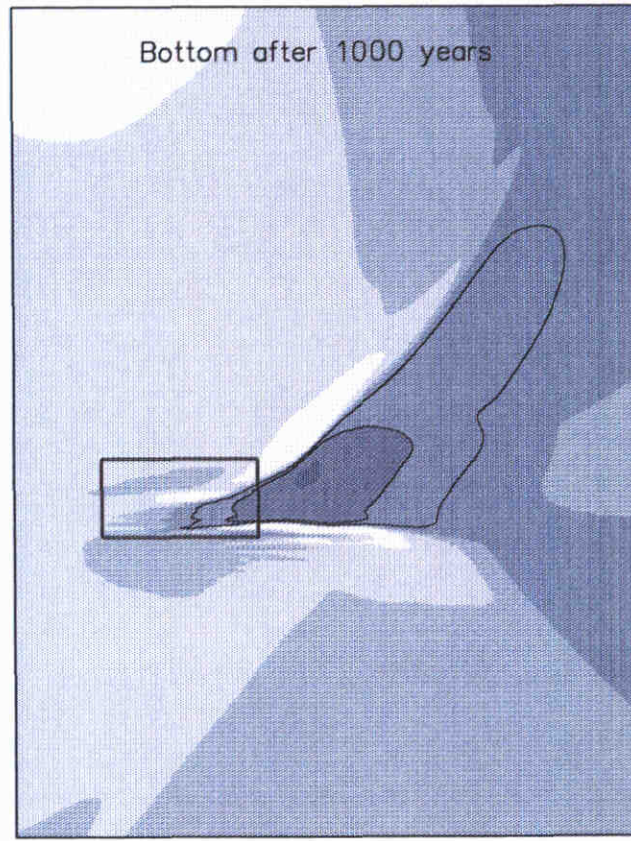
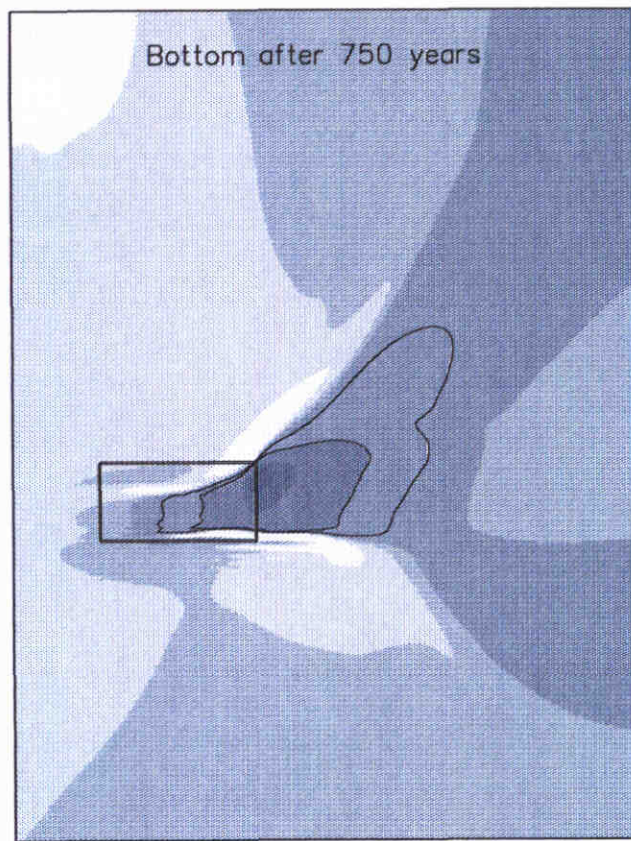
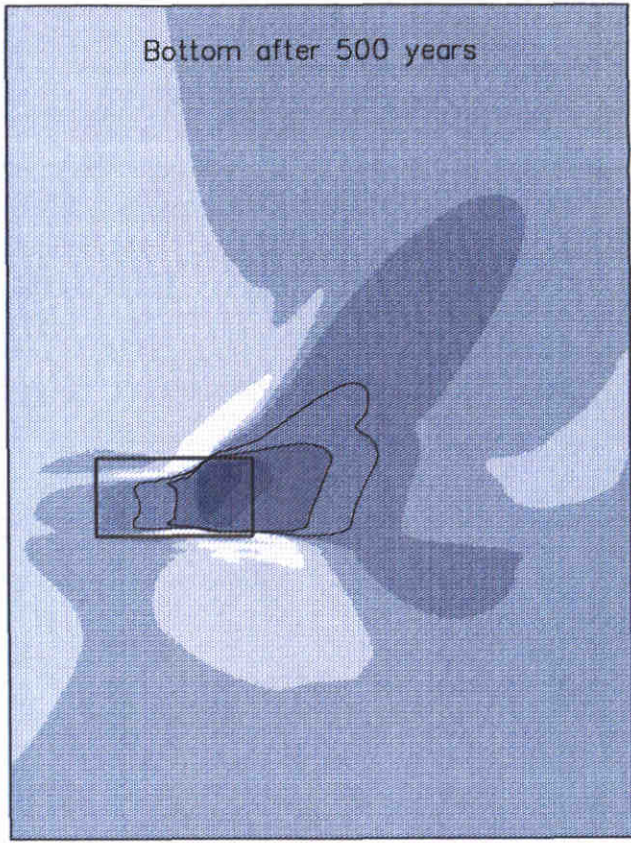
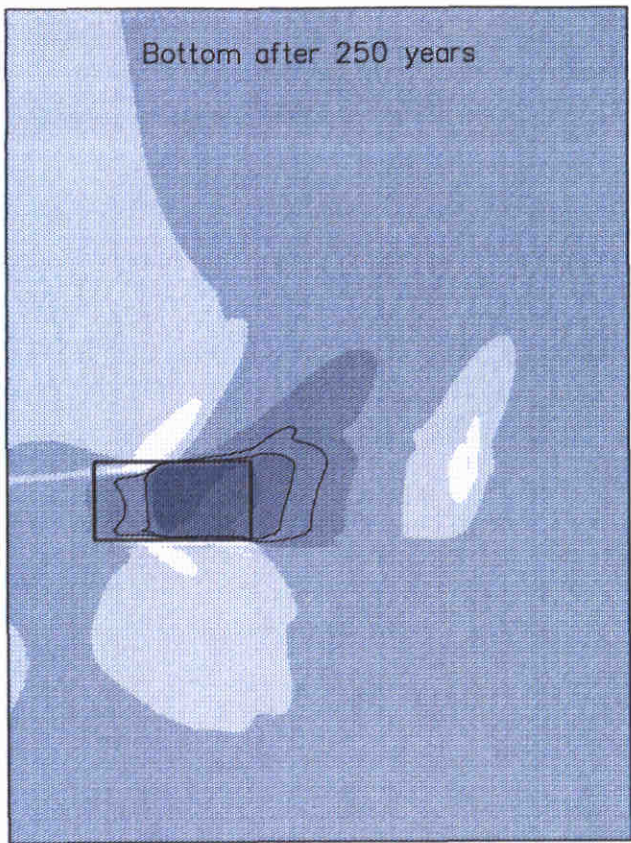
Figure 8.24a

Figuur 8.24b: Bottom levels in the center longitudinal section of a parallel $24 \times 5 \text{ km}^2$ sandpit, in case of increased velocity of M0 component



Figuur 8.24c: Bottom levels in the center cross-section of a parallel $10 \times 5 \text{ km}^2$ sandpit, in case of increased velocity of the M0 component



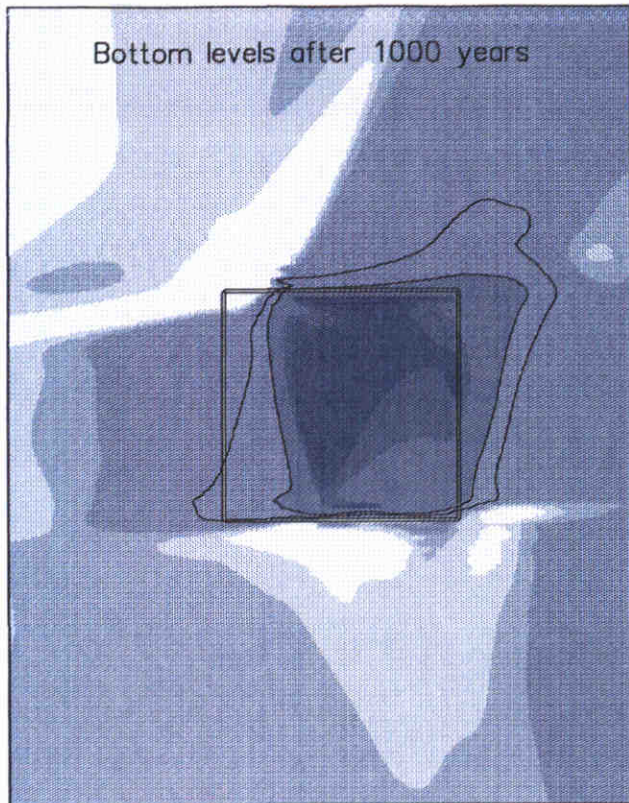


<19.0	<21.0	<29.0	<31.0
<20.0	<25.0	<30.0	>31.0

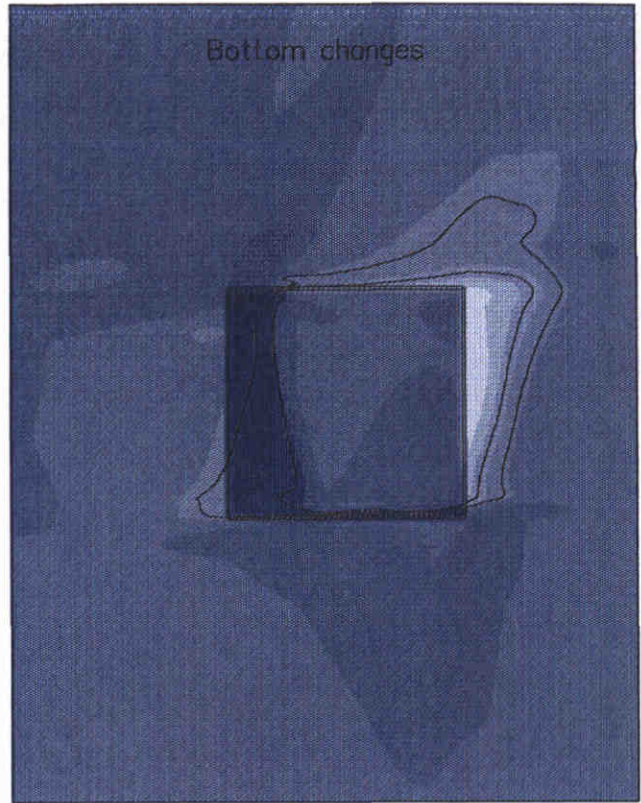
Bottom levels [m]

Parallel 10x5 km² sandpit; velocity variant

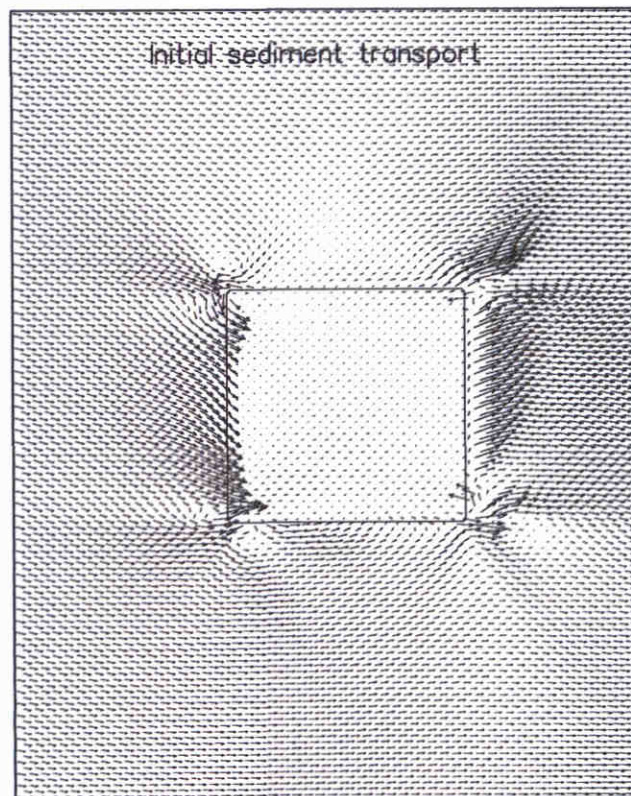
Morphological development in time



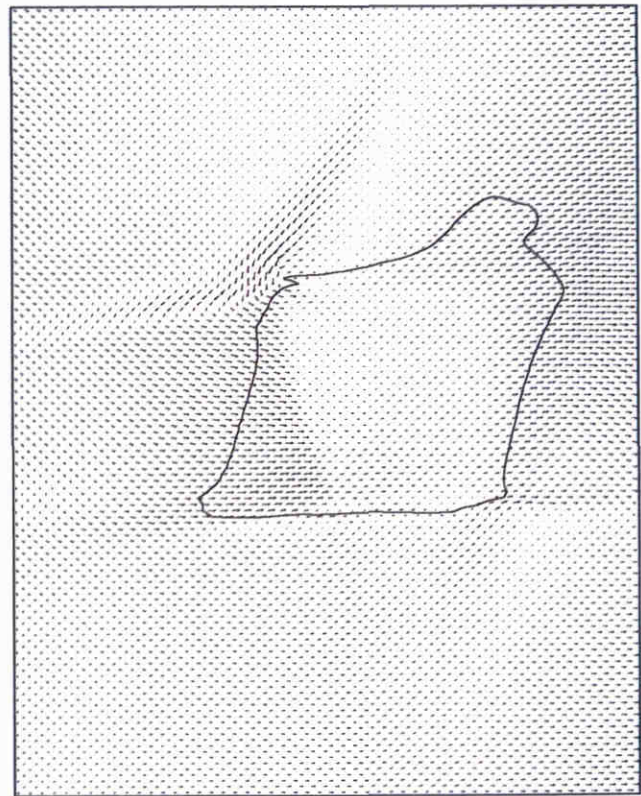
<19.5	<20.5	<29.5	<30.5
<20.0	<25.0	<30.0	>30.5



<-10.0	<-4.0	<2.0	<8.0
<-8.0	<-2.0	<4.0	<10.0
<-6.0	<0.0	<6.0	>10.0



→ $2.0 \times 10^{-6} \text{ m}^2/\text{s}$



Bottom levels and changes [m]; sediment transport [m^2/s]

+45 degrees rotated 10x10 km² sandpit

Morphological results after 1000 years

Figure 8.26b: Bottom levels in the center longitudinal section of a parallel $10 \times 10 \text{ km}^2$ sandpit

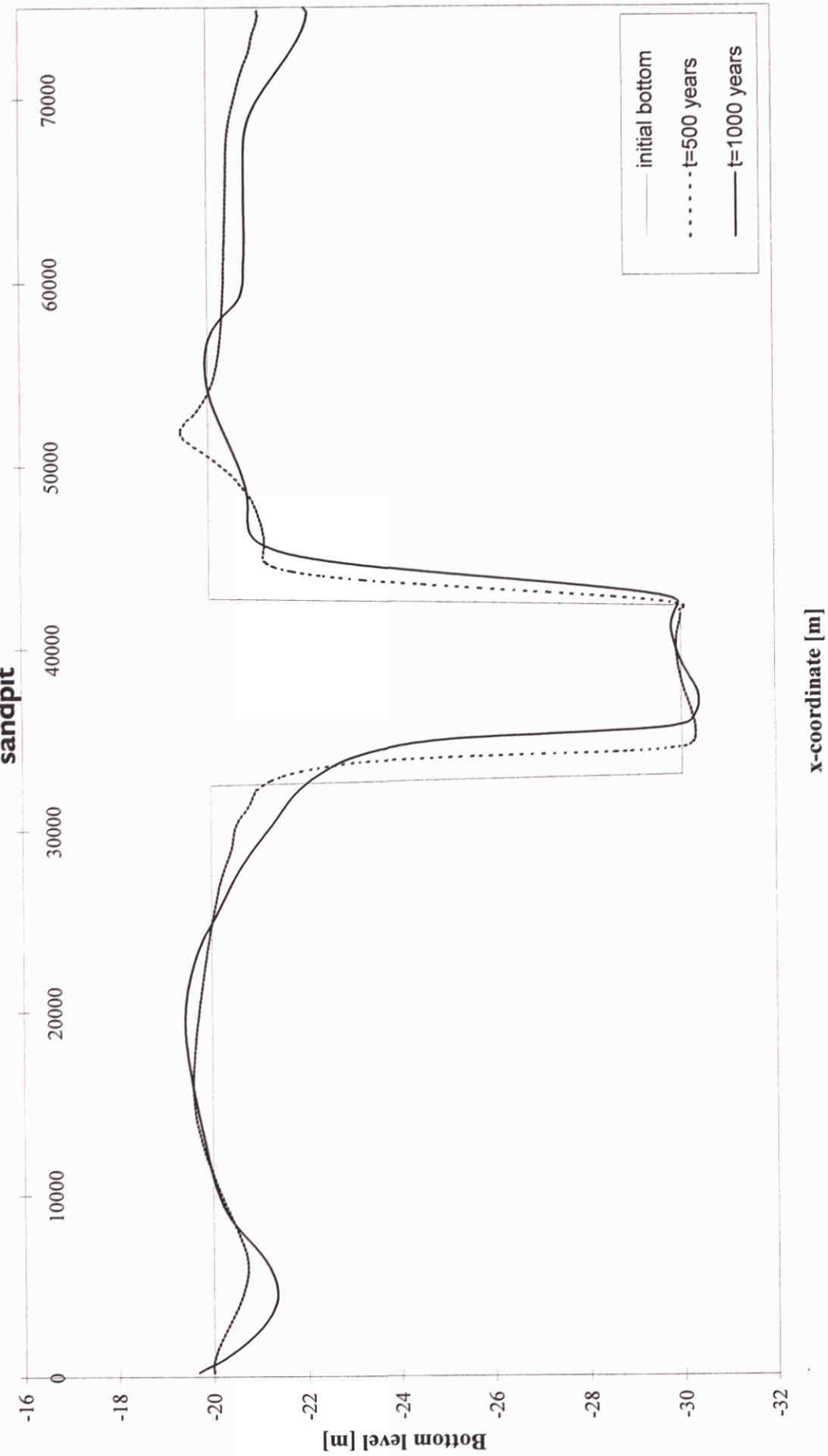
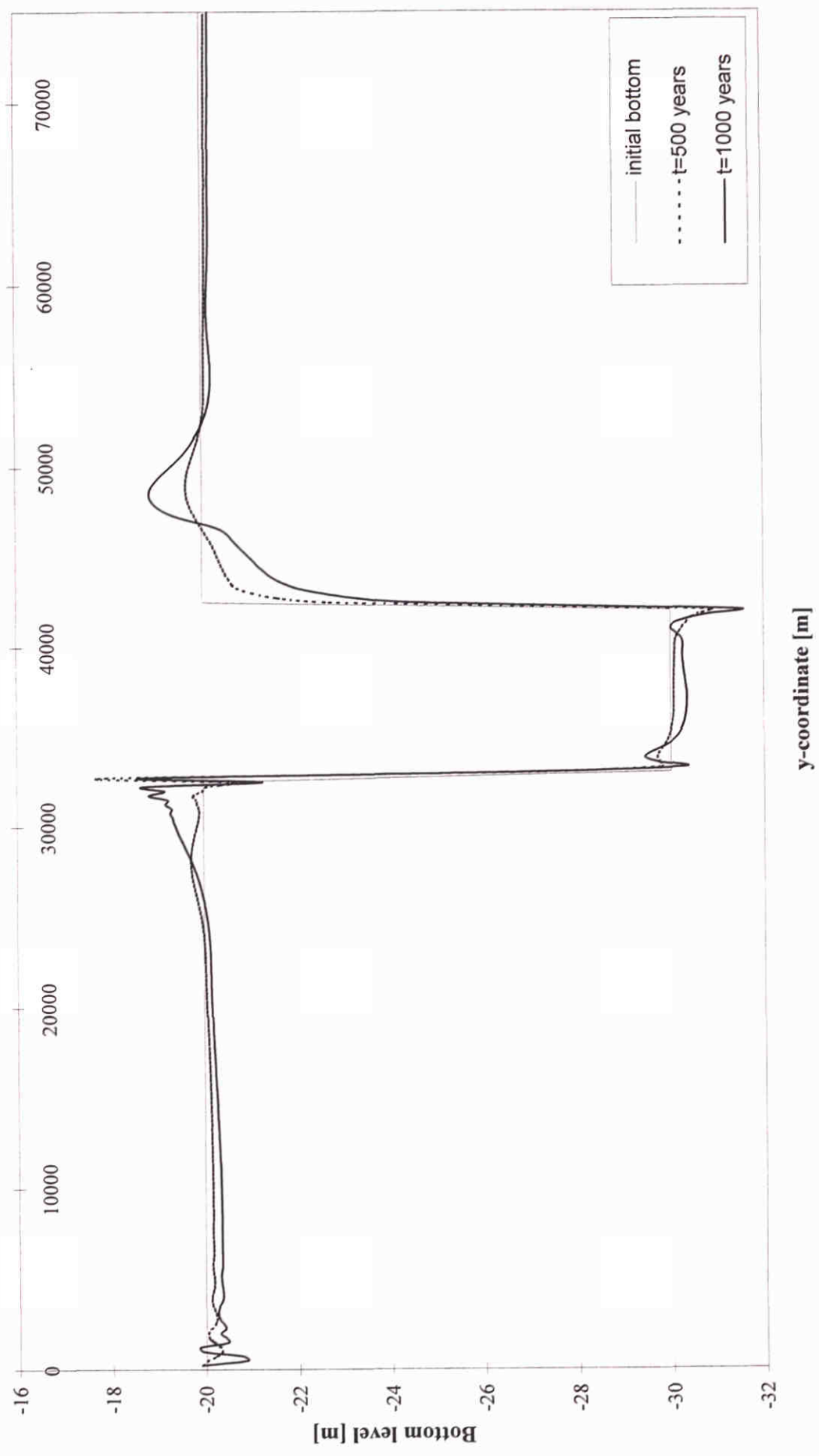
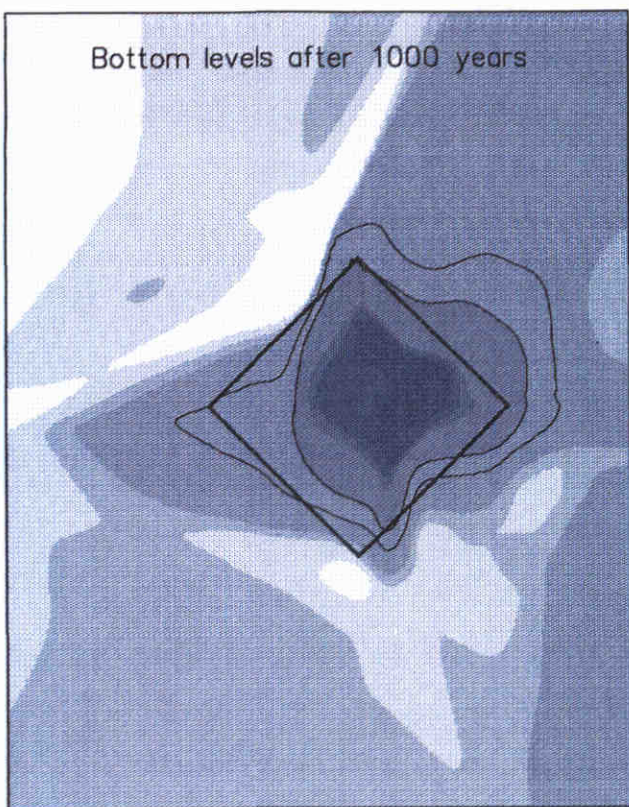
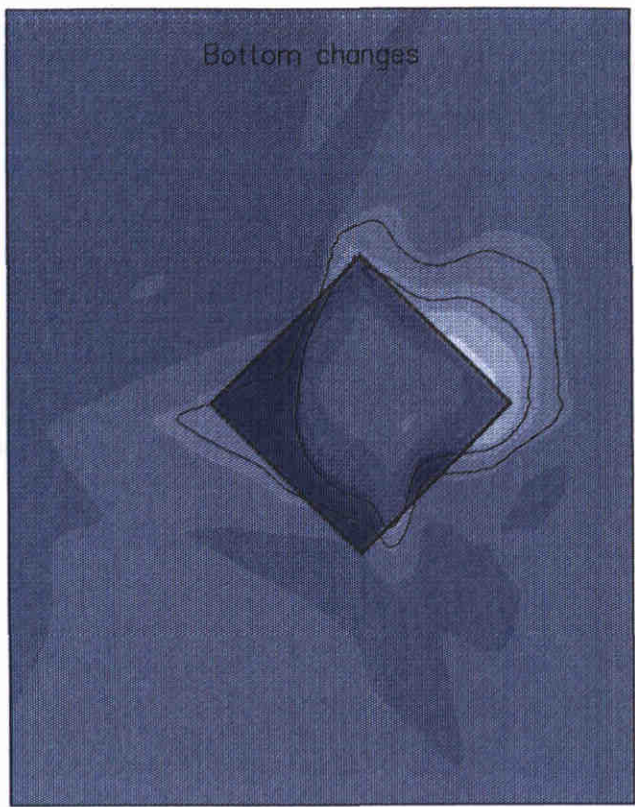


Figure 8.26c: Bottom levels in the center cross-section of a parallel $10 \times 10 \text{ km}^2$ sandpit

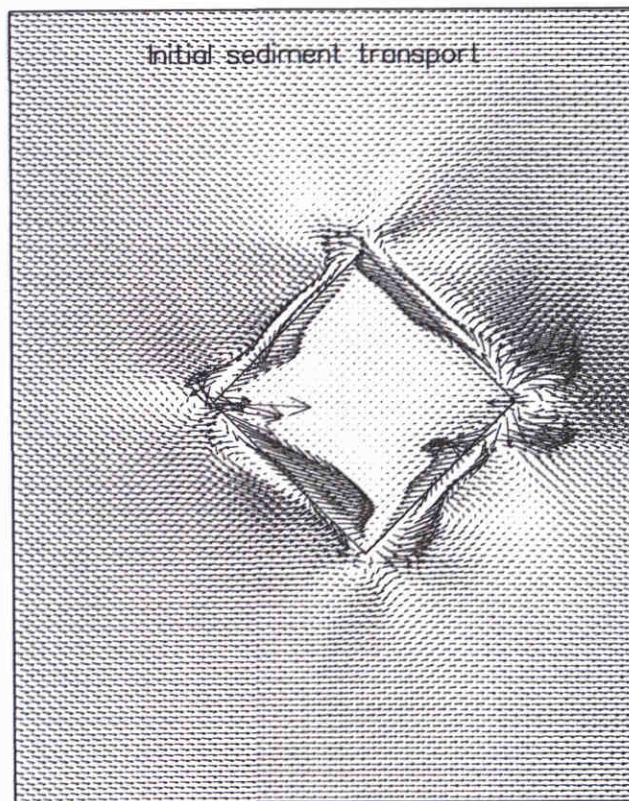




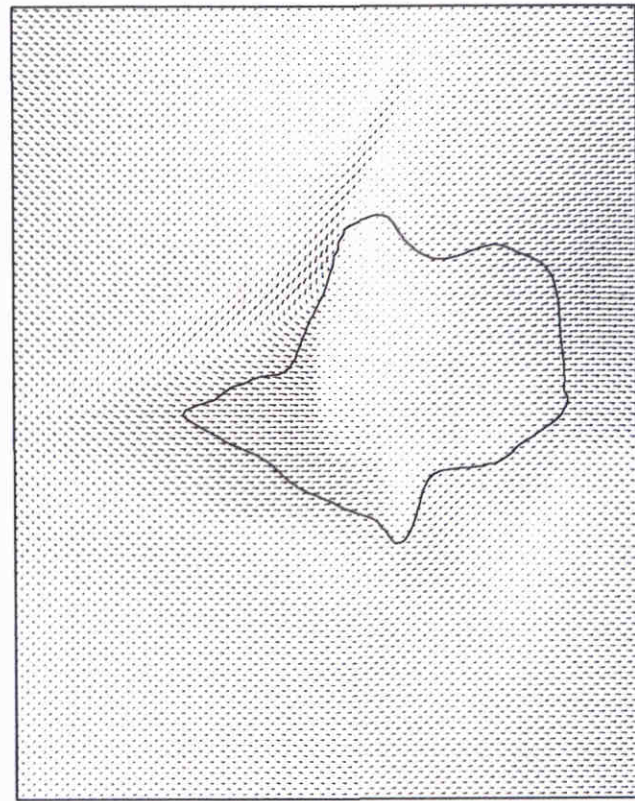
<19.5	<20.5	<29.5	<30.5
<20.0	<25.0	<30.0	>30.5



<-10.0	<-4.0	<2.0	<8.0
<-8.0	<-2.0	<4.0	<10.0
<-6.0	<0.0	<6.0	>10.0



→ $2.0 \times 10^{-6} \text{ m}^2/\text{s}$



Bottom levels and changes [m]; sediment transport [m^2/s]

+45 degrees rotated 10x10 km² sandpit

Morphological results after 1000 years

Figure 8.27b: Bottom levels in the longitudinal section of a +45° rotated 10x10 km² sandpit

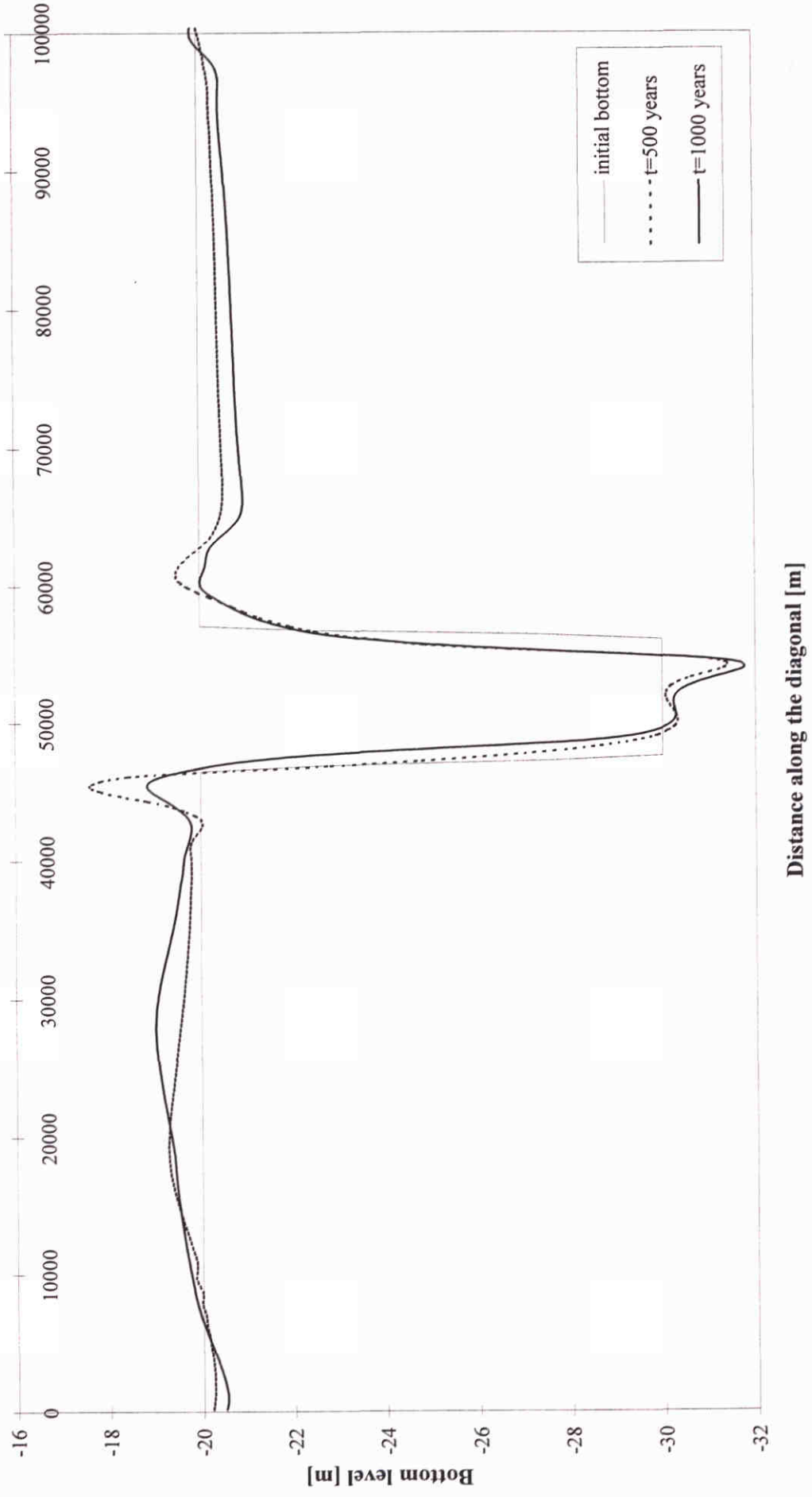
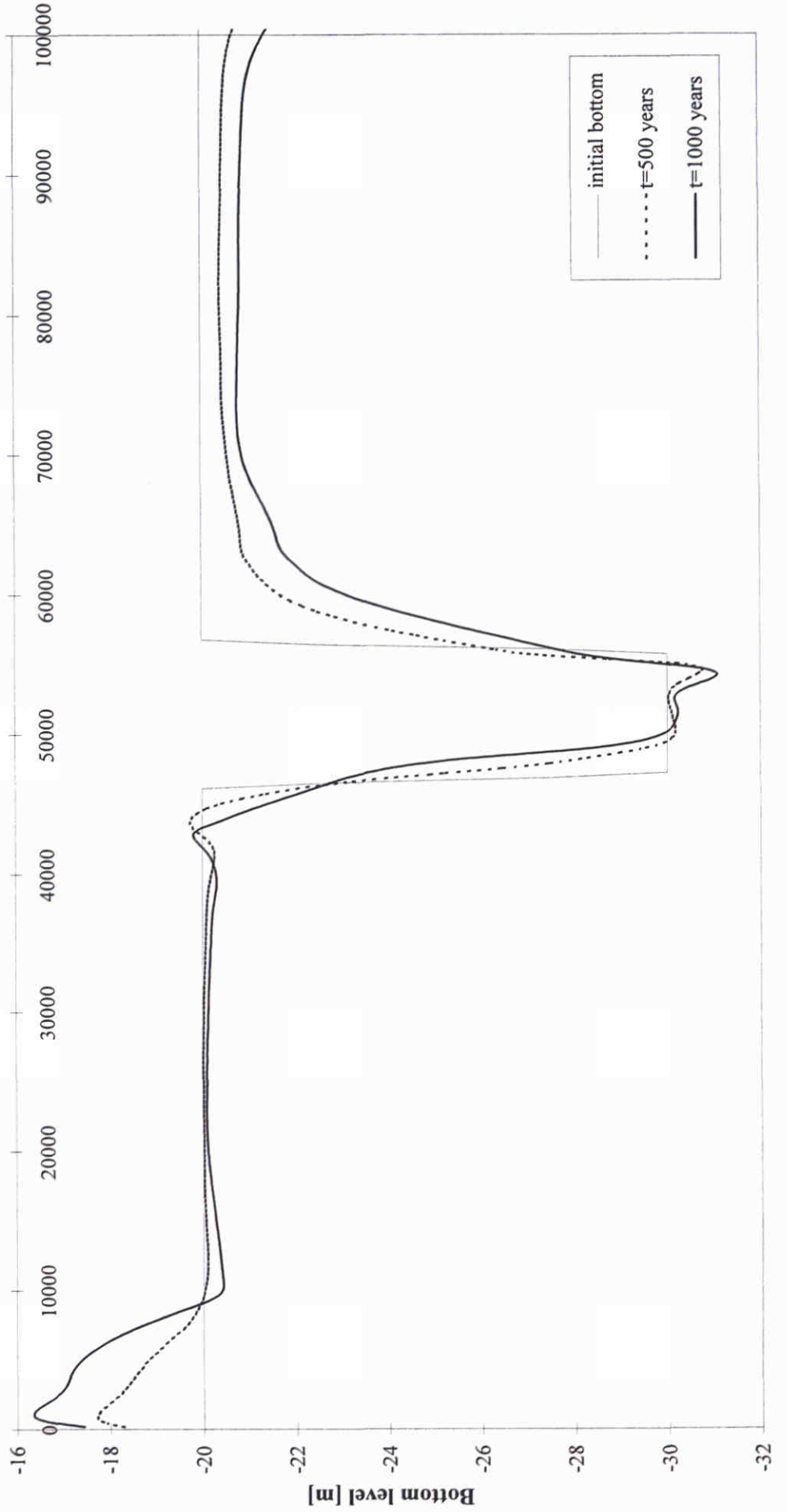
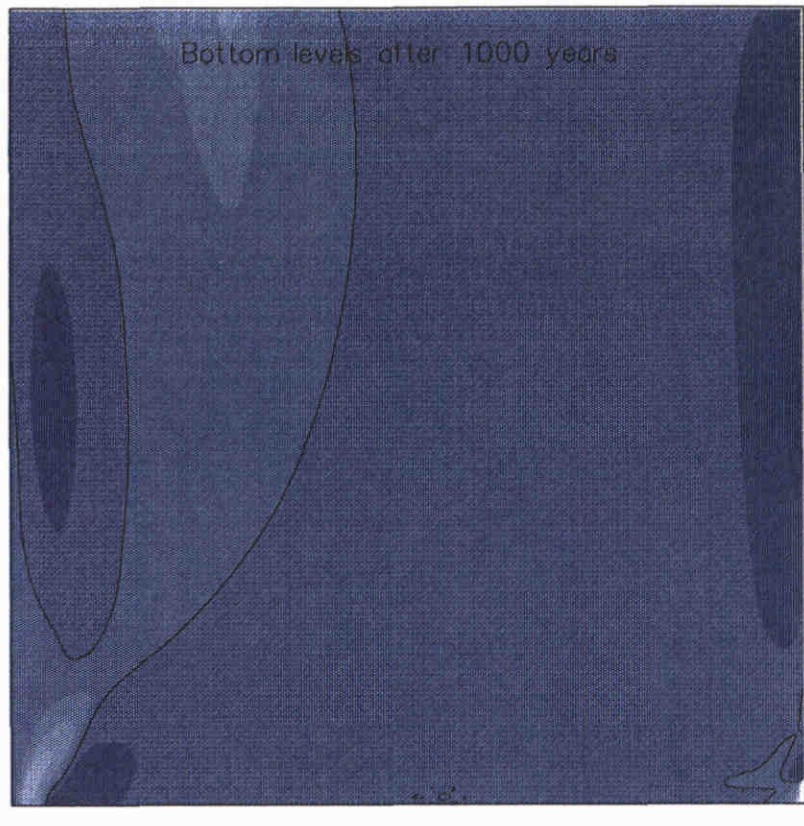


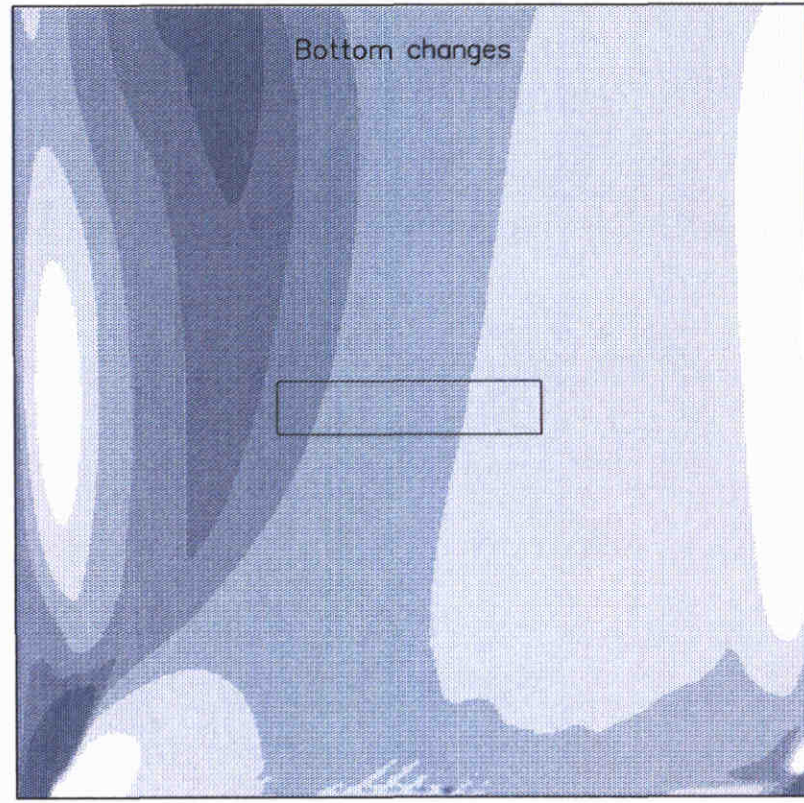
Figure 8.27c: Bottom levels in the center cross-section of a +45° rotated 10x10 km² sandpit



Distance along the diagonal [m]



<14.0	<16.0	<18.0	<20.0	<22.0	>23.0
<15.0	<17.0	<19.0	<21.0	<23.0	

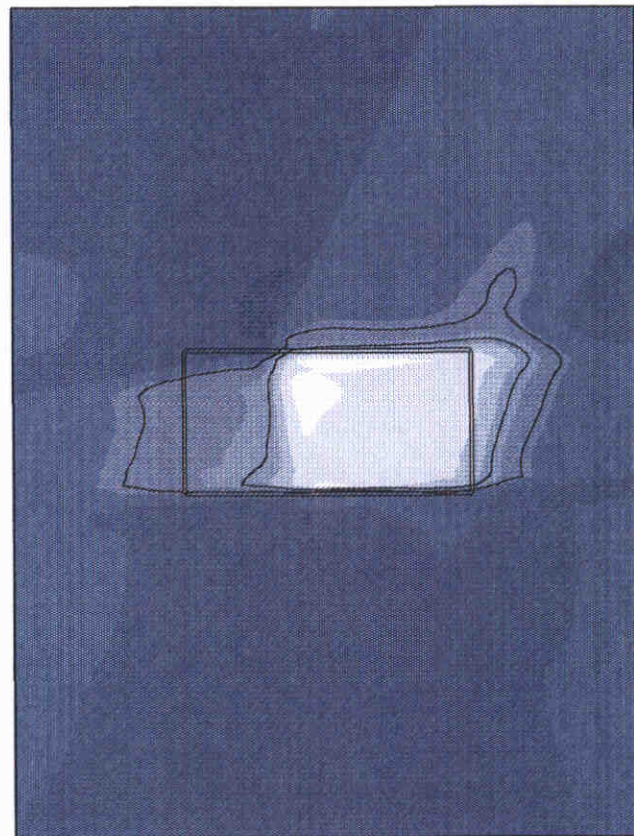
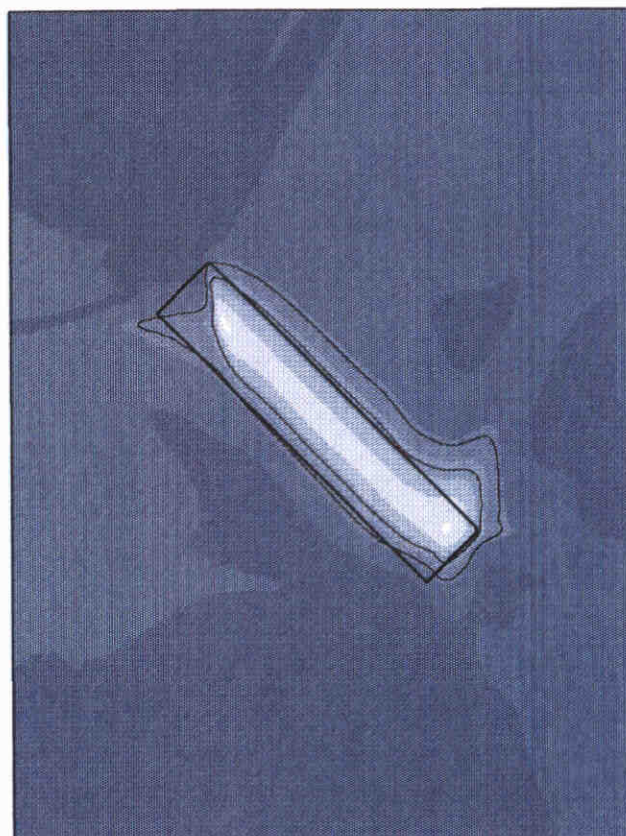
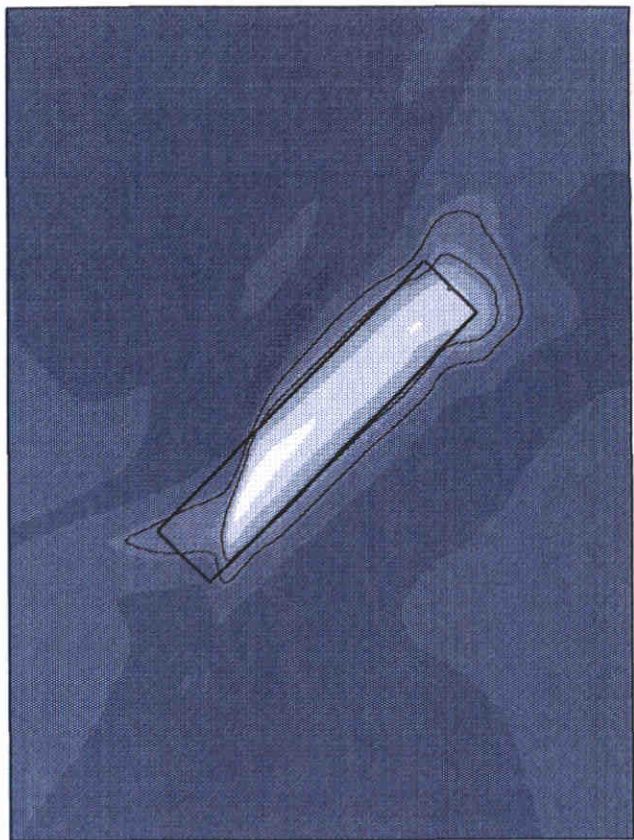
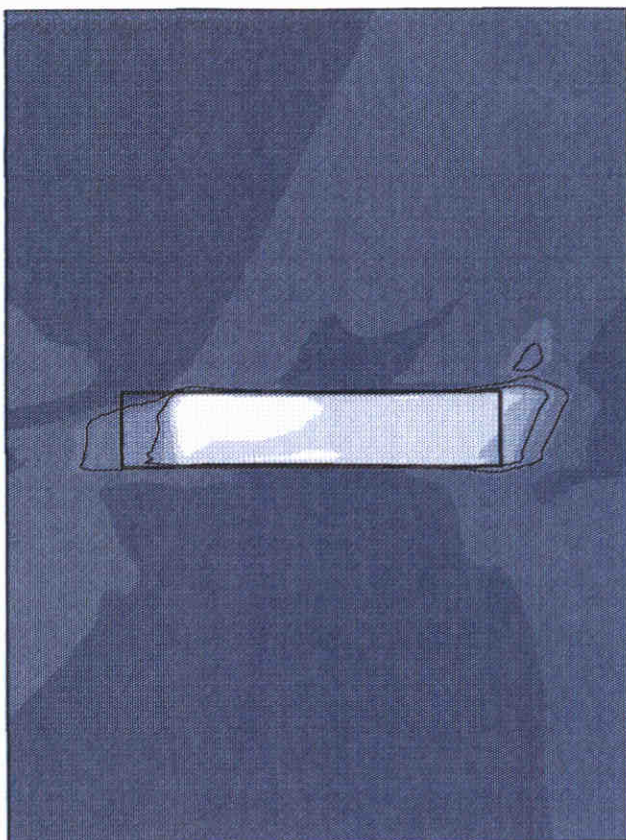


<-1.0	<0.0	<1.0
<-0.5	<0.5	>1.0

Bottom levels and changes [m]

Flat bottom without a sandpit

Morphological results after 1000 years

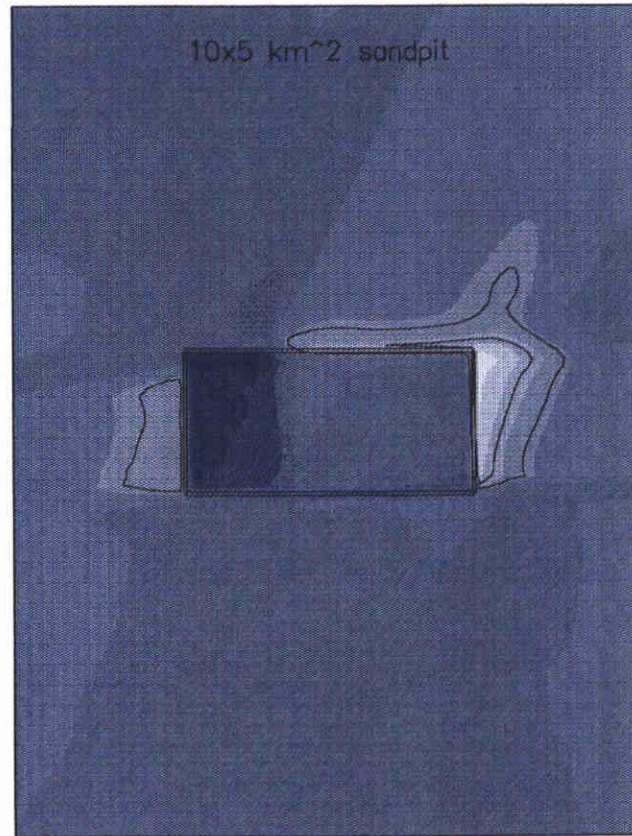
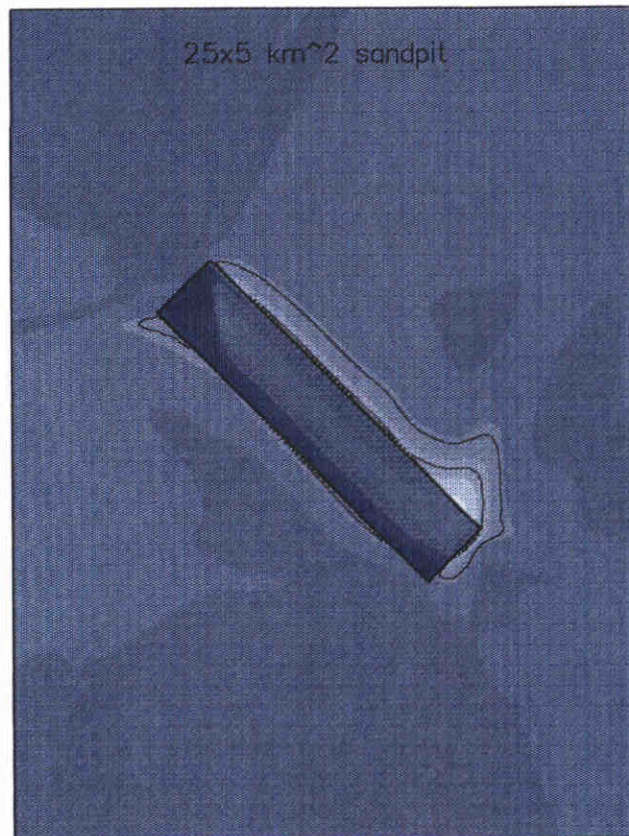
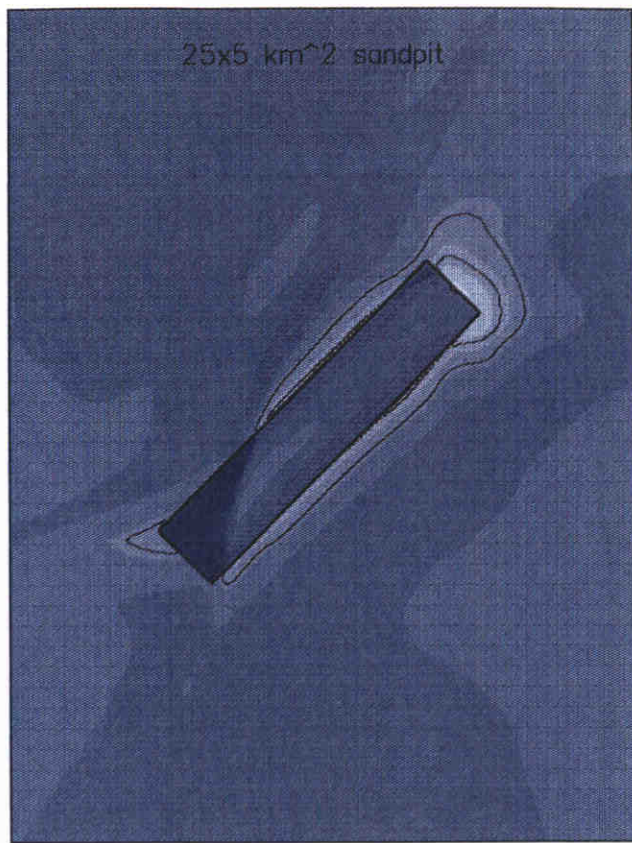
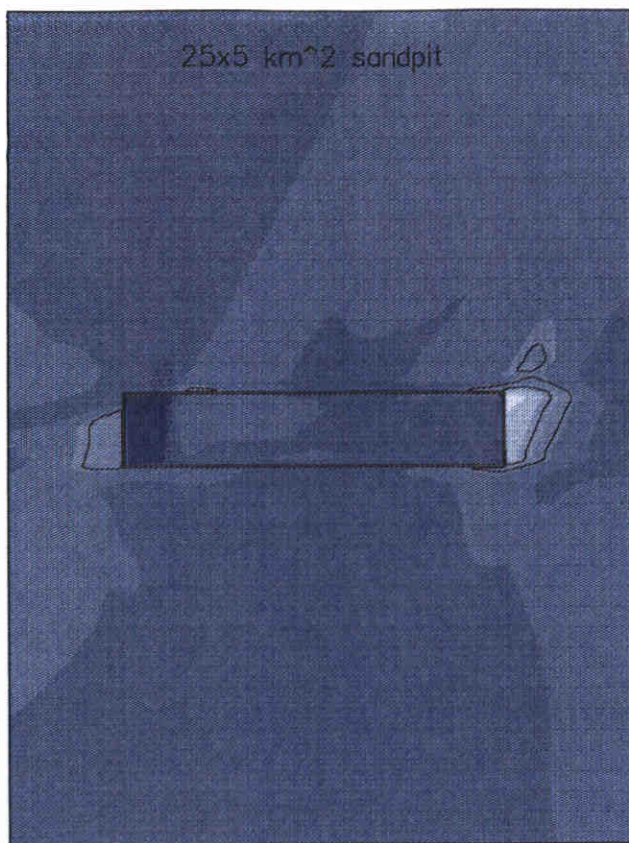


Bottom levels [m] with respect to undisturbed sea bottom

Correction for the influence of the boundary conditions

Morphological results after 1000 years





<-10.0	<-6.0	<-2.0	<2.0	<6.0	<10.0
<-8.0	<-4.0	<0.0	<4.0	<8.0	>10.0

Bottom changes [m]

Correction for the influence of the boundary conditions

Morphological results after 1000 years



wL | delft hydraulics

**Rotterdamseweg 185
postbus 177
2600 MH Delft
telefoon 015 285 85 85
telefax 015 285 85 82
e-mail info@wldeflt.nl
internet www.wldeflt.nl**

**Rotterdamseweg 185
p.o. box 177
2600 MH Delft
The Netherlands
telephone +31 15 285 85 85
telefax +31 15 285 85 82
e-mail info@wldeflt.nl
internet www.wldeflt.nl**

